Organic Petrology of Coals and Dispersed Organic Matter in Rocks from the TUNA FIELD, GIPPSLAND BASIN

A report prepared for ESSO AUSTRALIA LTD.

by

A.J. Kantsler, L.L. Ingram and A.C.Cook

Department of Geology
University of Wollongong
P.O. Box 1144
WOLLONGONG N.S.W. 2500

September, 1980

Organic Petrology of Coals and Dispersed Organic Matter in Rocks from the TUNA FIELD, GIPPSLAND BASIN

A report prepared for ESSO AUSTRALIA LTD.

by

A.J. Kantsler, L.L. Ingram and A.C.Cook

Department of Geology
University of Wollongong
P.O. Box 1144
WOLLONGONG N.S.W. 2500

September, 1980

1. Introduction

Following discussions with Esso Australia Ltd. in mid-1979 concerning the lack of knowledge about the effects of hydrocarbons on the physical properties of coal and dispersed organic matter (dom) it was decided to initiate a research project on the organic petrology of core samples from reservoir rocks in the Tuna Field, Gippsland Basin. The aim of the project was to investigate what, if any, maceral-maceral or maceral-hydrocarbon interactions occurred. Off-structure variation in organic matter is a further aspect of the study. Samples from the Tuna-1 well had previously been examined by A.C. Cook in 1971 and G.C. Smith in 1976. It had been noticed by the latter worker that the results of the 1971 vitrinite reflectance analyses were offset slightly towards lower ranks as compared with the 1976 results and it was thought that desiccation of the low rank samples during their shelf-life could be responsible. The effects of shelf-life and desiccation are also considered in this work using samples from the reservoir horizons in the recently drilled (1978) Tuna A-5 and A-15 wells as a control. Information from these samples is supplemented by data from the Tuna-2 and Tuna-3 wells at the extremities of the field (Figure 1) in order to establish any likely effects due to lateral and vertical rank and type variation.

The results presented in this report are a synthesis based upon a review of the data obtained from the samples submitted for analysis. Sampling density is obviously biased towards the M-1.2 and T-1 Reservoirs and it is not known how representative the samples are of the sequence penetrated, e.g. the samples bias towards the more carbonaceous rocks is not known. The number of samples obtained within each horizon is not the same either within, or between wells and this places further limitations on over-generalization from the results presented here.

In all, 104 core samples of coal and other sedimentary rocks were supplied for analysis. The results are considered with the other Tuna-1 data of Cook (1971 - 6 samples), Smith (1976 - 13 samples), Emmett-Smith (1978 - 2 samples) and Kantsler (1980 - 27 samples). The latter data were obtained from a suite of 33 samples of core and cuttings supplied for analysis by R.T. Mathews (University of Melbourne) as part of another, independent, research project.

Relatively little is known of localized rank variation in oil fields. Although rank varies relatively systematically over large areas, it is believed that significant local variation may also occur. The present

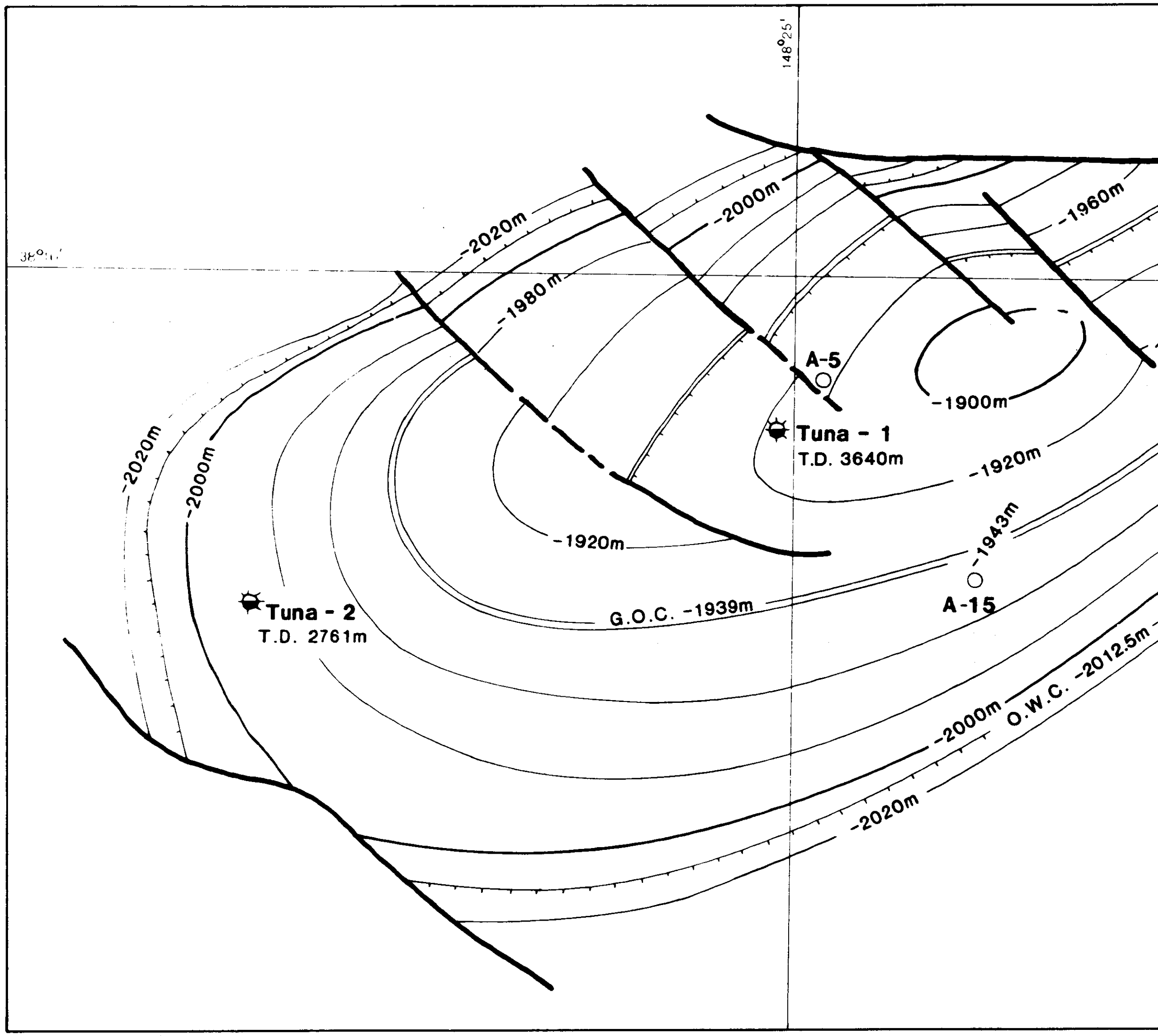

Figure 1

TUNA FIELD

STRUCTURE MAP
TOP OF T-1 RESERVOIR

Contour Interval: 20m   Datum: Sea Level

SCALE:- 1:25 000

0 — 1 km

study provides an ideal opportunity for the further consideration of such ideas, including the possibility that vitrinite reflectance 'noise' (often disregarded in assessing downhole rank variation) may relate to lithology, and thus 'plumbing' of the section under consideration. Small variations in vitrinite type (Brown et al, 1964) and the presence of hydrocarbons may also contribute to local variation.

2. Procedure

Full details of the procedures used are given by Cook (1979). The following represents a brief summary of the conditions under which maximum reflectance is measured and organic matter type ascertained.

All samples were mounted on an "as received" basis in a cold-setting polyester resin. Standard grinding and polishing procedures (chromium sesquioxide followed by magnesium oxide in a water slurry) were used.

Vitrinite reflectance measurements were made in oil-immersion (n = 1.518) at a wavelength of 546nm at a temperature of 23°C $\pm$ 1°C. A maximum of fifty measurements was taken on both coal grains and on discrete particles (phytoclasts) of vitrinite occurring as dom in accordance with the practice recently proposed by the SAA (1980). Maceral analyses were carried out using both incident white light and violet excitation (3mm BG3 filter with TK400 dichroic mirror and a K490 suppression filter).

3. Vitrinite Reflectance

3.1 Results of Vitrinite Reflectance Analyses

The reflectance values for the Tuna-1, Tuna-2, Tuna-3, Tuna A-5 and Tuna A-15 wells are listed in Tables 1-5 respectively together with a brief description of sample type. Reflectance profiles for the drilled sections in each of these wells are presented in Figures 2 to 6 respectively and are accompanied by detailed profiles of reflectance variation through the most densely sampled sections of each well, i.e. the M-1.2 and T-1 reservoirs.

TUNA-1

Figures 2A and 2A-1 show the results of the 90 vitrinite reflectance analyses measured on samples from Tuna-1. The two data points above the Latrobe Group (? Lakes Entrance Formation) are in good accord. They indicate minimal burial metamorphism of the sediments younger than 40 My and little section loss at the unconformity. Data from the level of the M-1.2 reservoir are also in good agreement (3 operators - 17 samples) and show only minor variation with lithology (fig. 2B) — the most noticeable feature

TUNA No.1

Reflectance Profile

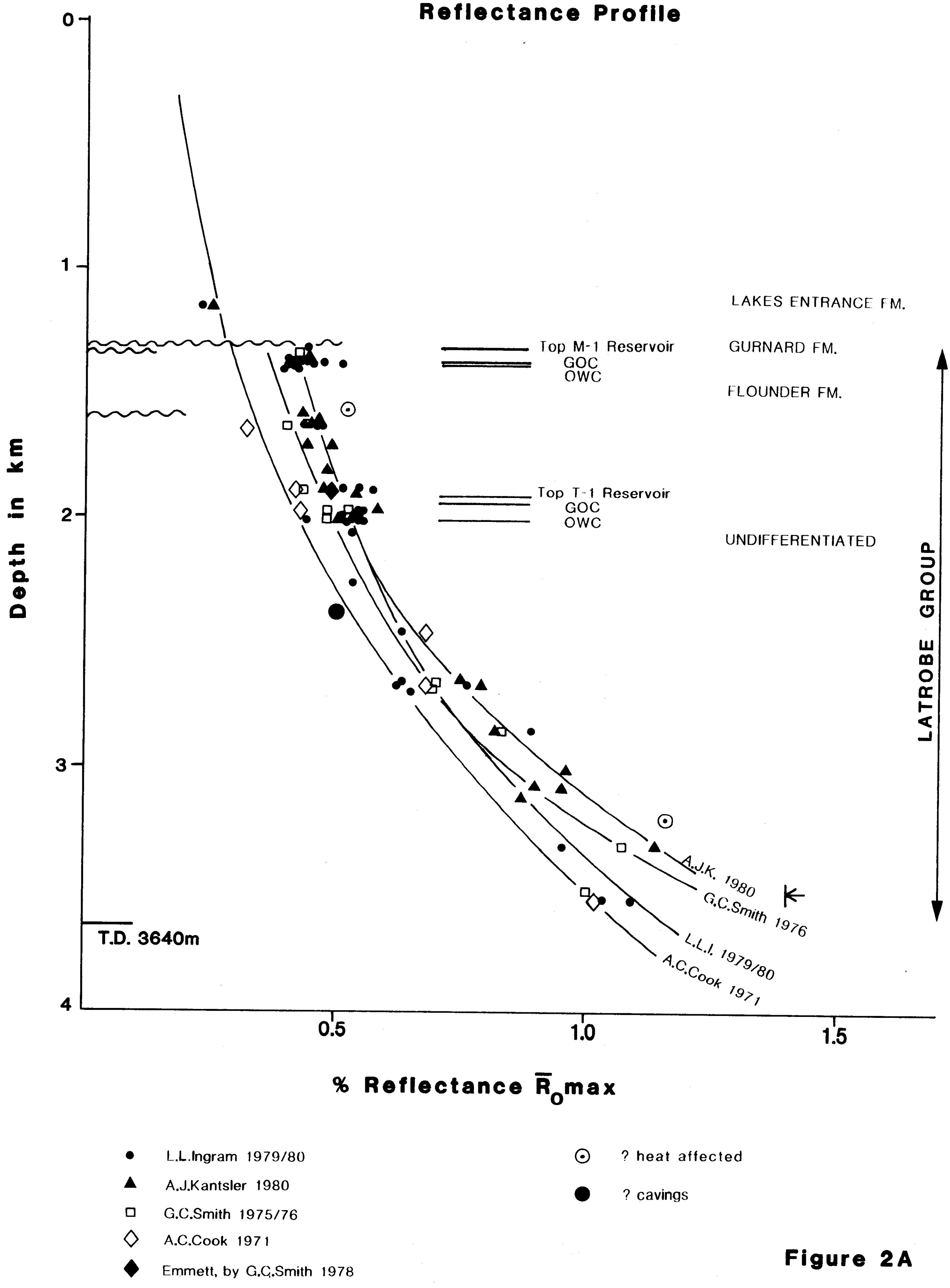

Figure 2A

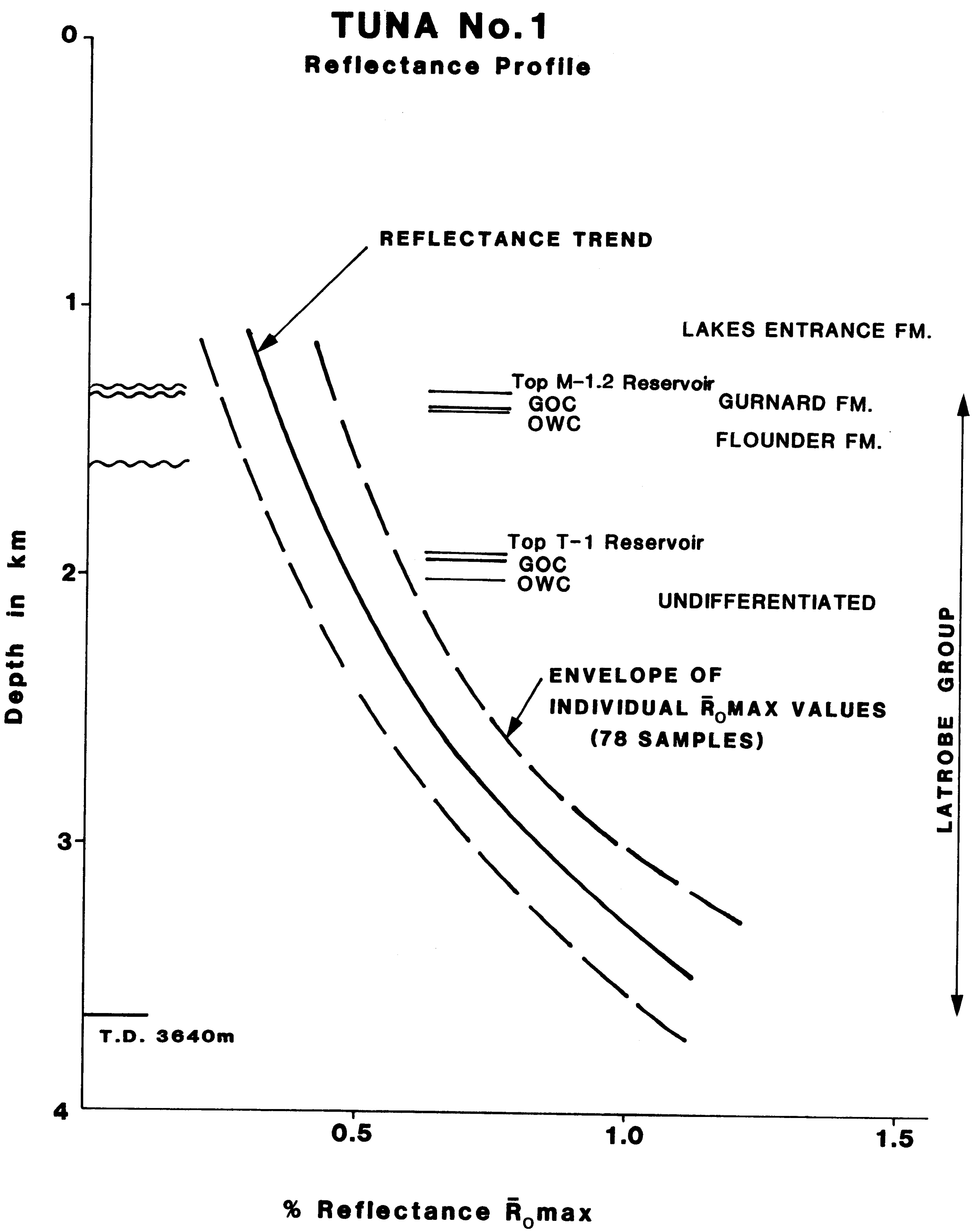

TUNA No.1
Reflectance Profile
REFLECTANCE TREND
LAKES ENTRANCE FM.
Top M-1.2 Reservoir
GOC
OWC
GURNARD FM.
FLOUNDER FM.
Top T-1 Reservoir
GOC
OWC
UNDIFFERENTIATED
ENVELOPE OF
INDIVIDUAL $\bar{R}_o$MAX VALUES
(78 SAMPLES)
LATROBE GROUP
T.D. 3640m
Depth in km
0
1
2
3
4
0.5
1.0
1.5
% Reflectance $\bar{R}_o$max

Figure 2A'

TUNA No. 1

Reflectance Profile M-1.2 Reservoir
(Data from L.L.Ingram only)

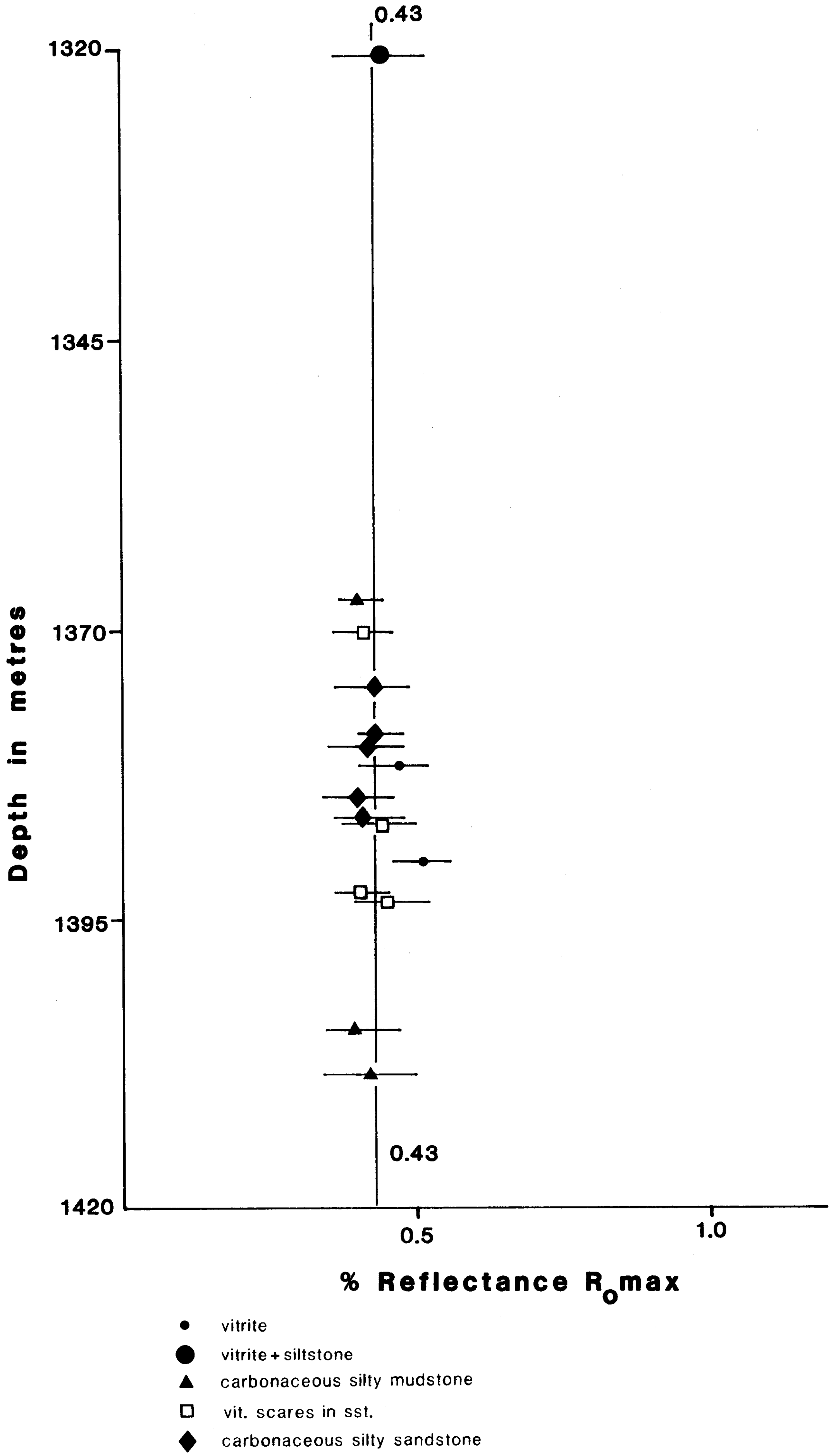

Figure 2B

being the offset towards higher reflectances of results from the two samples containing thick layers of vitrinite. Between the M-1.2 and T-1 reservoirs, most reflectance results (fig. 2A) show a range of about 0.1% R_o, which is considered high but not abnormal for 3 operators working on different samples. Exceptions are the 1971 data of A.C. Cook, which are consistently lower than the 1979-80 reflectance population. It is perhaps also significant that the 1976 data of G.C. Smith have a tendency to occur at the low rank end of the reflectance range.

In the T-1 reservoir, the population of reflectance results is tightly grouped and most points lie within a range of 0.07% R_o. Several samples lie outside this range, among which are: a lower result by A.C. Cook (1971), a high result by A.J. Kantsler (1979) from a cuttings sample which could be heat affected (see discussion), and a low result by L.L. Ingram (1980) from coal scares in a quartz sandstone (fig. 2C). Figure 2C shows little systematic variation of R_o with sample lithology and that the single low result is an exception. Again, it is worth noting that the 1976 data of G.C. Smith occur at the low rank end of the main reflectance population.

Below the T-1 reservoir, the reflectance data (fig. 2A) show greater variation which cannot be entirely isolated by operator, year of analysis or sample lithology (fig. 2D). In general, samples containing discrete layers or grains of vitrinite lie close to the arbitrary line drawn through the data in Figure 2D. Samples comprised largely of sandstone invariably yield results which lie on the low reflectance side of this arbitrary line (in particular the three sandstone samples between 2660 and 2680m and the sandstone samples at 3539m). Most carbonaceous shales yield data which lie close to, or on the high rank side of, this line. Cuttings samples typically have a very wide range of reflectance results as compared with the core samples (fig. 2D). This is probably a combination of artefacts due to drying and caving, and the effects associated with a greater range of host rock lithologies.

Little of the variation observed can be attributed to operator bias as each operator has analyses which lie above and below the general 'trend'. It seems most likely therefore that sample type and sample quality are the overriding factors which control the reflectance data. Further, beyond the brown coal rank stage there is no longer any association between year of analysis and lower R_o results.

TUNA-2

Figure 3A shows the results of reflectance analyses from the Tuna-2

TUNA No.1

Reflectance Profile T-1 Reservoir
(Data of L.L.Ingram only)

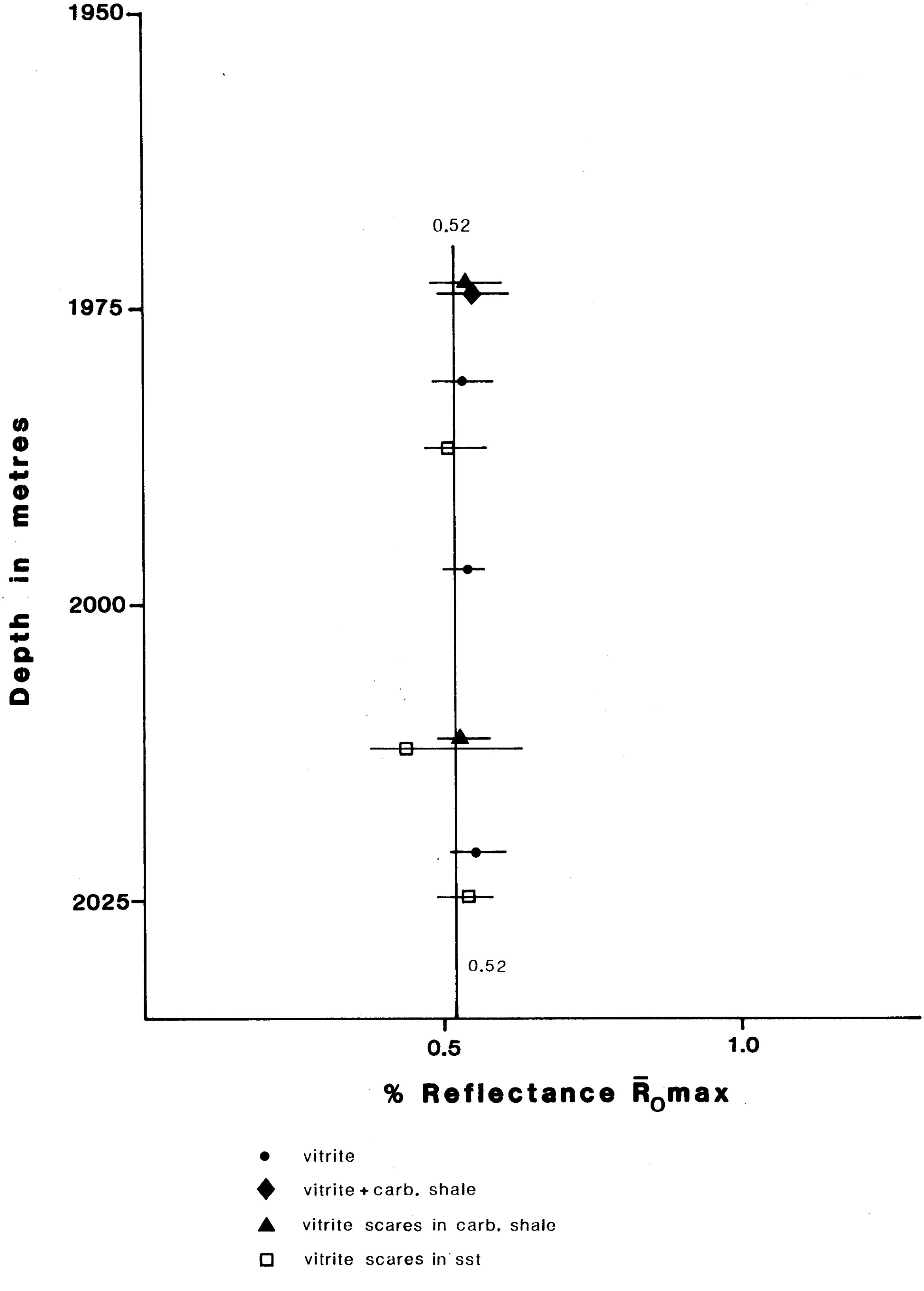

Figure 2C

TUNA No.1

Reflectance Profile Below the T-1 Reservoir

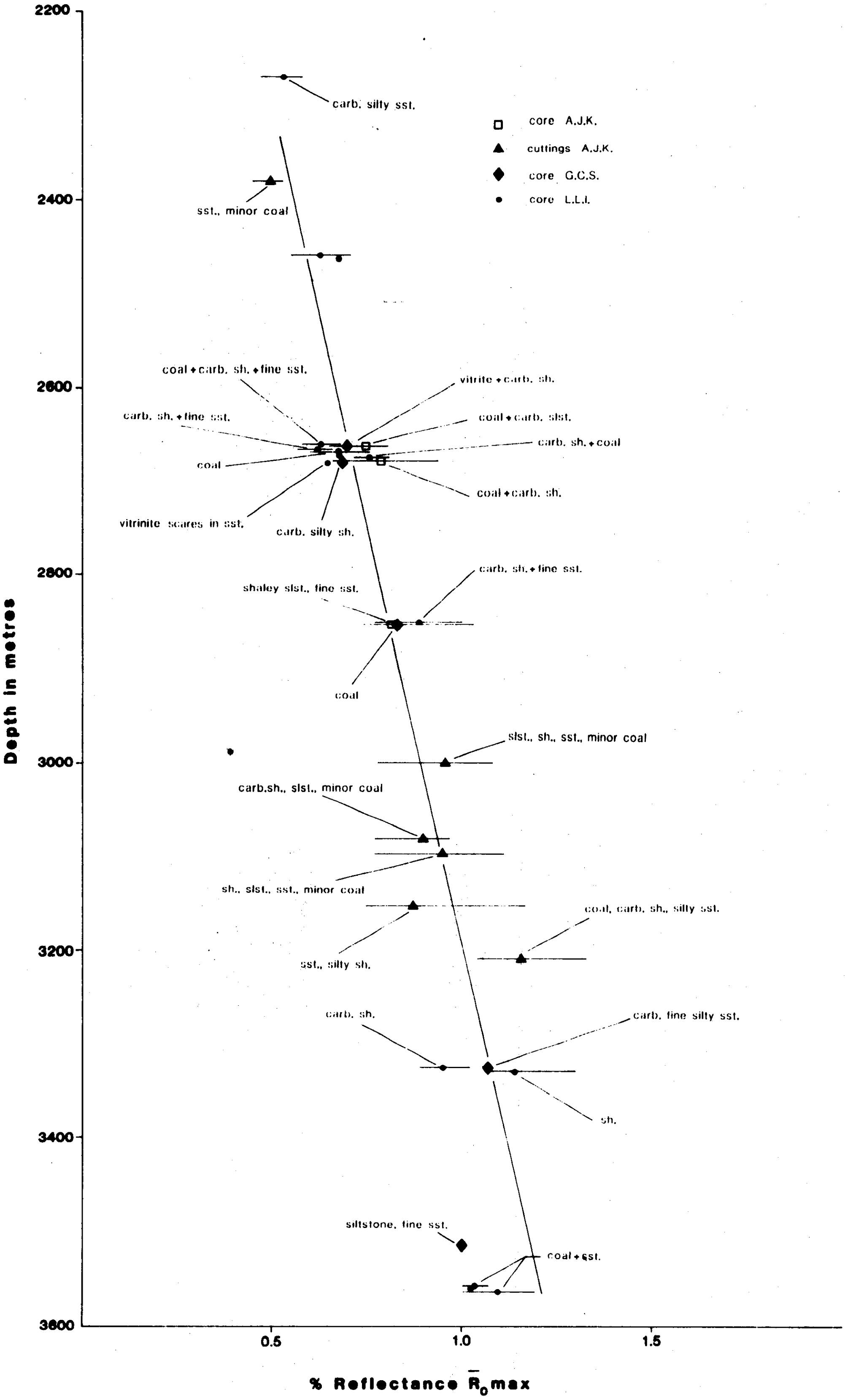

Figure 2D

well. Although similar to the Tuna-1 analyses, they have a tendency to be lower both in the M-1.2 reservoir and below the T-1 reservoir but are the same in the T-1 reservoir. In the M-1.2 reservoir the results were all measured on very small particles of vitrinite occurring as dom in fine silty sandstones and sandy siltstones. In the Tuna-1 data set vitrinite reflectances for such rocks are typically below the average trend. However, Figure 3B shows a lack of relation between vitrinite reflectance and host lithology, with one significant exception where the vitrinite may have been oxidised prior to, or during, deposition. The latter result is considered anomalous.

In the T-1 reservoir, reflectance again varies little (fig. 3C) with only a weak tendency for results from discrete layers of vitrite to be higher than the normal. Most of the reflectance data were measured from thick vitrite or clarite layers. The variation which does occur appears to fall within the limits of the experimental error of the method.

The three samples below the T-1 reservoir are each comprised largely of coal with some carbonaceous shale. When compared with the Tuna-1 data, these results lie toward the low rank side of the reflectance profiles illustrated in Figure 2A, outside the curves of A.C. Cook and G.C. Smith. The explanation for this departure is found in the gross sandstone lithology of this part of the Tuna-2 sequence.

TUNA-3

The Tuna-3 reflectance profile (fig. 4A) is similar to that for Tuna-1 but is weighted towards a higher gradient by the slightly higher results from the T-1 reservoir. In contrast, the gradient of the Tuna-2 reflectance profile is slightly lower because of the control exerted by the samples below the T-1 reservoir.

Silty, fine sandstones in the M-1.2 reservoir at Tuna-3 are similar to those encountered in both Tuna-1 and Tuna-2 and yield similar vitrinite reflectance values. In the T-1 reservoir, R_0 data were obtained mostly from thick layers of vitrite (as were the T-1 data from Tuna-2) and this may explain the increase in mean reflectance as compared with the T-1 data from Tuna-1. The data occur within a range of 0.10% R_0 and show some slight variation with lithology — most of the vitrite layers associated with sandstone being of less than average reflectance (Fig. 4B) whereas those associated with carbonaceous shale have a tendency to be slightly higher than average.

TUNA No.2

Reflectance Profile

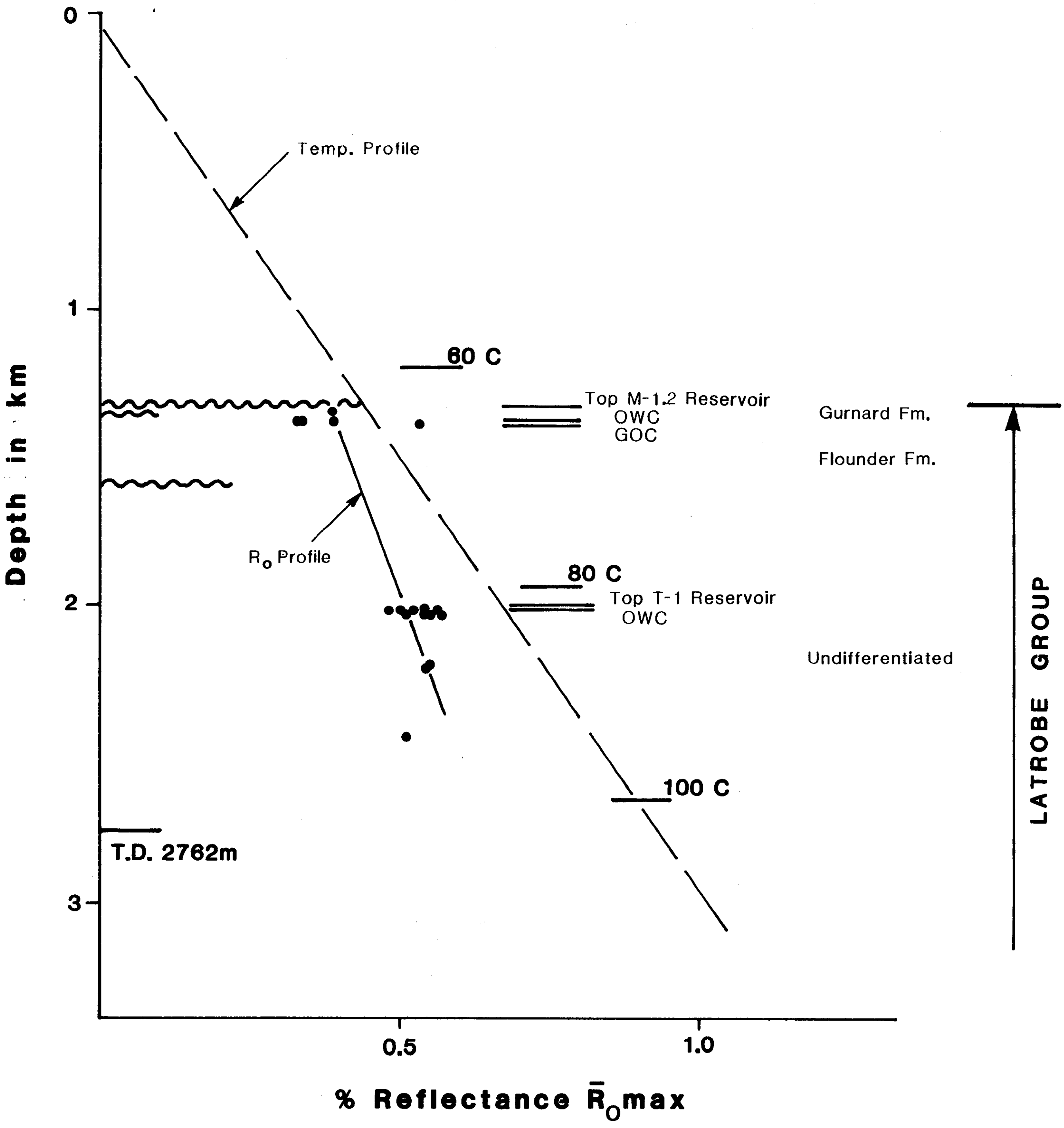

Figure 3A

TUNA No.2

Reflectance Profile M-1.2 Reservoir

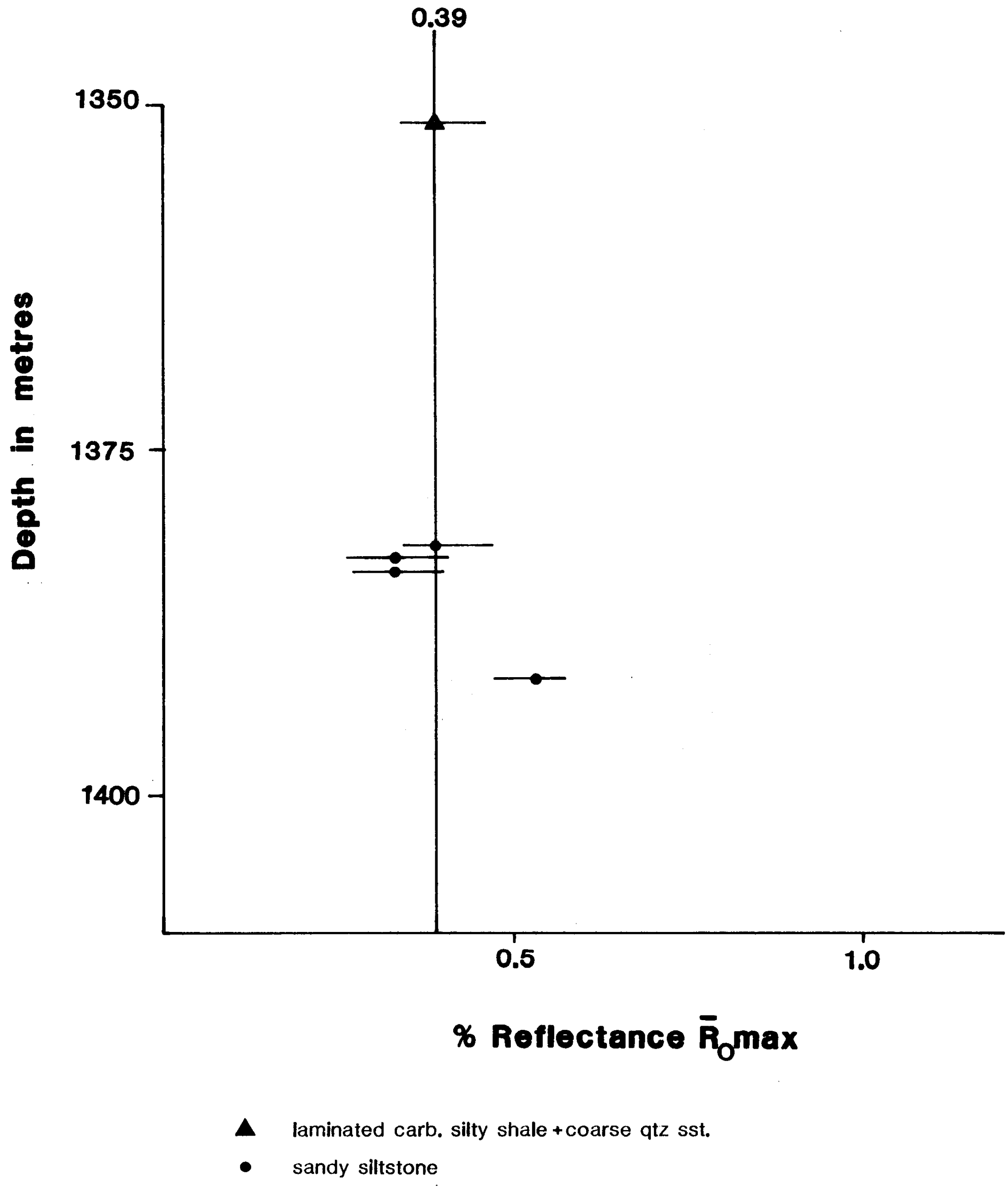

Figure 3B

TUNA No. 2

Reflectance Profile T-1 Reservoir

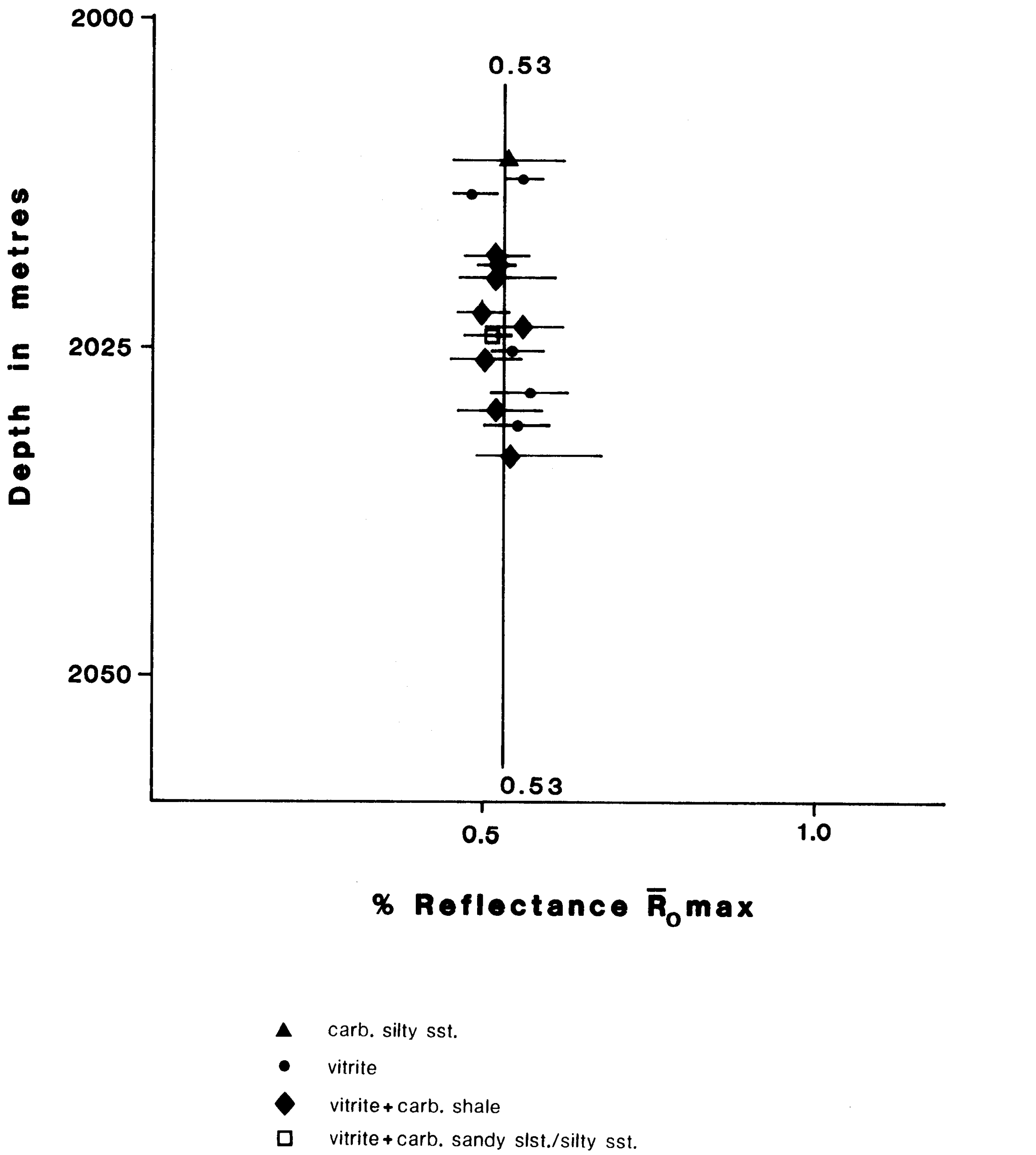

Figure 3C

TUNA No.3

Reflectance Profile

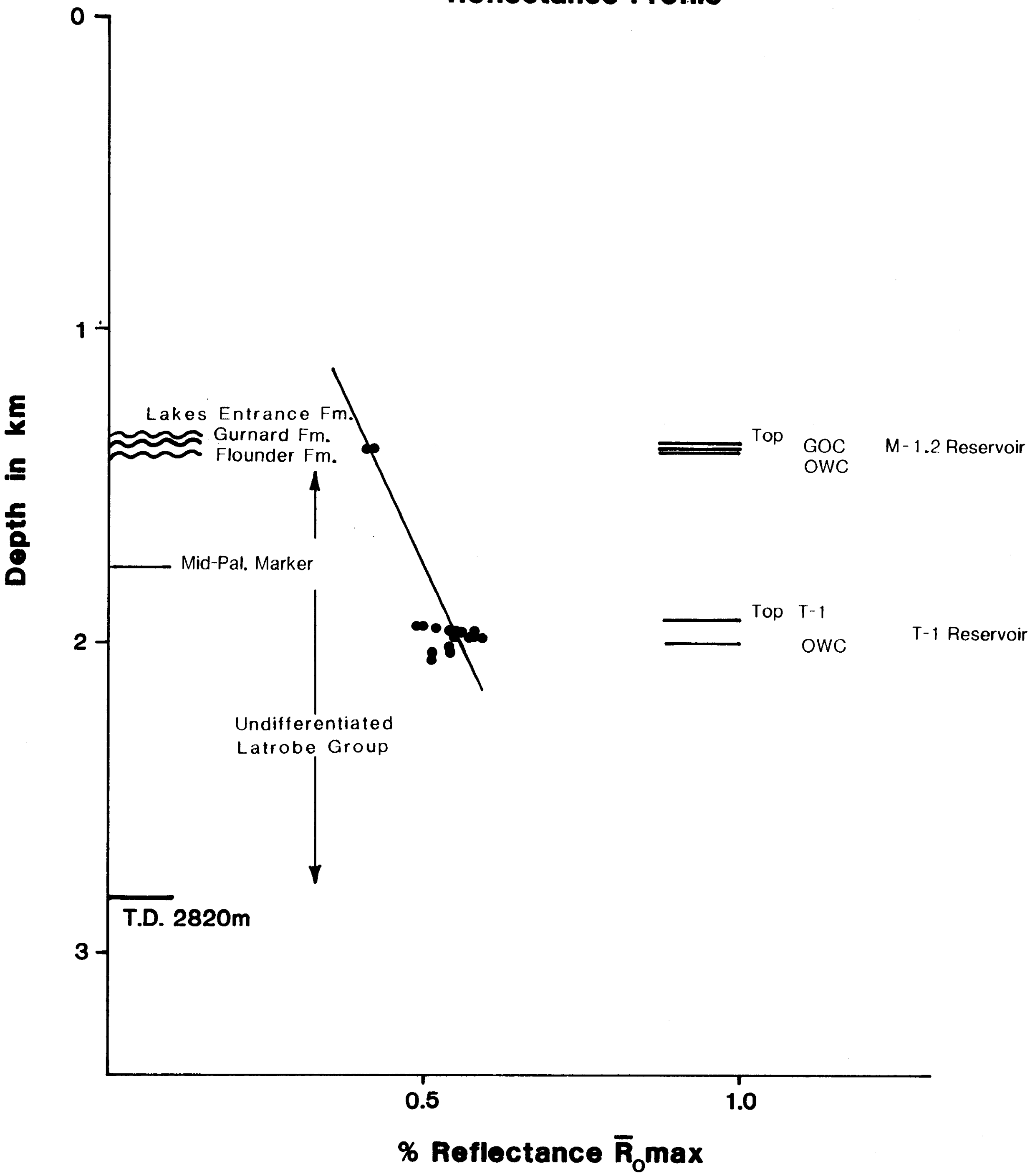

Figure 4A

TUNA No.3

Reflectance Profile for T-1 Reservoir

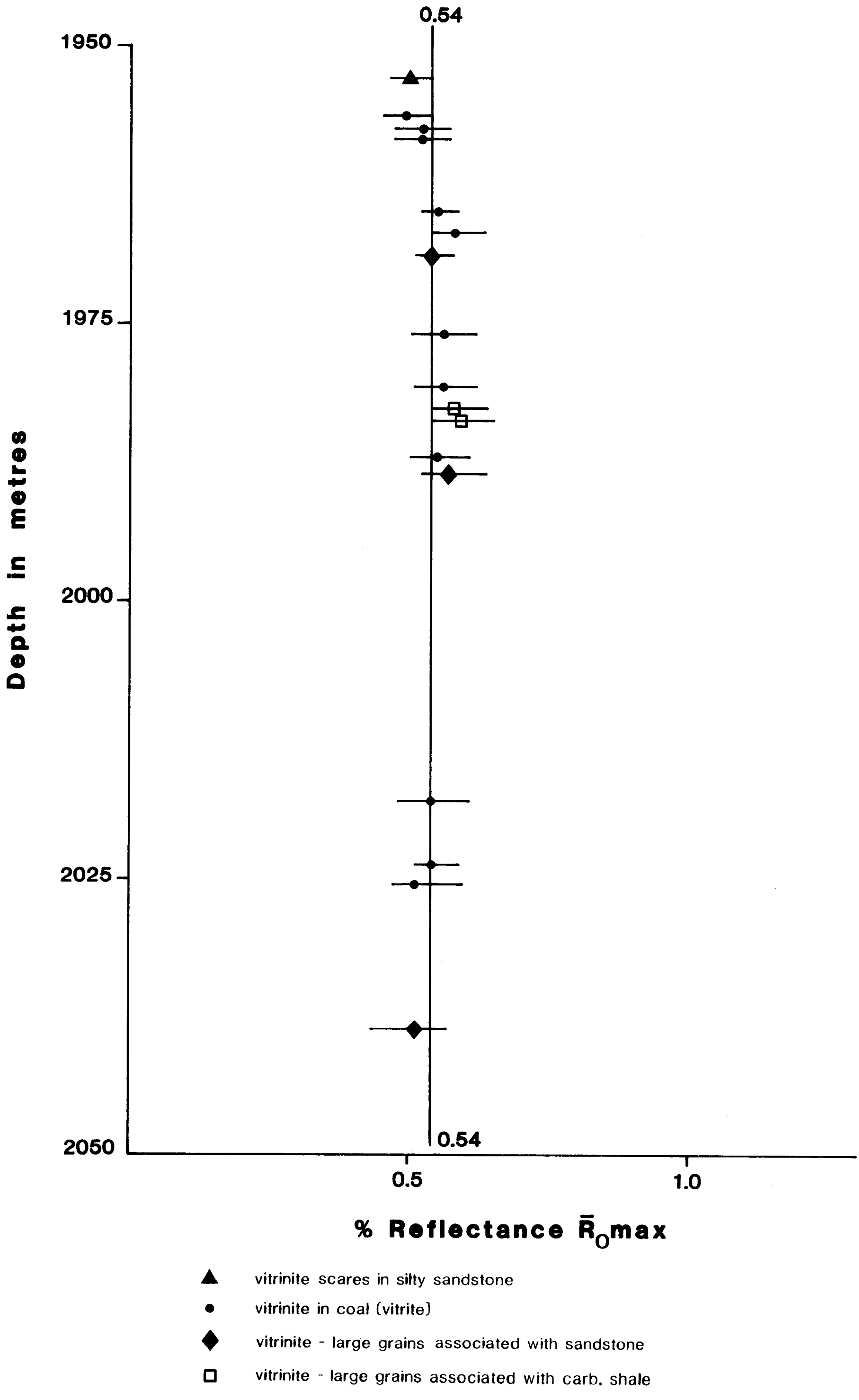

Figure 4B

TUNA A-5 AND TUNA A-15

The Tuna A-5 and A-15 reflectance profiles (figs. 5A and 6A) are very similar to that of Tuna-3. Data from the M-1.2 reservoir are similar to data from Tuna-1 and Tuna-2. Data from the T-1 reservoir are also in accord with data from the other wells. As with the reflectance data from the T-1 reservoir in Tuna-3, the Tuna A-5 and A-15 T-1 data are, on average, of slightly higher reflectance than the T-1 data from Tuna-1 and Tuna-2. The increase stems from measurements made on thick layers of vitrite and clarite or prominent coal scares in sandstone or shales. Figures 5B and 6B illustrate the lack of any systematic variation in results from the T-1 reservoir.

3.2 Discussion of Vitrinite Reflectance Results

Vitrinite reflectance data obtained from vitrite layers in coals and sediments of the T-1 reservoir show 'normal' scatter (consistent with experimental error) in each of the Tuna wells examined. Reflectances are consistent between wells with the exception of Tuna-2 where they are marginally lower. As such, T-1 reflectance data provide a reliable control point in the establishment of a reflectance profile.

Reflectance data from the M-1.2 reservoir are also consistent within and between wells, despite the fact that they were obtained variously from discrete particles of vitrinite and from thin layers of vitrinite interbedded with other sediments. They also provide a reliable control.

Between the M-1.2 and T-1 reservoirs, data from Tuna-1 show a range of results similar to those described above. They also show that the reflectance values determined by A.C. Cook in 1971 consistently lie at the low rank end of the reflectance range. This trend continues into the T-1 reservoir. Similarly, the data of G.C. Smith (generated in 1976) tend to occur at the lower rank end of the reflectance ranges measured by L. L. Ingram and A.J. Kantsler during 1979-80. The suggestion has been made that desiccation of low rank samples during their shelf-life may be responsible for this change in reflectance. A study by Chandra (1966) on the effect of storage on the reflectance of coal showed that storage of coals of sub-bituminous to anthracite rank for 10 years led to changes in reflectance of the order 0.01% to 0.10% R_0. However, this variation was by no means systematic and in most cases (including that of the sub-bituminous rank coal), was associated with a decrease in reflectance. Furthermore, Chandra's study was rather limited in scope and his results cannot be regarded as conclusive as most lie within the range of experimental error of the original analyses.

TUNA No. A-5

Reflectance Profile

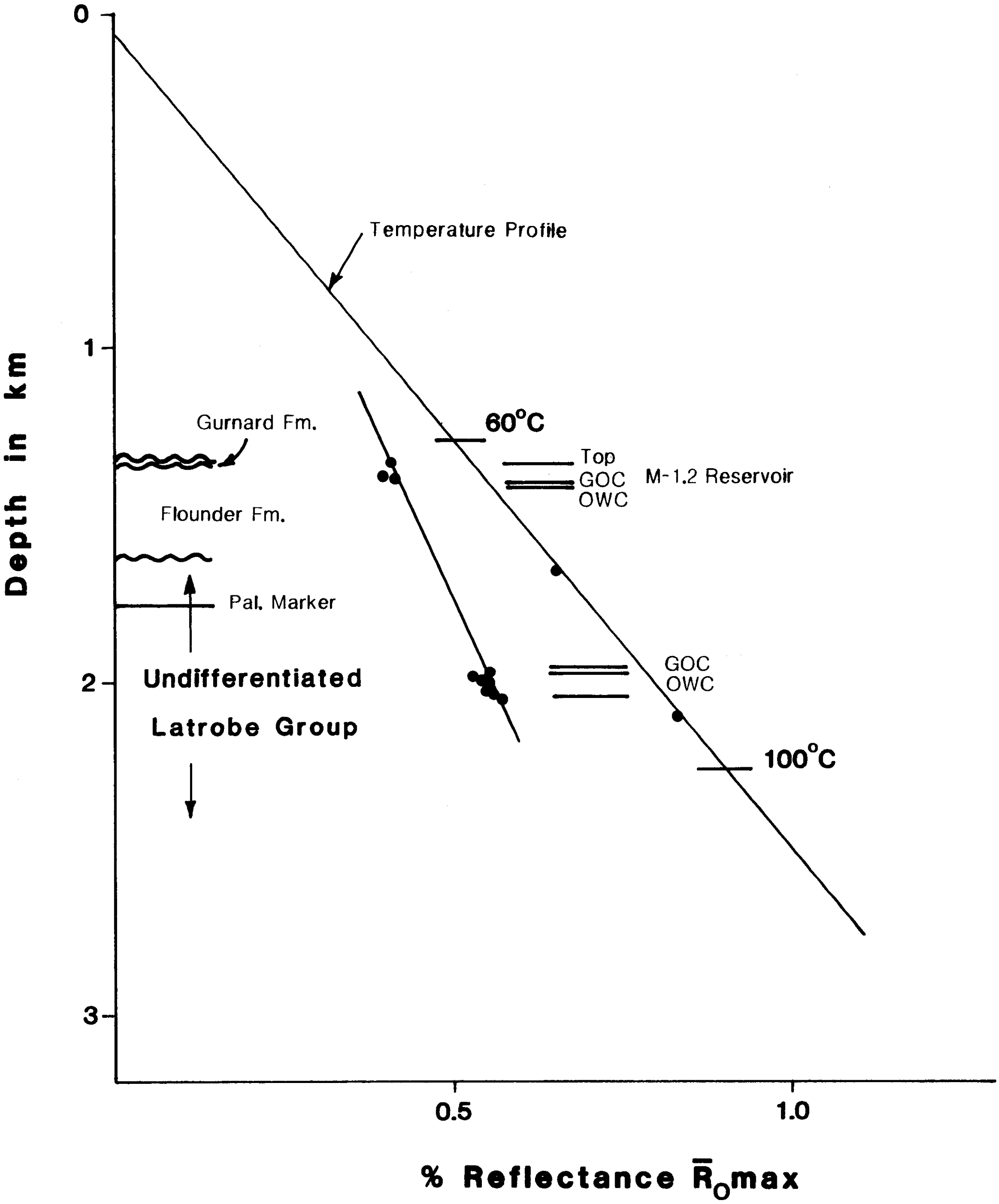

Figure 5A

TUNA No. A-5

Reflectance Profile T-1 Reservoir

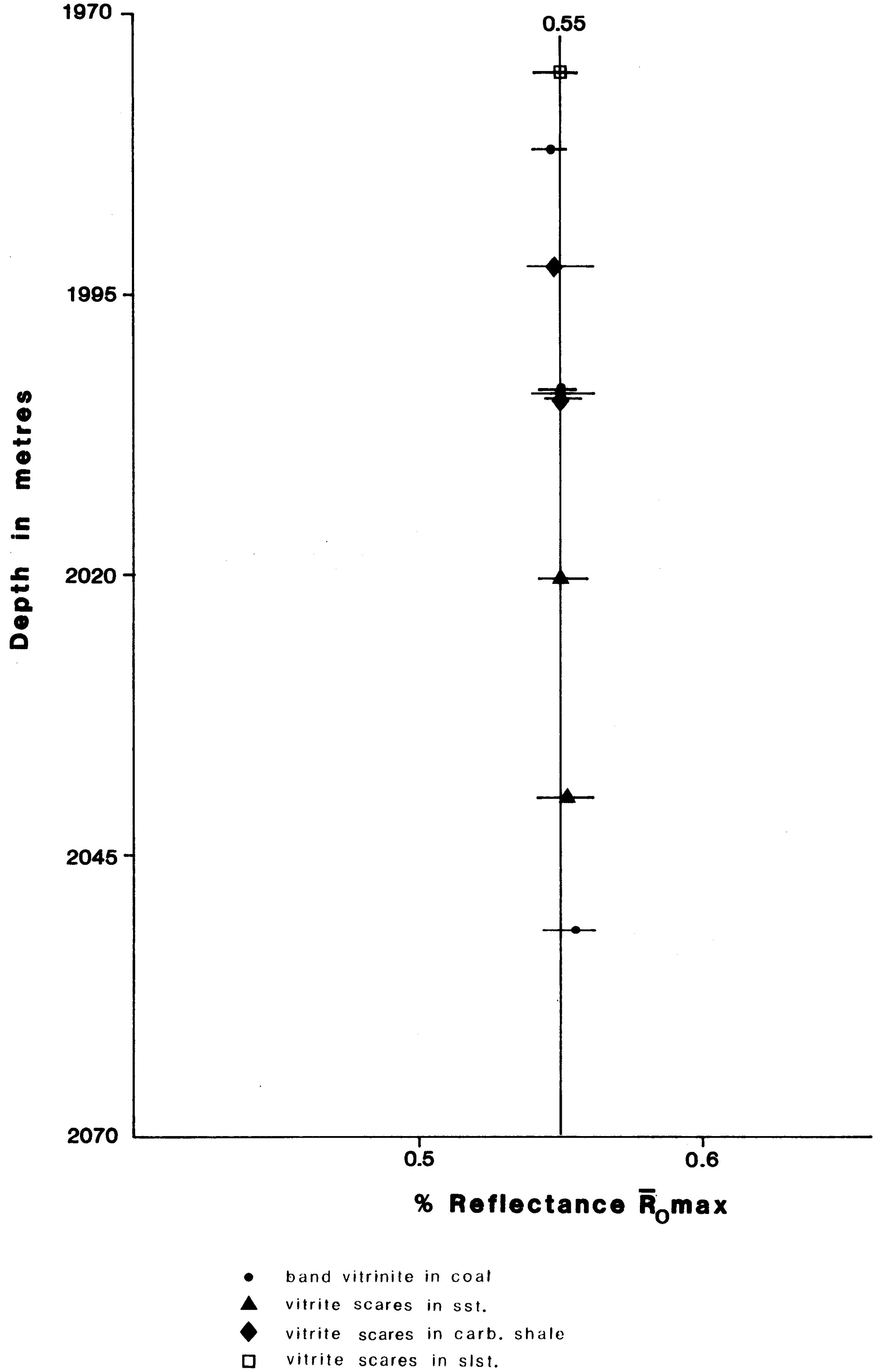

Figure 5B

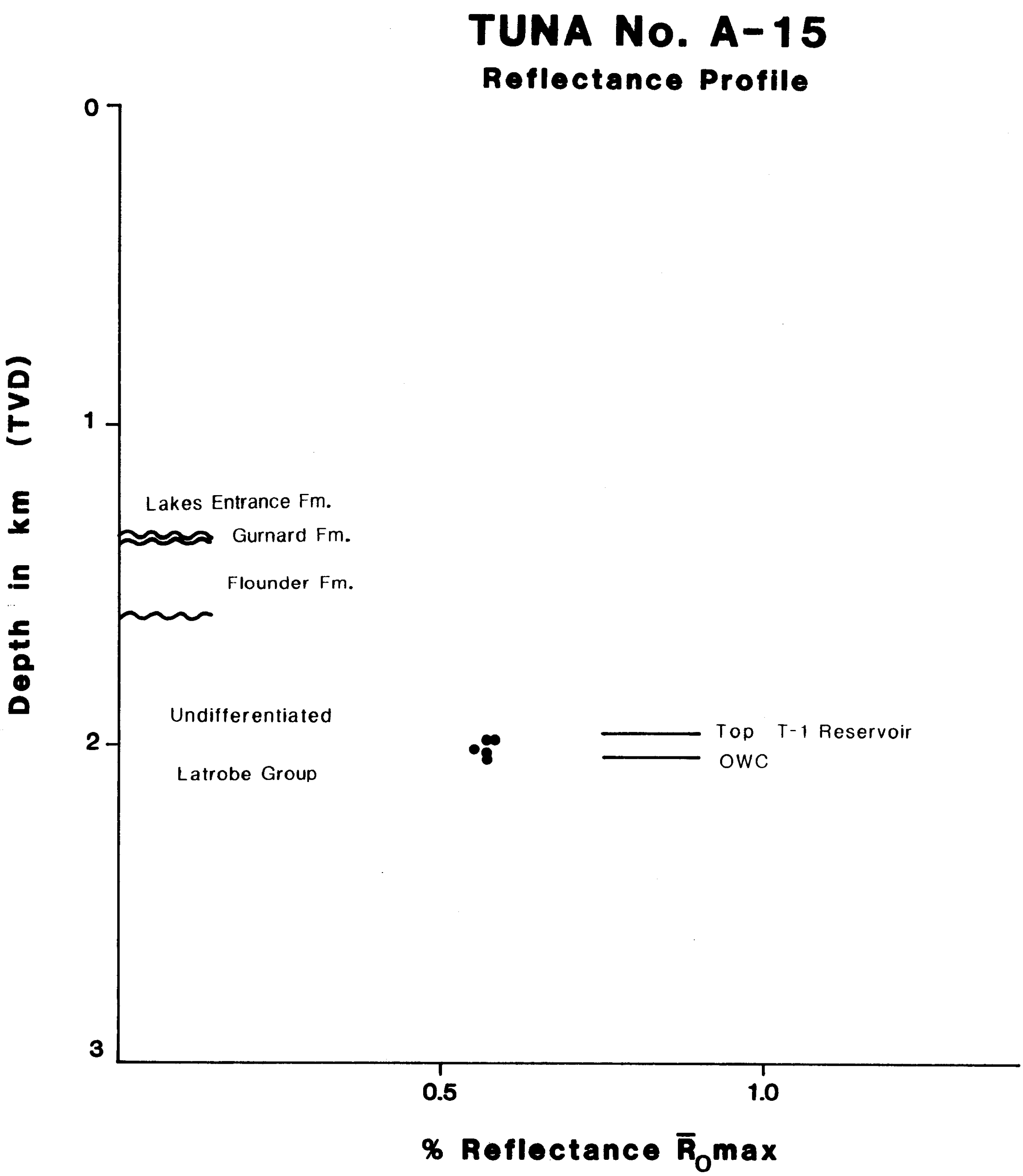
TUNA No. A-15
Reflectance Profile
0
1
2
3
Depth in km (TVD)
Lakes Entrance Fm.
Gurnard Fm.
Flounder Fm.
Undifferentiated
Latrobe Group
Top T-1 Reservoir
OWC
0.5
1.0
% Reflectance $\bar{R}_o$max

Figure 6A

TUNA No. A-15

Reflectance Profile T-1 Reservoir

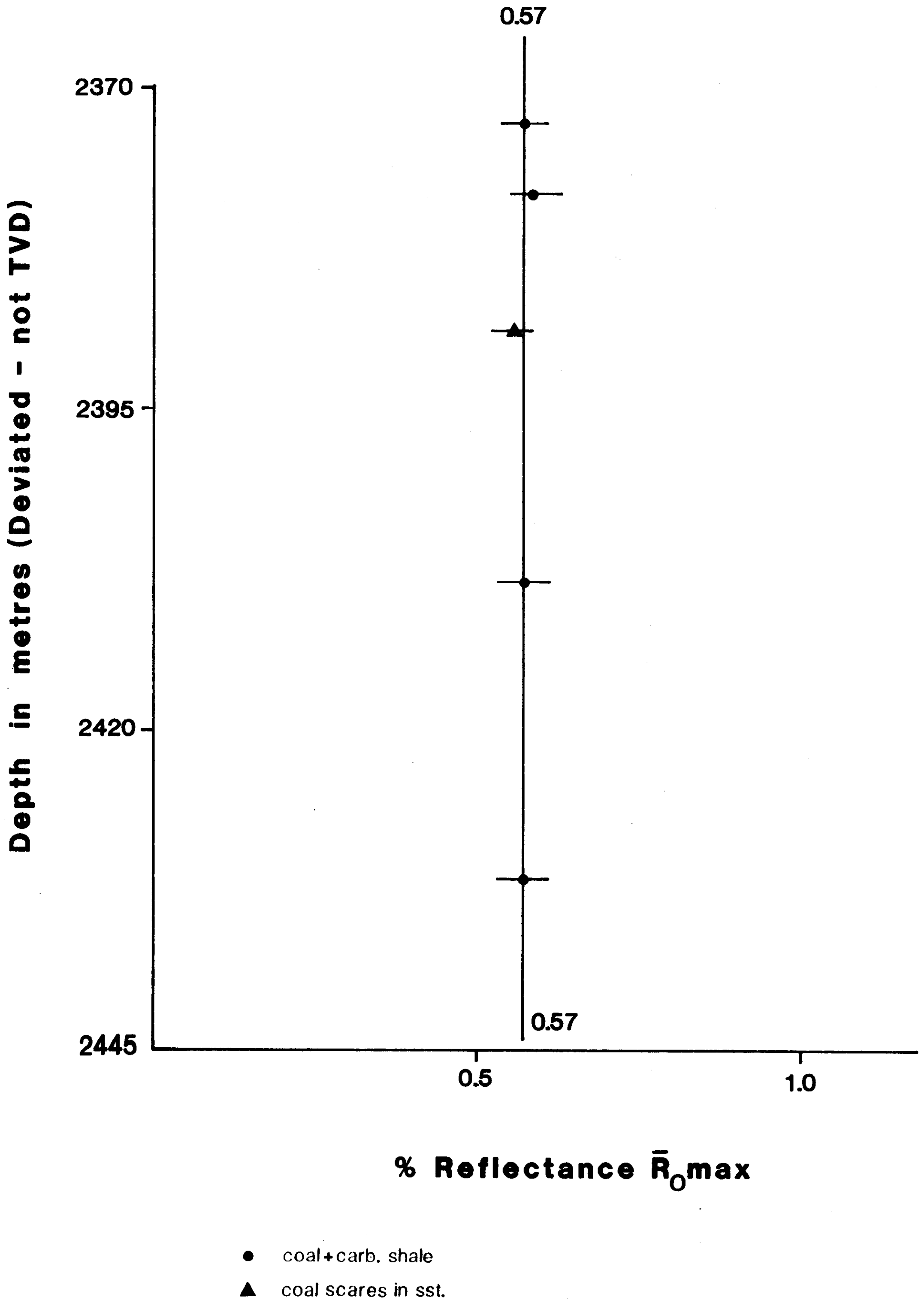

Figure 6B

Cook's measurements were made 3 years after the Tuna-1 well was drilled (1968), Smith's 8 years after drilling, and those of the present study 11 years subsequent to drilling. In order to establish better control with respect to the problem of shelf-life, samples from the M-1.2 and T-1 reservoirs in the recently drilled (1978) Tuna A-5 and A-15 wells were examined. Maximum elapsed time since drilling is 2 years. As shown by the reflectance profiles, the recent samples do not show lower reflectances — a fact which suggests only a slight contribution (if any) from the effects of shelf-life to the problem of lower reflectances in the earlier generated data.

It has also been suggested that the change in wavelength of the reflectance measurement standard from 525nm to 546nm and the change in the refractive index standard (1.515 or 1.518) between 1971 and 1976 may also have contributed to the increase in reflectance of samples from Tuna-1 measured more recently. Consideration of the work of Jakeman (1973) on the dispersion of the optical properties of vitrinite suggests that a shift in wavelength from 525nm to 546nm combined with the change in refraction index is likely to be associated with a negligible net change.

Sample variation (i.e. variation of R_0 with lithology) and operator bias may also have contributed to the differences between the results but this explanation seems unlikely given the occurrence of prominent layers of vitrinite in most of the samples examined. The occurrence in this study of several results of lower reflectance (about 0.32%R_0) in the M-1.2 reservoir from Tuna-2 suggests that sample variation is inherently more likely as a cause of variation in results.

The repeated upgrading of the instrumentation and the quality of the standards used for reflectance measurements over the period 1971 to 1979 (e.g. introduction of the MPV1 photometer in 1972, and synthetic spinel and garnet standards in 1979) revealed the slightly inferior performance of the equipment and glass standards used previously. Again, this may account for some systematic differences. No significant/systematic operator bias is shown in results for all four analysts using equipment in its present configuration, although variation may occur with individual samples (see below).

Below the T-1 reservoir, results are equally variable but are more obviously related to sample quality — e.g. some cuttings samples (particularly at 1588m, 3003m, 3213m) examined by A.J. Kantsler show evidence of heat alteration from high-temperature drying and yield higher reflectance results. The very tight carbonaceous, fine silty sandstone at 3516.2m is also associated with high vitrinite reflectance as is the carbonaceous shale at

3325.9m examined by both G.C. Smith and A.J. Kantsler. L.L. Ingram, in her measurement of the latter sample, obtained a significantly lower result, suggesting some operator bias in the selection of vitrinite for measurement. In this instance, the low result lies on the trend (fig. 2A) controlled by the coal-rich samples at 3539m (the base of the sampled interval). The coal-rich samples are inherently more reliable for R_o determination than fine, discrete particles of vitrinite occurring as dom in shales and fine sandstones.

Examination of all the samples and reflectance data cited in this report reveals that data generated from band vitrinite in coals and prominent scares of vitrinite in sandstones, siltstone and shales have more stable reflectance populations than the very fine particles of vitrinitic dom referred to above.

It appears, therefore, that slight variation in R_o with lithology may occur. Reflectance data from vitrinite associated with sandstones tend to be slightly less than 'average' whereas data from shales tend to be slightly more than average. However, it is equally clear that such trends are not universal and that in several cases little real variation in R_o with lithology occurs as the results remain within the experimental error of the method.

Having established reliable control points for the construction of a vitrinite reflectance profile in the M-1.2 and T-1 reservoirs, and knowing that the coals at the base of the sequence yield more consistent results than the dom in shales and sandstones above, which of the data points between the T-1 reservoir and the basal coal are the most reliable indicators of rank? The data from the interval 2660-2680m are illustrated in Figure 6. Samples varied from coarse sandstones with thin stringers of vitrinite, to coal, to carbonaceous shale devoid of macroscopically visible vitrinite. R_o data from vitrinite associated with sandstones are typically low. Those from the carbonaceous shales are generally high. Reflectance data from wide vitrite layers in coal also vary within the range 0.07% but have an obvious mean at about 0.70% and so this point is also used to construct the profile illustrated by the heavy line in Figure 2A[1].

Consideration of all the above data shows clearly that the determination of vitrinite reflectance from many samples at the same stratigraphic level is not the most effective method of obtaining data for the construction of a vitrinite reflectance profile. Rather, a large number a samples uniformly distributed throughout the section penetrated is a far more useful approach and 'noise' can be more readily averaged out.

TUNA No. 1

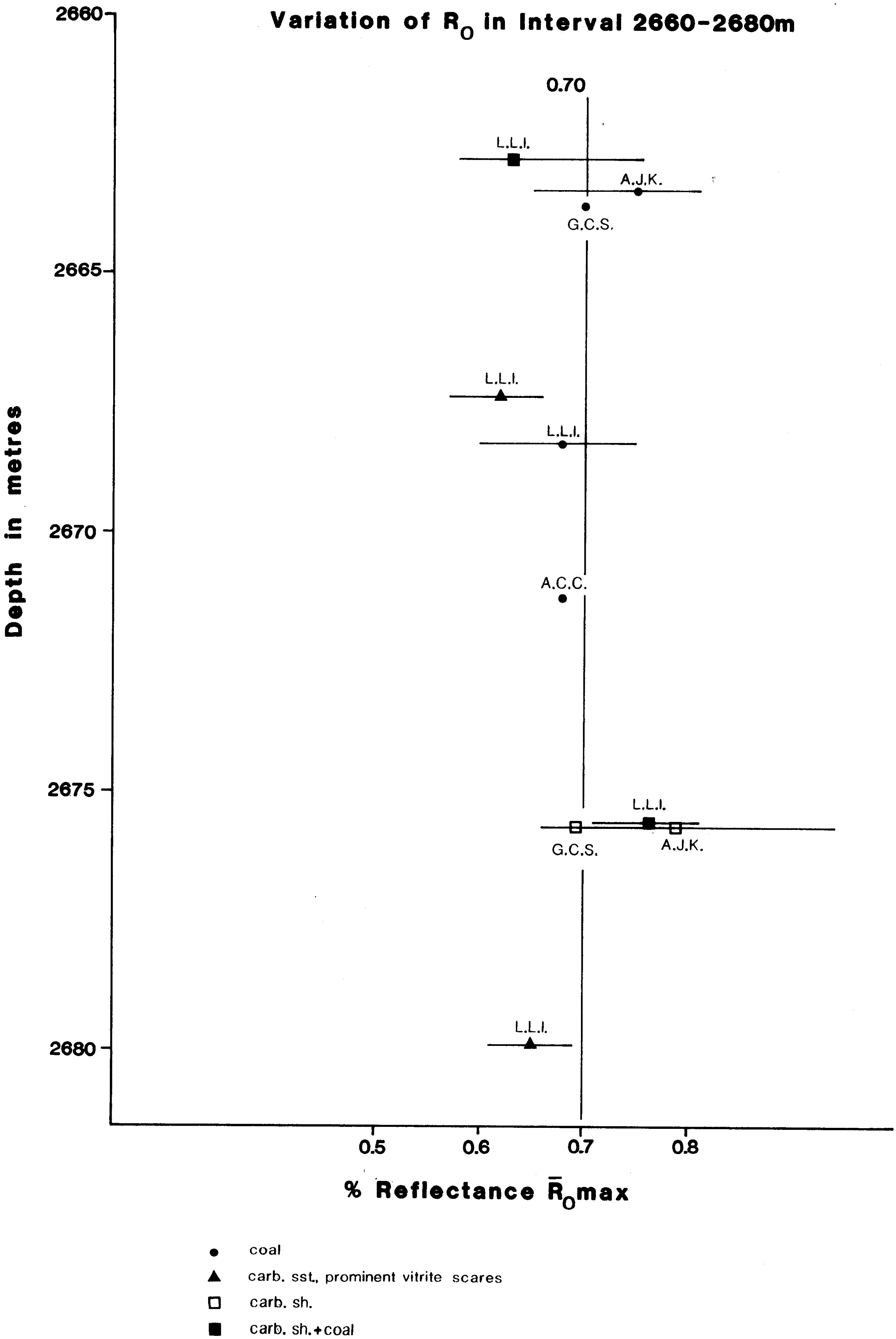

Figure 7

Figure 8

LOG PLOT VITRINITE REFLECTANCE Vs DEPTH

TUNA No.1

HYDROCARBON PRESERVATION WINDOWS

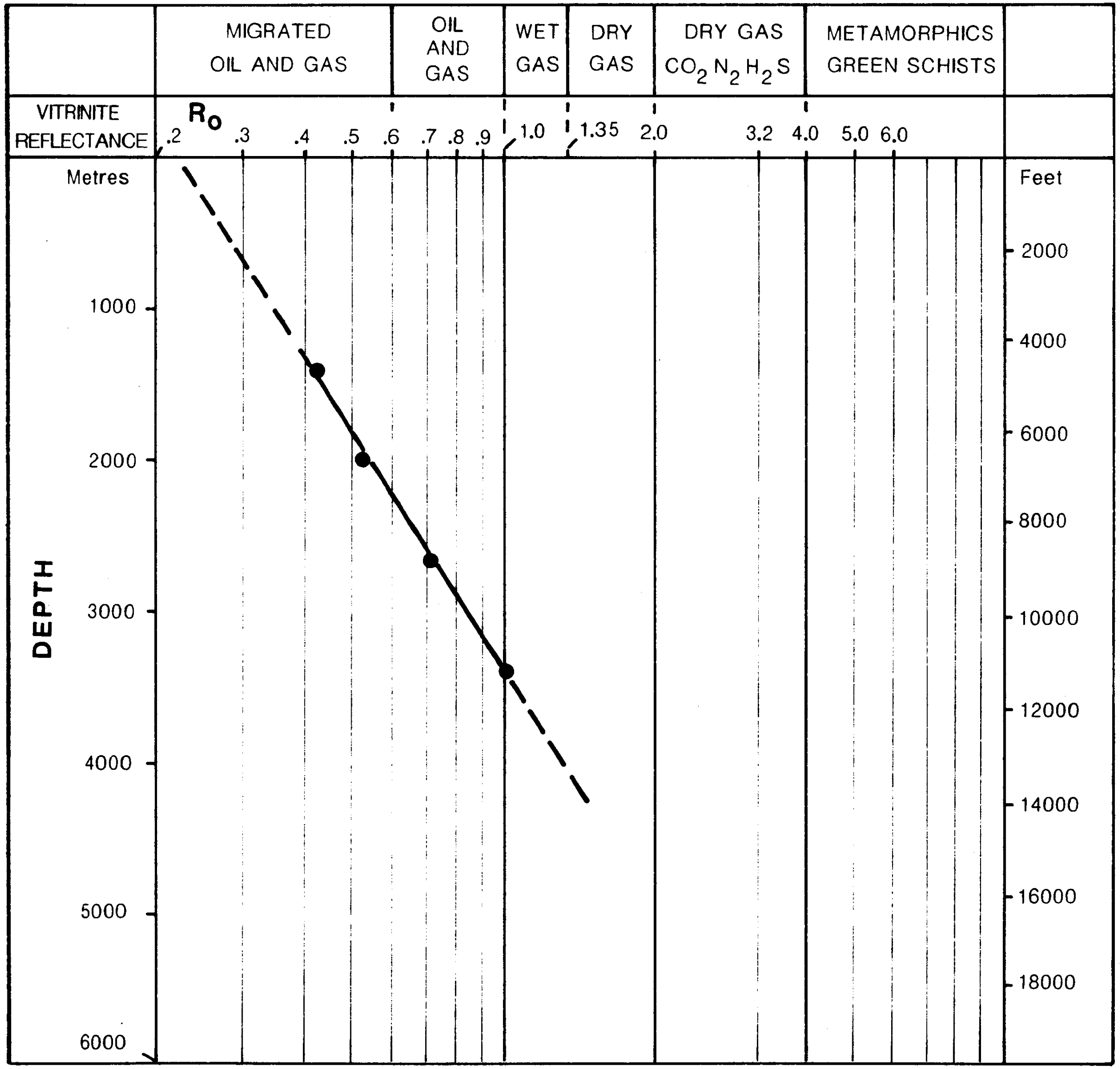

HIGHEST R_o ASSOCIATED WITH COMMERCIAL GAS 3.2

However, the Tuna-1 exercise demonstrates quite clearly the importance of having the petrologist doing the reflectance work interpret the trend of the data in the light of his observations and experience. A bald presentation of results without qualification will not be conducive towards meaningful risk analysis. At the same time, provision of basic lithologic and stratigraphic data is a great aid in allowing the petrologist to make the most judicious reflectance 'pick'.

Significance of the Reflectance Results

The vitrinite reflectance profile (Figure 2A-1) can be used to establish various hydrocarbon generation windows (Figure 8). The top of the liquid window corresponds to a vitrinite reflectance of about 0.5% R_o — i.e. about the level of the T-1 reservoir. Initial maturity occurs at 0.4% R_o in some sedimentary basins where the thermal drive is sufficiently high (e.g. the Los Angeles Basin) or where the organic matter type is suitable. This situation may obtain in the M-1.2 reservoir at Tuna-1 (where R_o = 0.40%) although it seems unlikely in view of the relatively low reservoir temperature of about 60-70°C. The probable zone of intense oil generation (0.6 to 0.9% R_o) occurs at about 2400 to 3100m but oil-generative section should occur down to an R_o of at least 1.0% (~3400m). The oil floor (1.35% R_o), as determined by both extrapolation of the curve in Figure 2A and the line drawn on the Log R_o vs depth plot (Figure 8), lies at a depth of about 4000m. Wet gas generation should span the depth interval 3000 to 4000+m.

Figure 2A also includes the 60°C, 90°C and 120°C temperature points. Together with the reflectance data, these temperature data can be used to delineate the most critical values in relation to the oil window in terms of generative temperatures for the Tuna section. Assuming limits of 60°C and 120°C and 0.5% R_o and 1.0%R_o as being the most favourable for oil generation, it appears that the section below the top of the T-1 reservoir to a depth of about 3200m is likely to be, currently, the site of most active oil generation. The data of Kantsler et al. (1978) indicate that a similar situation is likely to obtain at the nearby Marlin field. The situation off-structure is unknown. Some of the reservoired oil may, of course, have been generated in the section below 3200m earlier in the maturation history of the sequence. In view of the gas-condensate discoveries at the 16km distant Flounder Field (where the top of the Latrobe Group is more deeply buried) the general relationships described above appear to be valid and discount the need for a very deep current source of hydrocarbons as has been postulated by Shibaoka et al. (1978) and Saxby (1978) for the Kingfish field.

4. Estimates of Palaeotemperature

Estimates of palaeotemperature using the models of Karweil (1956) as modified by Bostick (1973) and Hood et al. (1975) as modified by Bostick (1979) are presented in Table 6. Isothermal estimates of temperature (as described by Kantsler et al. (1978)) for the Tuna samples are all lower than Tpres suggesting either that the Karweil/Bostick model is fundamentally wrong in its approach or that present temperatures have not acted over the entire burial history of the Tuna coal. Both causes are likely as the Karweil/Bostick model assumes rapid attainment of present temperature. As the Gippsland Basin has a long history of continuous subsidence, temperatures are not likely to have risen as fast as assumed in the model. Estimates of Tgrad based on a gradual increase in temperatures(see Kantsler et al., 1978) vary from being <Tpres to being >Tpres. The first condition is consistent with an history of an accelerating rate of subsidence. This is to be expected since the burial curve for Tuna shows a break at the top Latrobe conformity. Tgrad < Tpres indicates relatively low burial temperatures and weak coalification prior to the more rapid burial and temperature rise associated with the Late Tertiary phase of sedimentation. The lower coals, having been buried more deeply and having been more coalified prior to Latrobe unconformity time, yield by contrast, model results consistent with more rapid coalification at an early stage (i.e. Tgrad > Tpres)

Estimates of palaeotemperature for the Tuna area of the Gippsland Basin suggest an attenuating thermal regime in the early Tertiary with temperatures declining from a likely Late Cretaceous-Early Tertiary heat flow peak overprinted by a later Tertiary thermal event either associated with, or lagging behind, known late-Tertiary subsidence.

5. Source Rocks

5.1 Generalized Description of Source Rocks

5.1.1 Above the M-1.2 Reservoir

The Lakes Entrance Formation samples examined for this study are silty calcareous mudstones containing minor dom — much of it replaced by pyrite. Small amounts of dinoflagellates/acritarchs (Plate 1) and translucent vitrinite are present but appear insignificant on a % volume basis.

5.1.2 The M-1.2 Reservoir (including the Gurnard Formation)

Dom Mostly carbonaceous, silty fine sandstone with common thin laminae, stringers and small particles of vitrinite and less common layers of coal. Vitrinite dominates the dom content. Vitrinite strands and vitrodetrinite are frequently oil stained, generally 'scruffy' and difficult to measure, and much of the vitrinite is so thin as to appear translucent in reflected light. Vitrinite is commonly associated with framboidal pyrite. Many vitrinite laminae are mantled by cutinite (Plates 2 and 3) and cutinite is probably the most common form of exinite. Resinite is also common and typically is associated with vitrinite. Sporinite and liptodetrinite are less common and are scattered more widely throughout the sediment matrix. Intertinite is rare but may locally be associated with vitrinite.

Coal Some samples contain discrete layers of coal, most of which are comprised entirely of texto-ulminite. Eu-ulminite is less common. Minor phlobaphinite and corpohuminite-rich layers (Plate 4). Oil-staining of polished surfaces of vitrinite is common. Exinite is present chiefly as resinite infilling cell lumens, or as fluorinite. Cutinite is rare and inertinite is not present.

5.1.3 Between the M-1.2 and T-1 Reservoirs

Coal Many coal horizons were sampled over this depth interval. All coals are vitrinite-rich with subordinate quantities of exinite and inertinite. Vitrite, clarite and duroclarite are the principal microlithotypes. Fractures in some coal grains are associated with exudations of a pale green fluorescing oil which etches the surface of the vitrinite in the vicinity of the fracture (Plates 5 and 6). Exsudatinite is commonly seen "streaming" from other exinite macerals such as resinite. Pyrite framboids are common throughout.

i) Vitrite is generally comprised of thin and thick layers of telocollinite/eu-ulminite and less common levigelinite. Some layers are rich in corpocollinite and are frequently associated with porigelinite-filled cell lumens. Elsewhere, minor infilling of cell lumens with resinite occurs.

ii) Clarite consists of the following assemblages:

corpocollinite/tellocollinite + suberinite (Plate 7).

Suberinite occurs either in well-preserved tissue or in dense laminar masses of collapsed suberin-rich tissue;

telocollinite + resinite where resin impregnated cell lumens or corpocollinite plus leaf resins occur in leaf remains; or

desmocollinite (densinite) + sporinite ± liptodetrinite ± suberinite (Plates 8 and 9) with abundant exinite widely dispersed throughout the desmocollinite groundmass.

Desmocollinite reflectance is commonly <0.25% possibly because of the widespread occurrence of resinite, suberinite, fluorinite and liptodetrinite (c.f. the intermaceral effects described by Hutton and Cook, 1980).

iii) Duroclarite consists of:

desmocollinite + inertodetrinite + sporinite + liptodetrinite + semifusinite. Thin bands, pods and lenses of semifusinite and fusinite, frequently with cellular structure intact. Minor, thin vitrite bands. Porigelinite or micrinite often infill intact cell lumens in vitrinite. Micrinite well developed locally. Minor sclerotinite and macrinite. Rare Botryococcus-related alginite. Macrinite and inertodetrinite abundant locally.

telocollinite + semifusinite + desmocollinite ± cutinite ± resinite ± sporinite ± fluorinite ± sclerotinite. Coal regularly interlayered.

Dom Most samples are carbonaceous shale and carbonaceous mudstone but some siltstones and sandstones were also sampled.

Shale and mudstone grains contain from 1% to 50% dom chiefly as laminae or stringers of vitrinite and as very common vitrodetrinite (or attrinite). Frequently, the vitrinite scares or stringers are characterised by a symmetrical arrangement of suberinite and corpocollinite-rich tissue. Locally, this suberinite-rich tissue collapses to form dense, tightly packed suberinite laminae. Large lenses of semifusinite and fusinite are commonly associated with the large vitrite layers. Inertodetrinite is scattered throughout. Exinite is usually abundant (10% to 40% in some layers) and is mostly found as sporinite and liptodetrinite (Plates 10 and 11) although cutinite, resinite, fluorinite and leaf resinite are all common. Cutinite and leaf resinite dominate the exinite content of some samples.

Siltstones and sandy siltstones contain common vitrinite laminae (up to 20% of some grains) but typically are not as rich in exinite as the shales. Cutinite and sporinite are the most common forms of exinite although some cuttings grains containing abundant alginite-B (see Hutton et al., 1980) are present in some samples (e.g. cuttings at 5230' in Tuna-1 — Plates 12 and 13).

Sandstones are mostly clean and barren of organic matter. Minor interstitial clay containing exinite but vitrinite fragments are rare. Some grains show a diffuse bright green or yellow fluorescence along inter-grain boundaries, which could be adsorbed oil.

5.1.4 The T-1 Reservoir

Coal Many layers of coal of varying thickness occur in the core samples taken from the T-1 reservoir. Again, the coals are vitrinite-rich and vitrite is by far the most common microlithotype, completely dominating most samples. However, minor exinite and inertinite are present in less common clarite and duroclarite-rich layers. Fine pyrite is present throughout and some lenses are heavily pyritised. Carbonate nodules are common and many have pyrite cores.

i) Vitrite layers are comprised almost entirely of eu-ulminite/telocollinite with cell structure still visible. Some texto-ulminite with phlobaphinite (Plates 14 and 15), and corpocollinite associated with either suberinite (Plate 16) or porigelinite (Plate 17). Many vitrite layers are associated either with resin-filled or resin-impregnated cell lumens — the resinite having a wide range of physical properties (Plates 18, 19 and 20). In some cases, resin invades the cell walls in what appears to be 'wound' tissue (Plate 21). In addition, many vitrite layers show pronounced oil staining with pale-green fluorescing oil infilling either intercellular spaces or partly vacant cell lumens (Plates 22 to 25). In other cases, oil appears to be emanating from, rather than being adsorbed into, porous corpocollinite (Plate 26). Oil released during the polishing process commonly stains polished surfaces (Plate 27 and 28).

ii) Clarite occurs as thin layers interlaminated with vitrite being comprised of:

telocollinite/corpocollinite + resinite + fluorinite;

telocollinite/corpocollinite + suberinite; or

desmocollinite ± suberinite ± resinite ± cutinite ± sporinite ± liptodetrinite.

Exinite is generally of small particle size and is scattered widely throughout these layers. Many vitrinites are oil-stained.

iii) Trimacerite occurs mostly as duroclarite but some clarodurite is also present.

Duroclarites are comprised of thin bands, lenses and granular fragments of semifusinite together with inertodetrinite and a variety of exinites (sporinite, cutinite, liptodetrinite, leaf resins, resinite and some fluorinite) in a matrix of suberinite-rich desmocollinite (Plates 29 and 30) accompanied by mineral matter such as quartz and clay (Plate 31).

Clarodurites are less common overall but achieve local predominance. Bands and lenses of fusinite and semifusinite dominate and are separated by thin interlaminations of desmocollinite containing common exinite as described above. Elsewhere, inertodetrinite and granular fragments of semifusinite dominate and these layers are associated with abundant exinite, minor interstitial desmocollinite, and vitrodetrinite (Plates 32 and 33).

iv) Inertite comprises large layers and lenses of fusinite occurring in small amounts in some samples. Like the texto-ulminites and eu-ulminites observed in some vitrite layers, the inertite shows a surprising lack of physical maturity (i.e. degree of compression) for coals buried to a depth of 2km. Most cell structures remain visible (Plates 34 and 35).

Dom The core samples from the T-1 reservoir commonly comprise either sandstone, silty sandstone, sandy siltstone or carbonaceous silty shales and shale.

The dom content of the shales is highly variable (ranging from <1% to >50%). Gradations into shaley coal occur (Plate 36). Vitrinite is common to very common, typically occurring in thin layers, in stringers, as granular fragments or as vitrodetrinite. Suberinite is common in the thick vitrinite layers. Many vitrinite layers are oil stained. Exinite is common throughout (5 to 10%) and is comprised largely of sporinite, cutinite and liptodetrinite (Plates 37 and 38) although resinite and fluorinite are common locally. Cutinite frequently mantles vitrinite scares associated with leaf resins. Inertinite is common as thin stringers, lenses and grains of fusinite and semifusinite and as disseminated inertodetrinite.

Sandstone Dom is comprised mostly of bands, lenses and thin stringers of vitrinite (either eu- or texto-ulminite) with rare suberinite-rich tissue. Some granular vitrodetrinite. Many vitrite layers are completely impregnated by resinite (both cell walls and lumens). Inertinite is common and is found either as lenses of semifusinite associated with vitrite layers, as discretely occurring lenses and fragments of fusinite and semifusinite, or as inertodetrinite. Apart from prominent scares of vitrinite and inertinite, dom is rare and only minor amounts of exinite (cutinite and liptodetrinite) occur interstitially to quartz grains. Most exinite is present in vitrite layers where cutinite, leaf resins and liptodetrinite frequently agglomerate to form clarite.

5.1.5 Below the T-1 Reservoir

Coal To a depth of 2675m (in the Tuna-1 well), most coal grains are comprised of compressed, physically mature, massive vitrite (usually telocollinite) and contain few inclusions apart from minor amounts of suberinite and resinite, the latter either infilling cell lumens or occupying intercellular spaces. The vitrinite is commonly oil stained. Below 2675m most cores were cut in carbonaceous shale and the only other very coaly samples occur at a depth of 3539-40m (Tuna-1). These lower coals contain a much higher proportion of inertinite but are described under dom as they usually occur as prominent scares in sandstone.

Dom Variable amounts of dom as described previously but with common exinite and inertinite.

Shales at the base of the sampled section contain relatively small amounts of dom (<2%) made up largely of inertodetrinite and oxidised vitrinite with a small population of finely degraded exinite. However, exinite fluorescence colours remain strong. Carbonate nodules common. Silty shales are dominated by oxidised vitrinite and inertodetrinite and also contain common, but very fine, exinite comprising cutinite, sporinite, liptodetrinite, fluorinite and trace alginite.

Siltstones Dom common to abundant. Mostly vitrinite, frequently accompanied by particles of cutinite and inertodetrinite. Vitrinite is present mostly as thin bands, lenses and stringers, frequently associated with cutinite. Exinite content varies from <1% to >10% and is comprised mostly of sporinite, cutinite, leaf resin, fluorinite and trace *Botryococcus*-related alginite. Many layers of well crystallised carbonate — ?dolomite.

Sandstone Thin stringers and fragments of vitrinite, together with bands of inertinite are common. Fragmented inertinite is frequently found in intergranular spaces (i.e. between quartz grains). Clean quartz sandstones are barren. Exinite content is low overall but cutinite and sporinite often occur in the matrix of 'dirty' sandstones. Silty sandstones contain up to 5% dom as fragmented inertodetrinite and as oxidised vitrinite. Many medium to coarse grained sandstones also have a well developed carbonate matrix which may cause loss of porosity.

Carbonate Carbonates are common in sediments below the T-1 reservoir, occurring as large nodules in shales and siltstones, as discrete layers, or as a matrix in many sandstones and siltstones. Dom content is low and is generally restricted to common inclusions of inertodetrinite, fragmented semifusinite or oxidised vitrinite. Some samples (e.g. 2338m, Tuna-1) contain large quantities of asphaltic pyrobitumen infilling intergranular spaces (Plate 39).

Below the T-1 reservoir mineral/matrix fluorescence (Plate 40) becomes more common and is most obvious at high ranks (>1%R_o) where it may relate to enhanced adsorption of oils by clay.

5.2 Variation in Maceral Composition of Coals and DOM

5.2.1 Above the M-1.2 Reservoir

Dom content (Table 7) is low in the calcareous mudstone of the Lakes Entrance Formation above the M-1.2 reservoir. The count of the single sample reported is verified by independent examination of other samples from the same core by two other operators.

5.2.2 The M-1.2 Reservoir

The four coals sampled are comprised almost entirely of vitrinite with only minor exinite.

Dom content as shown by Tables 8.1, 8.2, 8.3 and 8.4 varies widely in these silty sandstones and sandy siltstones and ranges from 3% to 28%. Dom is comprised largely of vitrinite with subordinate exinite and only rare inertinite (see Table 12 for averages over entire field). Dom content therefore reflects the composition of the accompanying coals. Vitrinite contents range from 1% to 23%, exinite from 1% to 6%, and inertinite trace to 2%.

Figures 9.1 and 9.2 show a general trend for vitrinite and exinite contents to decrease with depth in the M-1.2 reservoir and for a broad sympathetic relationship between vitrinite content and exinite content.

5.2.3 Between the M-1.2 and T-1 Reservoirs

The six coals sampled in this interval from the Tuna-1 well are all vitrinite-rich (Table 9) and generally contain little or no exinite or inertinite until they approach the T-1 reservoir (Table 9, Figure 10.1). The two coals immediately above the T-1 reservoir contain large amounts of exinite (8 to 16%) and substantial inertinite (up to 8%).

Dom content in the carbonaceous shales and mudstones accompanying the coals (Table 9) is high and ranges from 12% to 41% (average 30%). Vitrinite again dominates, but is accompanied by a large population of exinite with only minor inertinite. Figure 10.2 is inconclusive because of the dearth of data, but a sympathetic relationship between vitrinite content and exinite content is again obvious in the lowermost sample.

TUNA No.1

Variation in Dom with depth in the M-1.2 Reservoir

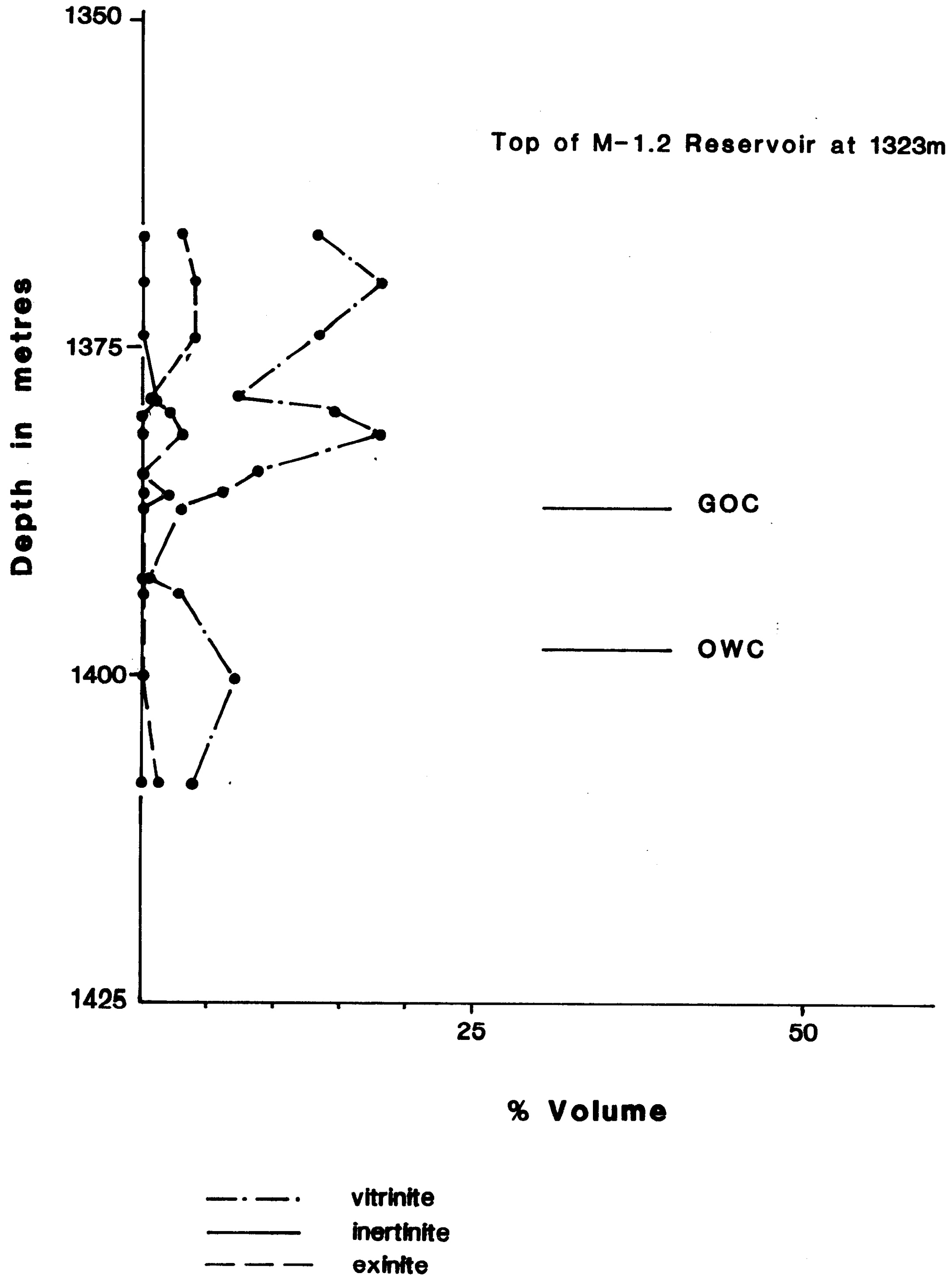

Figure 9.1

TUNA NO.2

Variation in Dom with depth in M-1.2 Reservoir

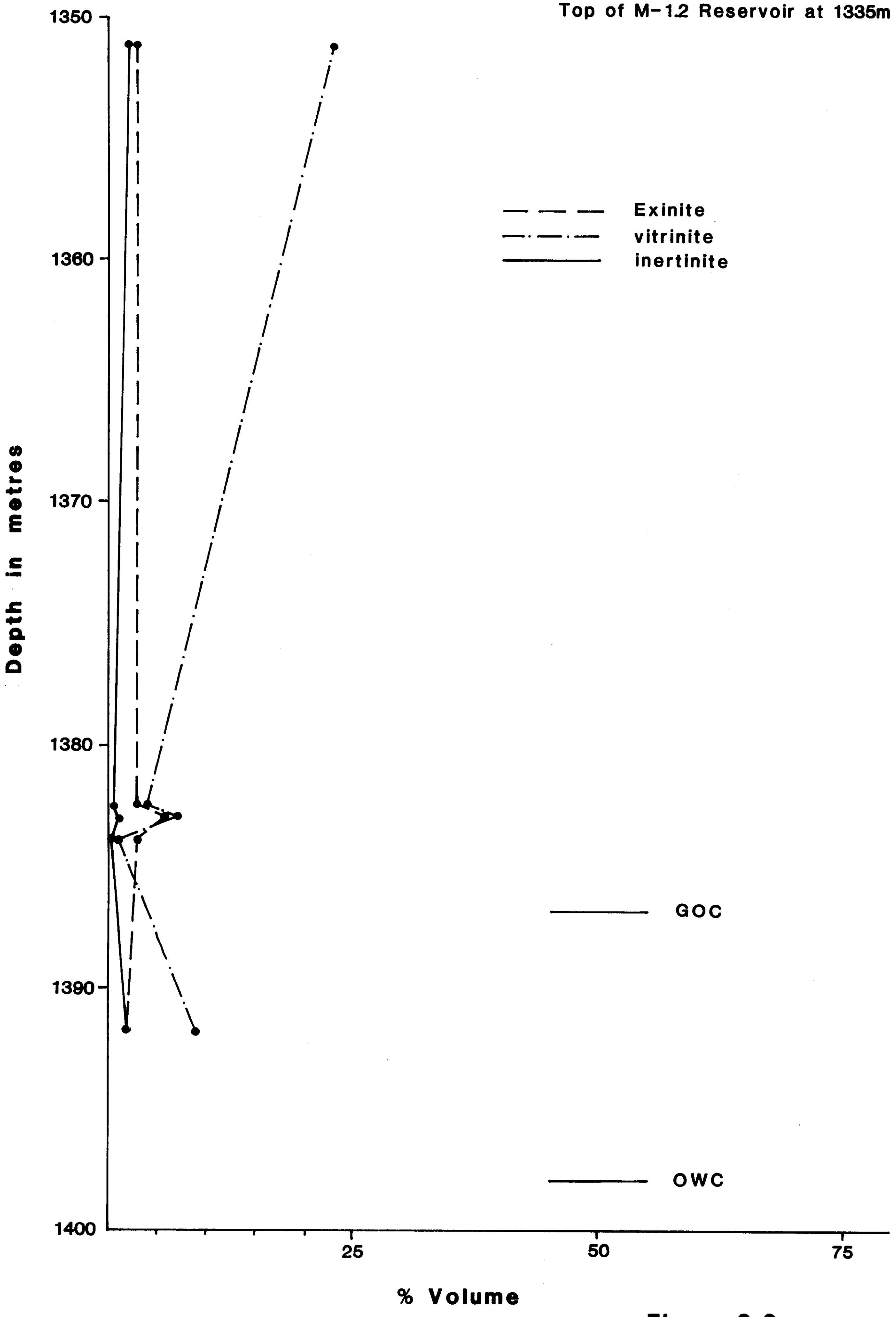

Figure 9.2

TUNA No.1

Variation in Maceral Composition of Coals between the M-1.2 and T-1 Reservoirs

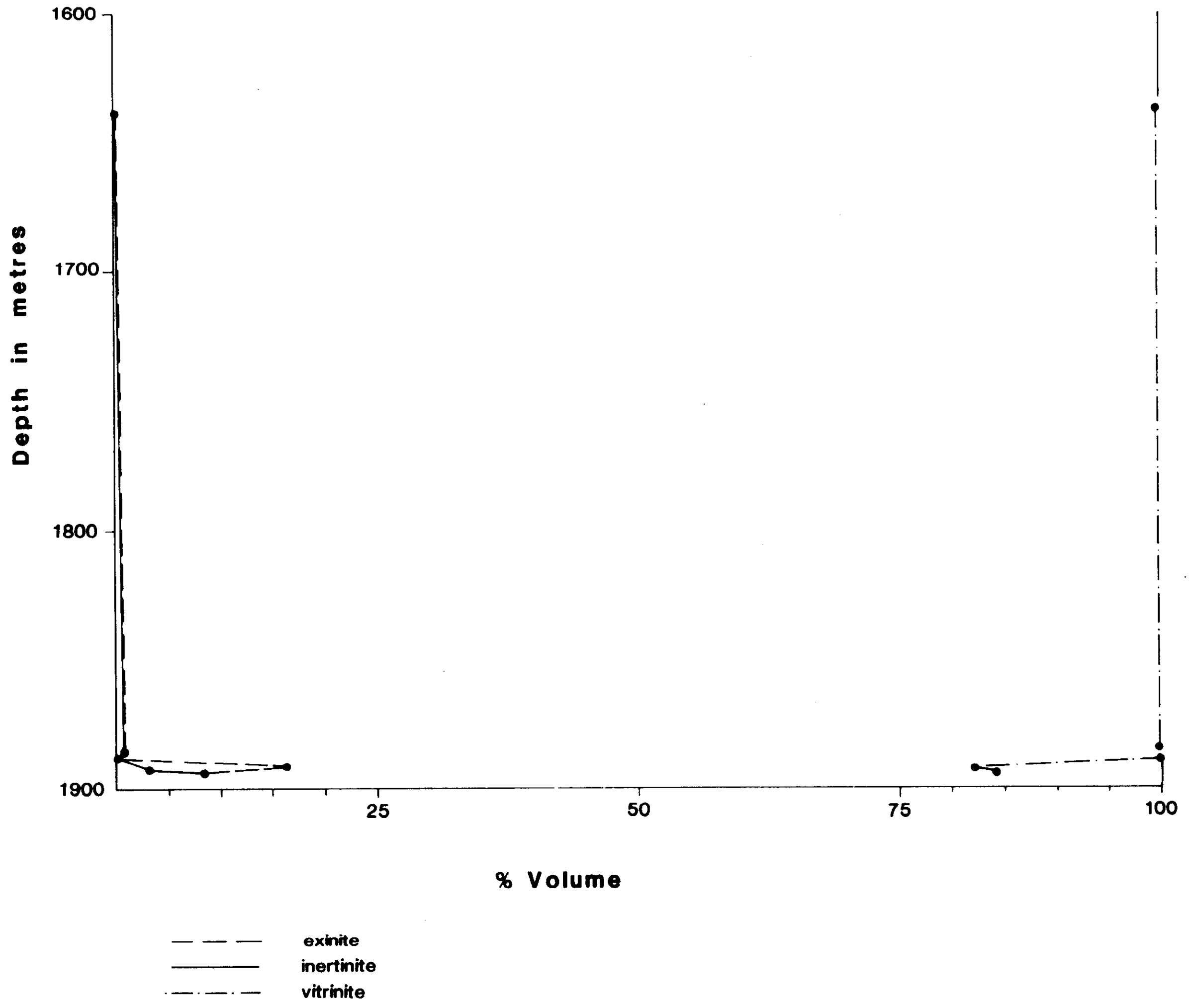

Figure 10.1

TUNA No.1

Variation in Maceral Composition of Dom between the M-1.2 and T-1 Reservoirs

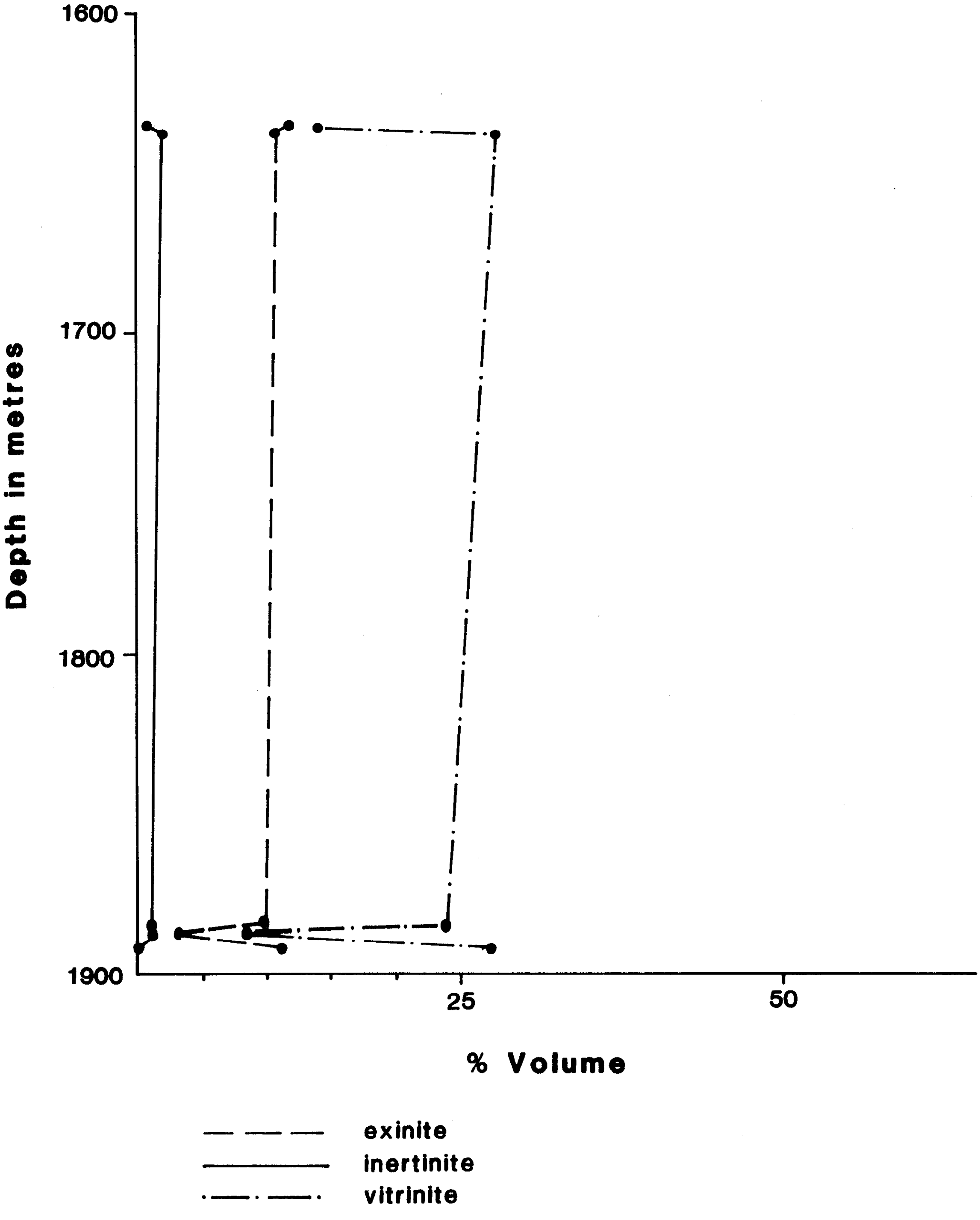

Figure 10.2

5.2.4 The T-1 Reservoir

Forty-three samples of coal from the T-1 reservoir were examined. Tables 10.1, .2, .3, .4, and .5 show that the coals are vitrinite-rich vitrites, clarites and duroclarites. Inertinite is absent in two-thirds of the samples but may comprise up to 14% of some other samples. On the other hand, exinite is found in two-thirds of the samples in amounts up to 15% by volume. Average maceral composition is shown in Table 12. Figures 11.1, .2 and .3 show that there is little systematic variation in maceral composition of coal, either laterally or with depth, in the Tuna 1, 2 and 3 wells but that there is a trend for high exinite contents to correlate with high vitrinite contents.

Abundant dom (average 25%, range 1% to 57%) is present in most of the forty-six samples of shale and sandstone taken from the stratigraphic interval of the T-1 reservoir. Vitrinite is invariably the dominant constituent (1% to 47%) and only in one instance is it exceeded by inertinite (1% to 17%). Exinite is ubiquitous (1% to 12%). Figures 12.1, 12.2, and 12.3 show that there is no systematic variation in maceral composition with depth in the reservoir but that there is a sympathetic relationship between % vitrinite and % exinite — a trend also noticed in the interval between the M-1.2 and T-1 reservoirs. In general, the shales contain more dom than the sandstones but the 'dirty' sandstones are not to be ignored as source rocks — frequently containing more than 10% organic matter as vitrinite and locally, as abundant exinite.

5.2.5 Below the T-1 Reservoir

Data below the T-1 reservoir are sparse and widely separated but the trend again (Tables 11.1 and 11.2) is for the 7 coals to be rich in vitrinite, poor in inertinite and to contain a small but pervasive content of exinite. Only one coal sample contained less than 95% vitrinite and it is this sample which contains the only significant inertinite content (6%). This high inertinite content is also associated with a high exinite content — a feature noted previously in coal samples from the T-1 reservoir.

Dom content below the T-1 reservoir is variable between 10% and 53% by volume (average 15%) but unlike the horizons above is not always dominated by vitrinite (Figure 13). Fig. 13 reveals no systematic variation in dom content with depth but does show that the inertinite content is more abundant and more pervasive. Tables 11.1 and 11.2 (and the samples themselves) indicate that this inertinite content is preferentially associated with the sandstones — a feature not evident in samples from, or above, the T-1 reservoir. Furthermore, the sympathetic relationship between exinite content and inertinite content noted previously no longer holds.

5.3 Discussion of Maceral Analyses

Substantial amounts of organic matter are present in the sampled section and relatively few samples contain <5% dom — most containing >10% dom.

Both the coals and dom are vitrinite-rich and, below the top of the T-1 reservoir, contain an appreciable amount of higher plant derived inertinite. Exinite is common to abundant throughout the sampled intervals. Table 12, which represents average maceral compositions at various levels in the Tuna Field, demonstrates these relationships and shows how the dom is likely to be perhydrous throughout the section because of the dominance of exinite over inertinite. Similarly, most coals are likely to be perhydrous to orthohydrous because of the presence of common suberinite (a maceral with chemical and optical properties are midway between those of the exinite macerals sporinite and cutinite and vitrinite). Exinite, on a % volume basis, ranges from trace to 12% in dom and trace to 16% in coal layers not including suberinite which often represents 5% to 20% of the vitrinite reported in Tables 7 to 11. However, below about 2500m, suberinite is no longer a very obvious constituent of the coals and vitrite scares. Much of the desmocollinite-like vitrinite is associated with low vitrinite reflectance (e.g. <0.25% where telovitrinite reflectance >0.50%) and a prominent dull orange-brown fluorescence, and is presumed to have source potential for liquids. The cause of this lower reflectance appears to be incorporation of resinite or suberinite into the vitrinite matrix. As well, micrinite, in its earliest stages of formation, is present in the vitrinite groundmass of many duroclarites and suggests partial condensation and disproportionation of resinous compounds formerly present in either cell lumens or cell walls.

The most common forms of exinite are sporinite, cutinite and liptodetrinite. Fluorescence colours and intensities show a progression in colour from yellow through orange to brown and a decrease in intensity from bright to dull over the rank range spanned by the Tuna-1 samples (e.g. sporinite at 1390m has a bright yellow fluorescence whereas at 3540m is dull orange/brown). Exsudatinite, although present in only minor amounts, occurs in many of the lower rank samples (down to a vitrinite reflectance of 0.4%) and indicates

TUNA No.1

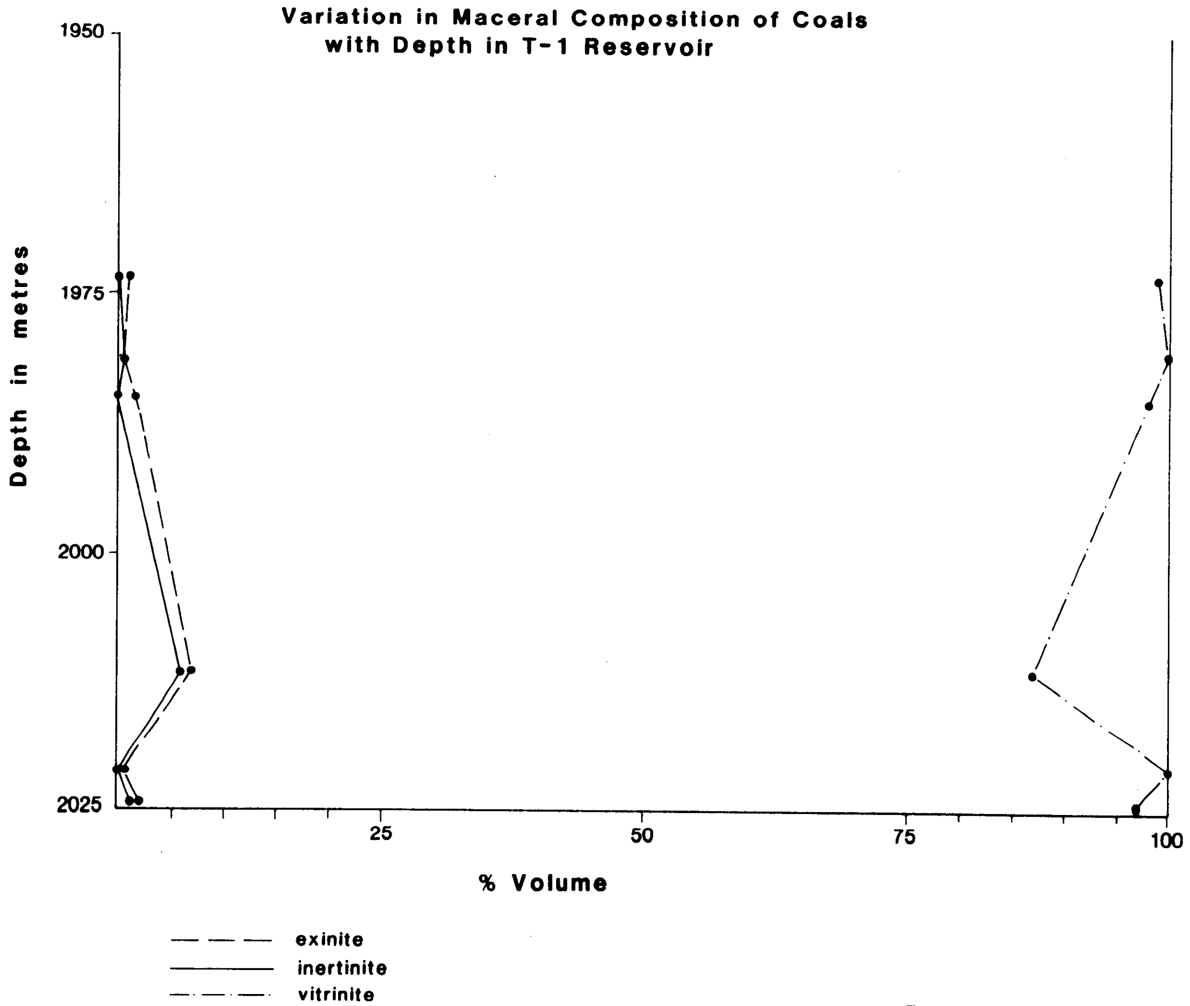

Figure 11.1

TUNA No.2

Variation in Maceral Composition of Coals with depth T-1 Reservoir

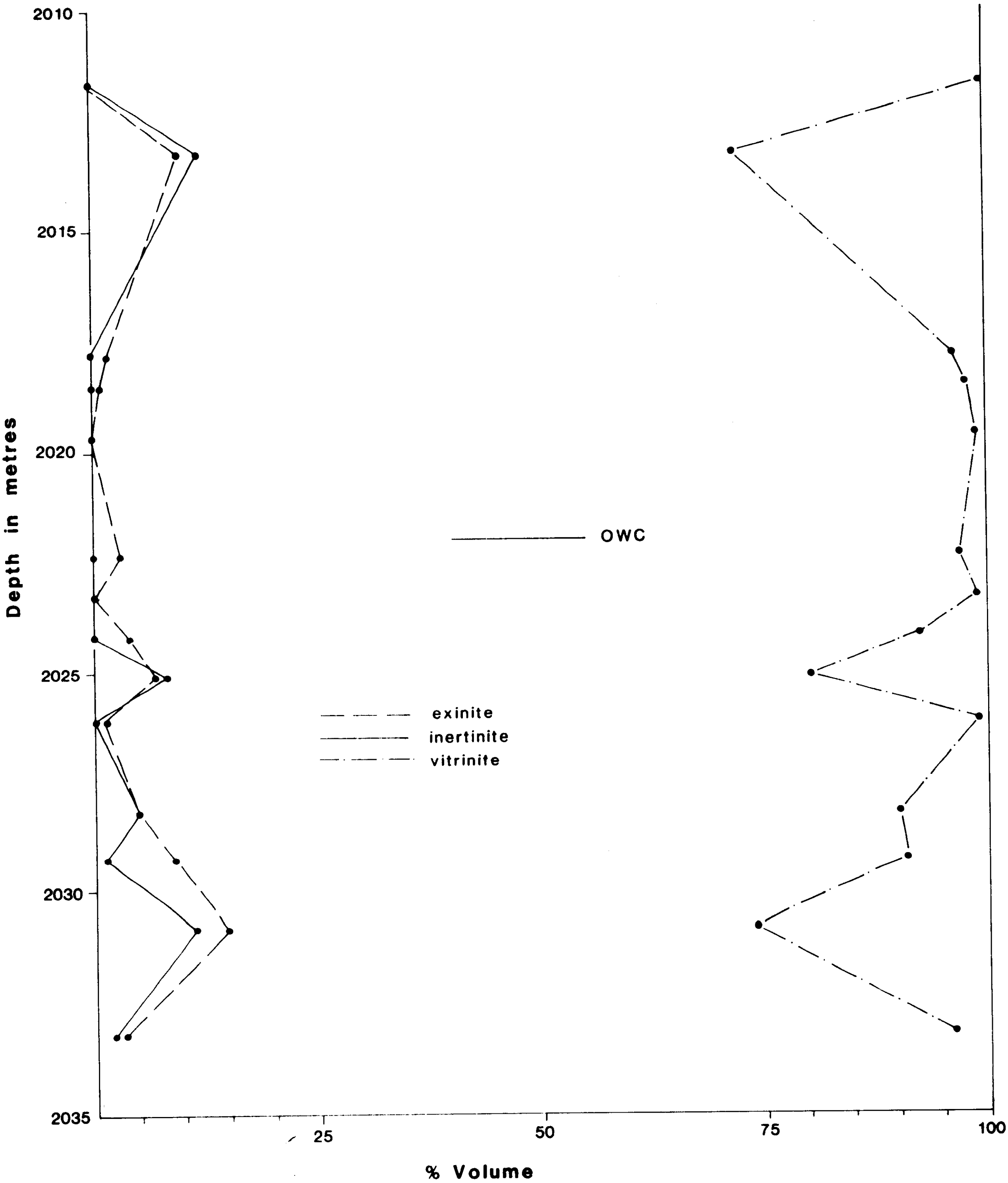

Figure 11.2

TUNA No.3

Variation in Maceral Composition of Coals with depth in T-1 Reservoir

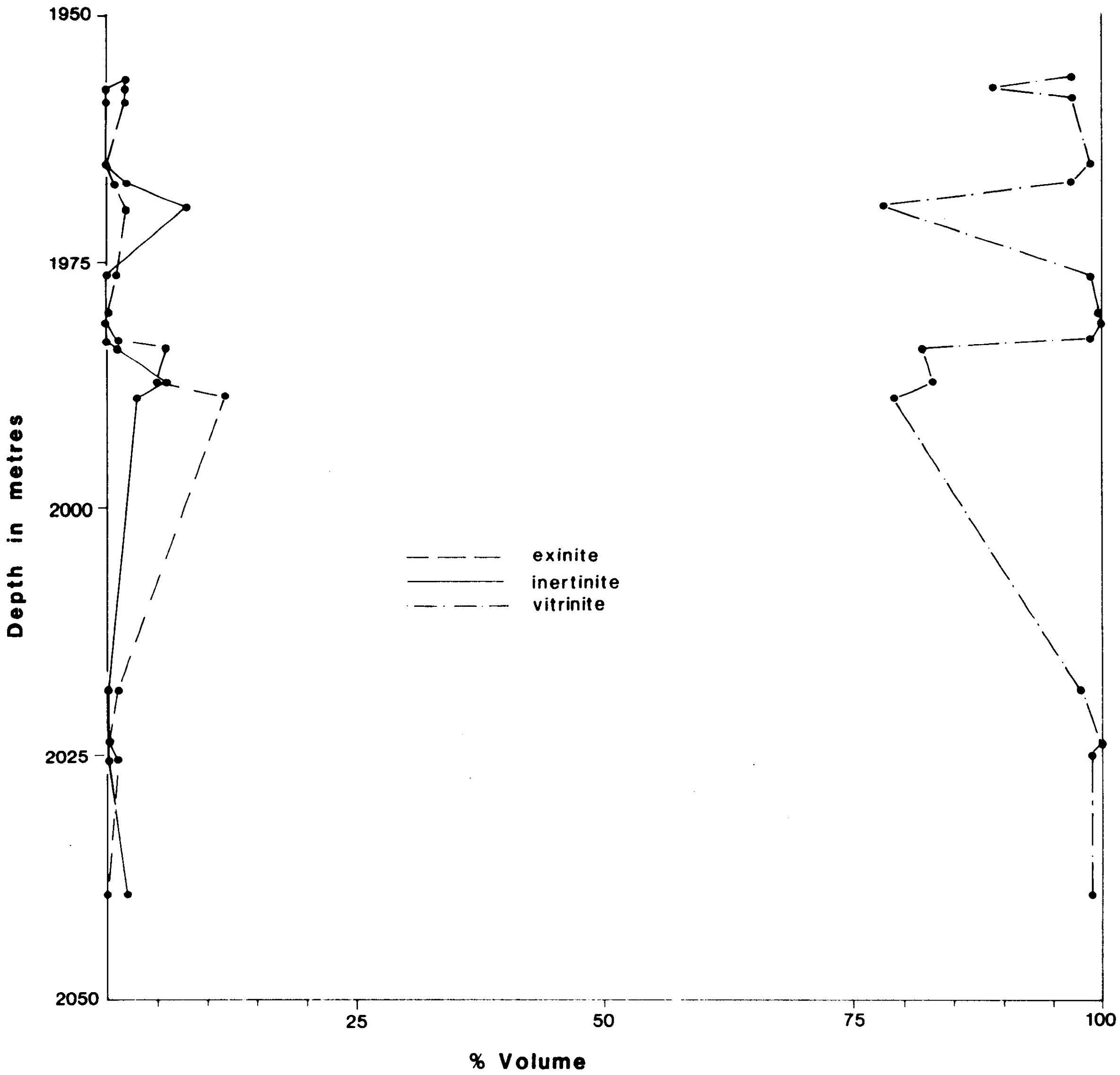

Figure 11.3

TUNA No.1

Variation in Maceral Composition of Dom with depth in T-1 Reservoir

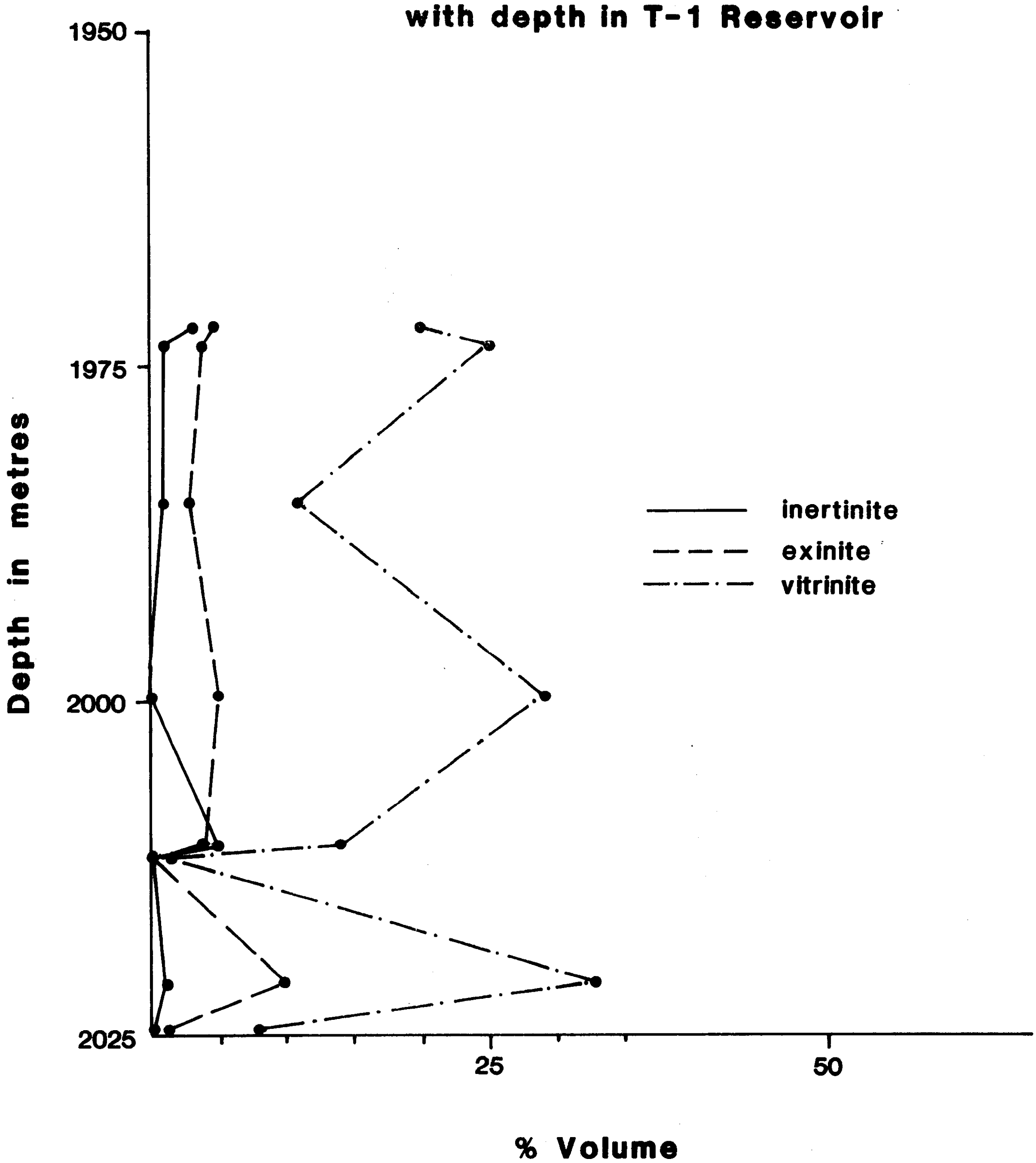

Figure 12.1

TUNA No.2

Variation in Maceral Composition of Dom with depth in T-1 Reservoir

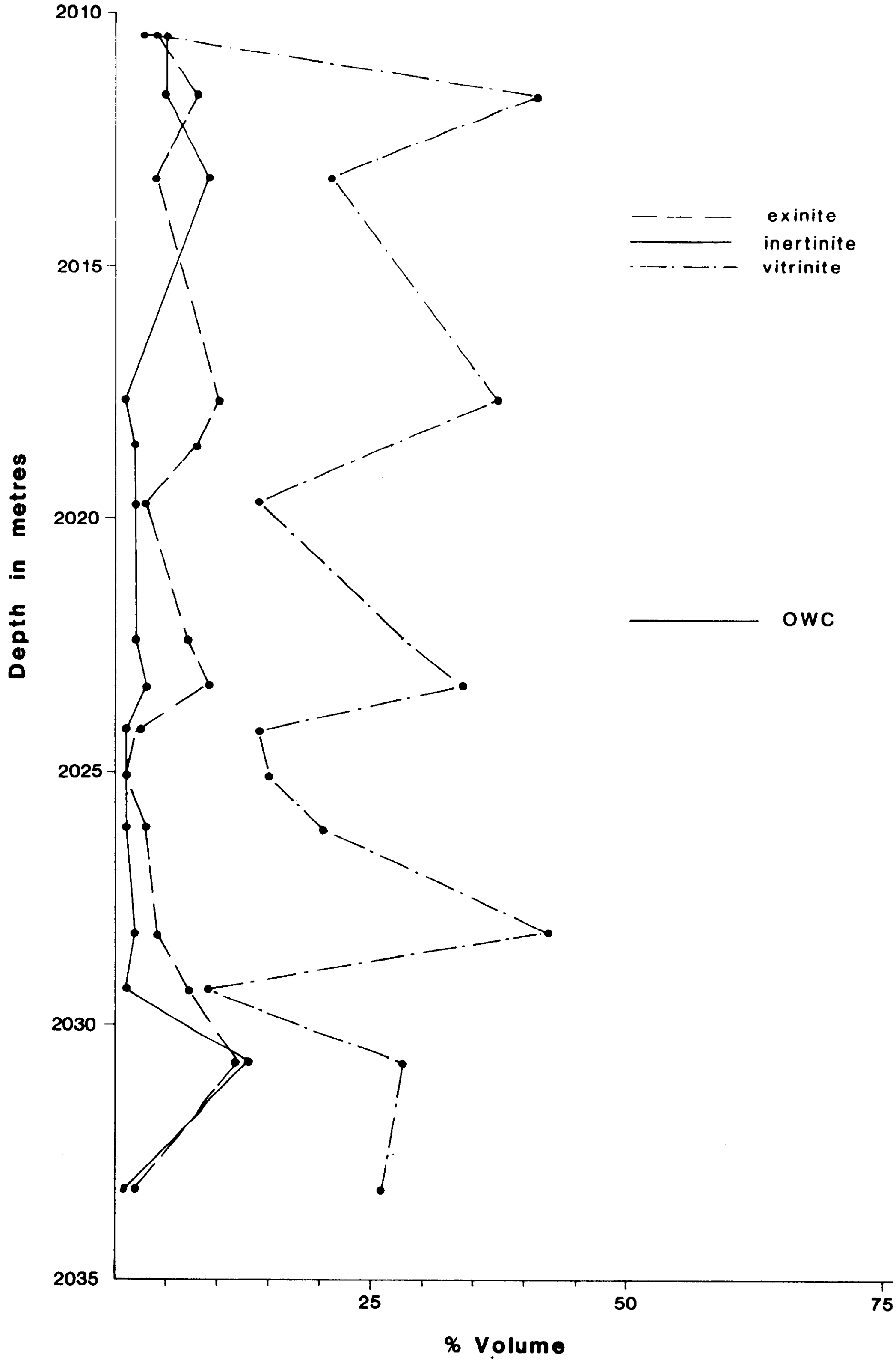

Figure 12.2

TUNA No.3

Variation in Maceral Composition of Dom with depth in T-1 Reservoir

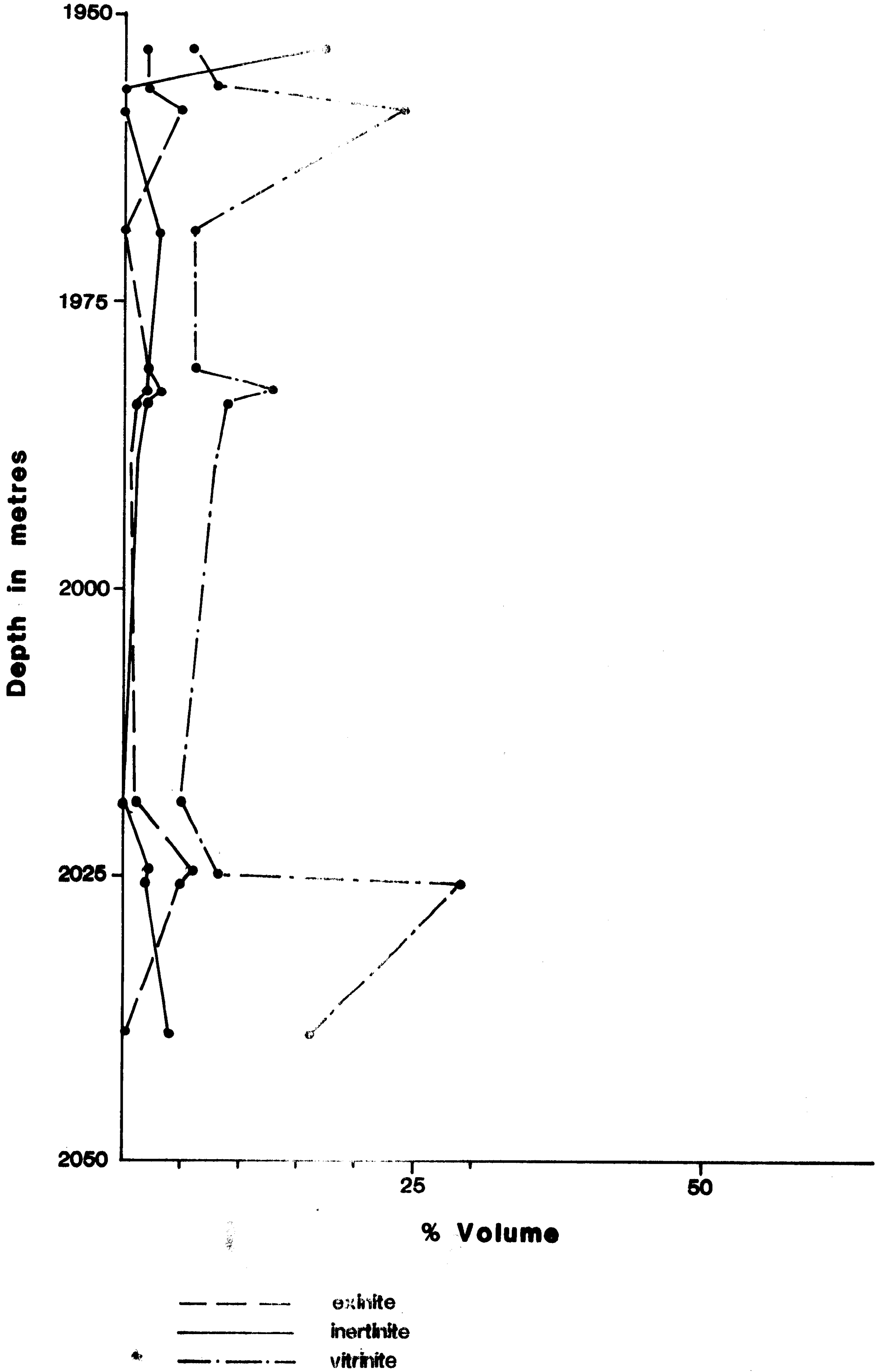

Figure 12.3

TUNA No.1

Variation in Maceral Composition of Dom with depth below T-1 Reservoir

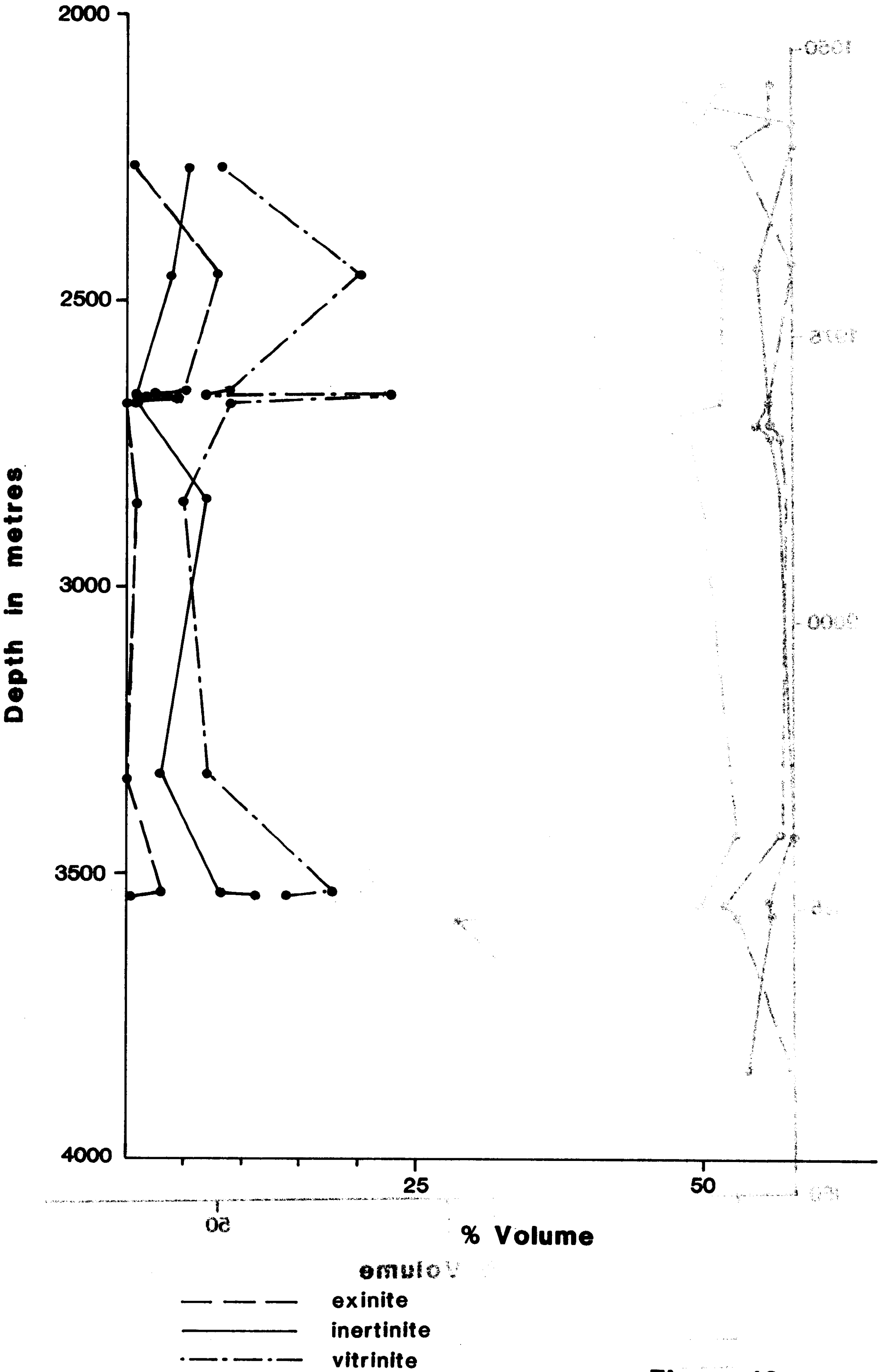

Figure 13

mobilization of hydrocarbons within the coals. Fluorinite and leaf resinite are a small but obvious component of the exinite content down to depth of about 2660m but are difficult to distinguish beyond that rank stage (i.e. about 0.70%).

Inertinite is present in many samples but does not become a significant component until the T-1 reservoir is reached (i.e. age of coals >65MyBP). Table 12 shows the trend for the increase in the percentage of inertinite (by volume) in dom with depth throughout the Tuna section.

We have noted above how some of the exinite macerals (suberinite, fluorinite, leaf-resinite) lose their petrographic identity over the rank range 0.6 to 0.7% Ro. It is also worth noting that much of the vitrinite and inertinite also undergoes pronounced physical and chemical change but at a vitrinite reflectance of 0.5% R_0. This corresponds to a depth of about 2000m or, the level of the T-1 reservoir. Here, the vitrinite cell structure becomes completely closed (i.e the vacant cell lumens or inter-cellular spaces associated with texto-ulminites become fully compressed). Some intercellular spaces in coals from the T-1 reservoir, which are infilled with oil (Plates 22 to 25), remain open probably because of the fluid pressure of the oil. This feature is no longer observed below the T-1 reservoir. Similarly, many inertinite bands have remarkably intact cell structures down to the level of the T-1 reservoir, but such well-preserved structure is rarely observed below this level.

The T-1 reservoir therefore appears to occur at the boundary between dominantly physical and dominantly chemical coalification (the brown coal/ sub-bituminous coal boundary). Is it merely coincidence that an oil reservoir occurs at a maturation level which coincides with the onset of rapid change in the nature of many coal macerals? We prefer to think not for the following reasons:

i) the immature Hapuku oil discovery occurs at a similar level of organic maturation, at temperatures of the order 85 to 95°C,

ii) temperatures in the T-1 reservoir are likewise about 90°C and must be considered generative in the light of the accumulated evidence relating temperatures to hydrocarbon occurrences,

iii) the zone from 2400 to 3100m (0.6 to 0.9%R_0), which we regard as the probable site of <u>most</u> active oil generation, coincides with the loss or change in petrographic identity of many exinite, vitrinite and inertinite macerals. Temperatures in this zone are of the order 100° to 120°C and are certainly likely to be generative in the light of

Philippi's 1965 data on hydrocarbon generation in the Miocene of California, and

iv) the T-1 reservoir is, not surprisingly, the site of heaviest oil staining of vitrinite. Why is it much heavier than in the M-1.2 reservoir? The answer can only be alluded to but it does appear that oil is actually emanating from, rather than being adsorbed into, the pore structure of many vitrinites (Plate 26) in the lower reservoir.

That vitrinite actually contributes to the oil yield is uncertain, but it is worth noting that none of the inertinites with open (and presumably porous) cell structures are associated with oil stain.

Finally, mineral fluorescence is not particularly obvious in either the M-1.2 or T-1 reservoirs. Appreciable orange clay fluorescence does, however, begin to occur beyond a vitrinite reflectance of 0.7% R_0 (Plate 40) and reaches a peak (in the Tuna-1 well) in the deepest samples. In many wells outside the Gippsland Basin, such clay fluorescence becomes most intense just below the oil floor (i.e. >1.35% Ro) prior to phasing out altogether in the semi-anthracite rank range (>2.0% R_0).

6. Conclusions

1. The effects of shelf-life on the vitrinite reflectance of coals from petroleum exploration wells appear to be minimal. Modernisation of equipment may cause a slight change in vitrinite reflectance as compared to results obtained 5 to 10 years ago, but such changes are likely to be small.

2. Sample quality, type, lithology and operator bias are more significant with respect to the results for vitrinite reflectance.

3. In general, reflectance results from dom and vitrinite scares in sandstones tend to be less than average whereas those from shales tend to be slightly above average. Certainly, some of the more anomalous data meet these criteria. However, the samples supplied do not meet the criteria for a well-designed experiment and these comments merely reflect broad trends.

4. Rank shows little lateral variation across the Tuna Field and most downhole reflectance data from the various wells sampled can be superimposed with few, if any, significant discrepancies. However, data from Tuna-2 do tend to lie towards the low side of the general downhole reflectance trend established for Tuna-1. This is seen more clearly

in Figure 14 — a generalized E-W section through the Tuna field. The cause of this variation appears to lie in the more massive, continuous nature of the sands encountered towards the base of the section drilled by Tuna-2. As compared with the alternating shale/sandstone sequence elsewhere, this more massive sandy sequence is likely to have a higher thermal conductivity and therefore a lower temperature gradient than that of the neighbouring wells.

5. Active oil generation is likely to be occurring currently over the depth interval 2000m to 4000m at temperatures in the range 90° to 170°C. Peak oil generation is thought to occur at about 2200m to 3100m, where many macerals (particularly suberinite) undergo marked change in their physical and chemical properties.

6. Initial generation of oil appears to be occurring in the T-1 reservoir where many vitrinites show pronounced oil staining. Oil staining of vitrinite is, however, common both above and below the T-1 reservoir and leads to pronounced change, as well as to some etching, of the vitrinite. The changes are distinctive as is the appearance of oil-saturated vitrinite. However, only a small proportion (<20%) of the vitrinite is so affected.

7. In contrast, clay mineral fluorescence does not appear to occur prior to a vitrinite reflectance of about 0.70% R_o.Mineral fluorescence becomes more pronounced at higher ranks and probably coincides with the transformation of smectite to random mixed layer clays.

8. Common to abundant exinite occurs in rocks throughout the sequence and most are considered to have good to excellent source potential. A local source up to 1000m below the T-1 reservoir is envisaged for the oil in the Tuna field but down-dip, off-structure sources are also likely.

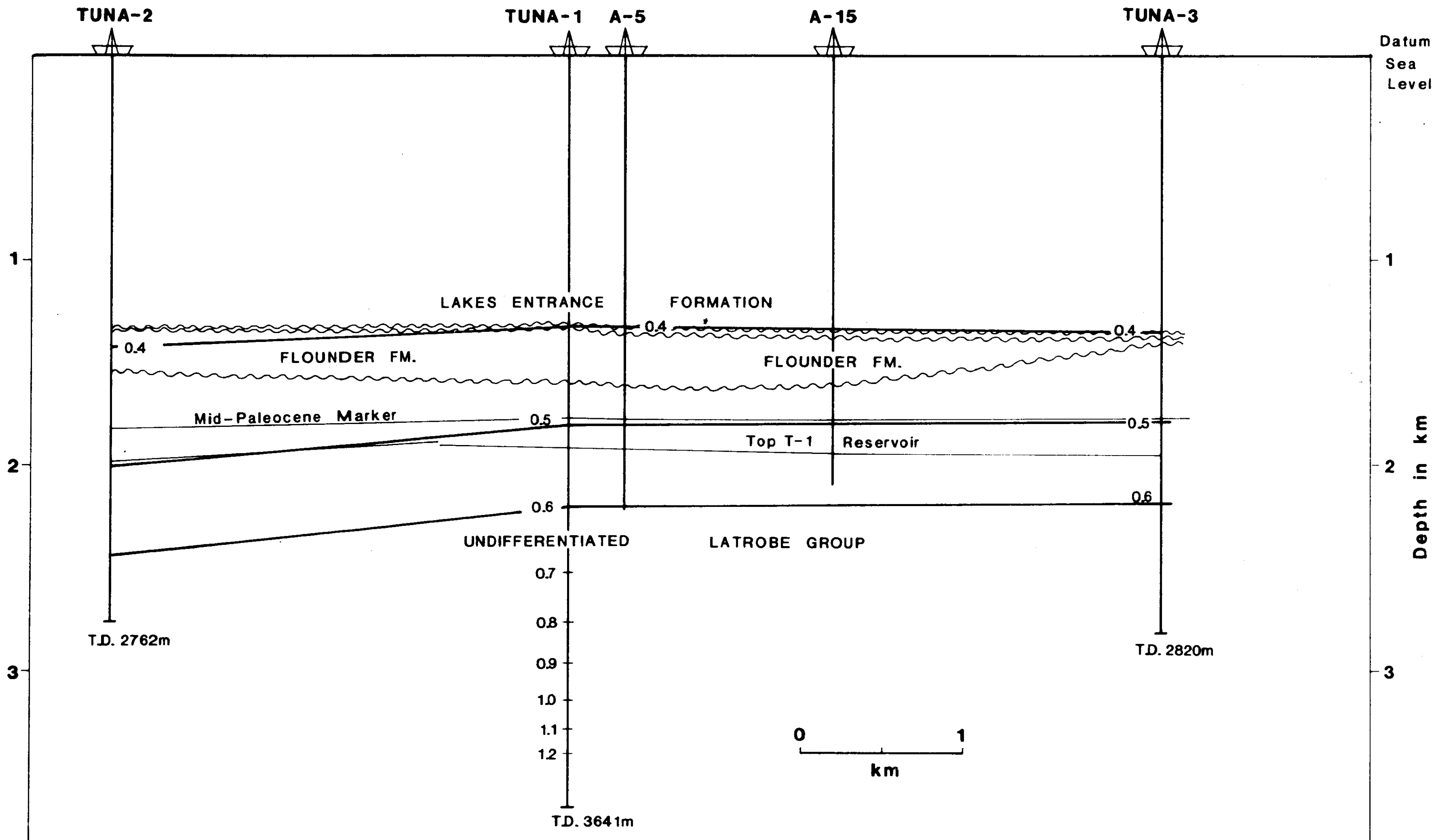

Figure 14 Generalized E-W Section Through the Tuna Field

7. REFERENCES

BOSTICK, N.H., 1973: Time as a factor in thermal metamorphism of phytoclasts (coaly particles); in Congres International de Stratigraphie et de Geologie Carbonifere, Septieme, Krefeld, August 1971. Compte rendu, 2, 183-193.

BOSTICK, N.H., 1979: Vitrinite reflectance; in Cook, H.E. (Ed.), Geologic studies of the Point Conception deep stratigraphic test well OCS-CAL 78-164 No. 1, Outer Continental Shelf, Southern California, United States, pp. 125-128. U.S.G.S. Open-File Report 79-1218, Menlo Park.

BROWN, H.R., COOK, A.C. and TAYLOR, G.H., 1964: Variations in the properties of vitrinite in isometamorphic coal. Fuel, 43, 111-124.

CHANDRA, D., 1965: Effect of storage of coals on reflectance and petrological composition. Econ. Geol., 61, 754-759.

COOK, A.C., 1978: Organic Petrology of Houtman No. 1. Unpublished report for Esso Australia Ltd.

HUTTON, A.C. and COOK, A.C., 1980: Influence of alginite on the reflectance of vitrinite from Joadja, N.S.W., and some other coals and oil shales containing alginite. Fuel, 59, 711-714.

HUTTON, A.C., KANTSLER, A.J., COOK, A.C. and McKIRDY, D.M., 1980: Organic matter in oil shales. Aust. Petrol. Explor. Assoc. J., 20, 44-67.

JAKEMAN, B.L., 1973: The dispersion of some optical properties of coal. Unpublished Honours Thesis — Wollongong University College.

KANTSLER, A.J., SMITH, G.C. and COOK, A.C., 1978a: Lateral and vertical rank variation: Implications for hydrocarbon exploration. Aust. Petrol. Explor. Assoc. J. 18, 143-156.

KANTSLER, A.J., COOK, A.C. and SMITH, G.C., 1978b: Rank variation, calculated palaeotemperatures in understanding oil, gas occurrence. The Oil and Gas Journal, Nov. 20, 196-205.

KARWEIL, J., 1956: Die Metamorphose der Kohlen vom Standpunkt der physikalischen Chemie. Z. Deut. Geol. Ges., 107, 132-139.

PHILIPPI, G.T., 1965: On the depth, time and mechanism of petroleum generation. Geochim. Cosmochim. Acta, 29, 1021-1049.

S.A.A. (Standards Association of Australia), 1980: Microscopical determination of the reflectance of coal macerals. Draft Standard.

SAXBY, J.D., 1978: The organic geochemistry of oil and gas generation and its application to Bass Strait and the Northwest Shelf. Aust. Petrol. Explor. Assoc. J., 18, 137-142.

SHIBAOKA, M., SAXBY, J.D. and TAYLOR, G.H., 1978: Hydrocarbon generation in Gippsland Basin, Australia — comparison with Cooper Basin, Australia. Am. Assoc. Petrol. Geol. Bull., 62, pp. 1151-1158.

TABLE 1

TUNA NO. 1

Vitrinite Reflectance Analyses

W.U. Sample No	Esso Sample No.	Depth ft.	Depth m	Core No.	$\bar{R}_o$max %	Range $R_o$max %	N	Sample Type	Description
9283[1]	B685	3795-802	1157.8	1	0.23	0.21-0.25	7	C	fine silty mudstone
4191[2]		3800	1158.5	1	-	-	-		pyritic shale, mudstone
9493A[3]		3800	1158.5	1	0.25	-	2	C	calcareous mudstone
9284[1]	B686	4330-3	1320.2	3	0.44	0.36-0.52	25	CC	coal and siltstone
9285[1]	B687	4485-8	1367.4	8	0.40	0.37-0.44	25	C	carbonaceous silty mdst.
9286[1]	B688	4494-7	1370.2	8	0.41	0.36-0.46	22	C	coal scares in sst
9287[1]	B689	4508-11	1374.4	9	0.43	0.36-0.49	25	C	carbonaceous silty sndst.
9288[1]	B690	4523-6	1379.0	9	0.43	0.40-0.48	20	C	" " "
9493B[3]		4524	1379.3	9	0.44	0.32-0.52	13	C	" " "
4192[2]		4524	1379.3	9	0.4			C	" " "
9289[1]	B691	4526-29	1379.9	9	0.42	0.35-0.48	25	C	" " "
9290[1]	B692	4532-35	1381.7	9	0.47	0.40-0.52	25	CC	coal + carbonaceous silty sandst
10080[1]	B639	4541-44	1384.5	10	0.40	0.34-0.46	25	C	fine silty sandstone
10081[1]	B640	4547-50	1386.3	10	0.41	0.36-0.48	23	C	laminated slst, sst
10082[1]	B641	4550-53	1387.2	10	0.44	0.37-0.50	25	C	laminated carb. s'st, slst
10083[1]	B642	4559-62	1390.0	10	0.51	0.46-0.56	25	CC	coal only
10084[1]	B643	4568-71	1392.7	11	0.40	0.36-0.45	25	C	quartz s'st.
10085[1]	B644	4571-74	1393.6	11	0.45	0.39-0.52	25	C	fine silty s'st
10086[1]	B645	4608	1404.4	12	0.39	0.34-0.47	25	C	carb. sandy slst
10087[1]	B646	4621	1408.4	12	0.42	0.34-0.50	25	C	" " "
9493[3]		5210	1588.4		0.52	0.37-0.62	18	B	coal, slst, sst
9495[3]		5230	1594.5		0.43	0.38-0.51	22	B	qtz sst, coal, abundant cavings

Table 1 (p.2)

W.U. Sample No	Esso Sample No.	Depth Ft.	Depth m	Core No.	$\bar{R}_o max$ %	Range $R_o max$ %	N	Sample Type	Description
9496[3]		5290	1612.8		0.46	0.40-0.55	24	B	carb. shale, coal, shale
10088[1]	B647	5368'6"	1636.2	13	0.43	0.3 -0.50	25	C	carb. sh.
10089[1]	B648	5375	1638.2	13	0.46	0.41-0.51	25	CC	coal + carb. shale
10090[1]	B649	5376	1638.5	13	0.47	0.45-0.50	25	CC	coal only
9497[3]		5375	1638.7	13	0.45	0.37-0.53	30	C	carb. shale + prominent vitrite scares
4193[2]		5375	1638.7	13	0.40			C	carb. mudstone
4194[2]		5376	1639.0	13	0.44			C	carb. shale + laminae of coal
898	S66[4]	5392	1643.9	13	0.32			C	vit. scares in carb. sh.
9498[3]		5610	1710.4		0.44	0.36-0.52	4	B	calcareous mudstone + coal
9499B[3]		5630	1716.5		0.49	0.39-0.58	11	B	calcareous mudstone + coal
9501[3]		5920	1804.9		0.48	0.33-0.59	11	B	shale, carb. shale, minor coal
10091[1]	B650	6190	1886.6	14	0.51	0.43-0.58		CC	coal + carb. shale
10092[1]	B651	6194	1887.8	14	0.54	0.48-0.58		C	sandy slst + minor coal
9502A[3]		6194	1888.4	14	0.47	0.42-0.51	20	C	carb. shale with thin vitrite scares
4195[2]		6194	1888.4	14	0.43			C	very carb. sh.
10093[1]	B652	6208	1892.1	14	0.54	0.48-0.60	25	CC	coal + carb. sh.
9502[3]		6211	1893.6	14	0.54	0.48-0.62	30	CC	coal only
Emmett[2]		6211-12	1893.6		0.49				
10094[1]	B653	6213	1894.2	14	0.57	0.54-0.61	25	CC	coal only
899	S67[4]	6213	1894.2	14	0.42			CC	coal. Thick vitrite plies
10095[1]	B654	6471	1972.8	15	0.54	0.48-0.60	25	C	carb. shale + sandy slst.
4196[2]		6471	1972.8	15	0.5			C	carb. silty shale
10096[1]	B655	6474-77	1973.7	15	0.55	0.49-0.61	25	CC	coal + carb. shale
9503A[3]		6477	1974.6	15	0.58	0.53-0.66	30	C	silty carb.sh with thin vitrinite scares
4197[2]		6477	1974.6	15	0.48			C	carb. shale + coal
10097[1]	B656	6498-501	1981.1	16	0.53	0.48-0.58	25	CC	coal only

Table 1 (p.3)

W.U. Sample No	Esso Sample No.	Depth Ft.	Depth m	Core No.	$\bar{R}_o max$ %	Range $R_o max$ %	N	Sample Type	Description
900	S684	6517	1986.9	16	0.43			C	coal. Vitrite
10098[1]	B657	6517	1986.9	16	0.51	0.47-0.57	25	C	coarse s'st + minor coal
10099[1]	B658	6550	1996.3	18	0.54	0.50-0.57	25	C	sst + carb. sh. + coal
4198[2]		6550	1997	18	0.48			C	sandstone + vit stringers
9503[3]		6551	1997.3	18	0.55	0.47-0.67	31	C	silty sst + carb. shale with thin vitrinite scares
9504[3]		6571	2003.3	19	0.50	0.45-0.53	30	CC	coal only
10100[1]	B659	6597	2010.7	19	0.53	0.49-0.58	25	C	silty carb. shale
10101[1]	B660	6600	2011.6	20	0.44	0.38-0.53	25	C	qtz. sst. + minor coal
10102[1]	B661	6629-32	2020.9	21	0.55	0.51-0.60	25	CC	coal
10103[1]	B662	6641-44	2024.5	21	0.54	0.49-0.58	25	CC	coal + qtz. s'st
Emmett[2]		6652-55	2028	21	0.52			C	
10104[1]	B663	7430-33	2265.0	22	0.53	0.47-0.58	25	C	carb. silty s'st
9505[3]		7670	2338.4					B	Mostly s'st + carbonate (?cavings)
9506[3]		7810	2381.1		0.59	0.52-0.70	30	B	mostly s'st + minor coal
10105[1]	B664	8067-70	2459.2	25	0.63	0.55-0.71	25	CC	coal + carb. sh.
901	S69[4]	8069	2460.1	25	0.68			CC	coal. Thick vitrite plies
10106[1]	B665	8734-43	2662.8	26	0.63	0.58-0.68	25	CC	coal +
9507[3]		8736	2663.4	26	0.75	0.65-0.81	30	CC	coal + carb. sh.
4199[2]		8737	2663.7	26	0.70			C	coal + carb. silty shale
10107[1]	B666	8749-52'	2667.0	26	0.62	0.57-0.66	25	C	carb. sst. + carb. silty sst.
10108[1]	B667	8752-55'	2667.9	26	0.68	0.60-0.75	26	CC	sst. + carb. sh. + coal
902	S70[4]	8762	2671.3	26	0.68			CC	coal. Thick vitrite plies.
10109[1]	B668	8776	2675.6	27	0.76	0.72-0.81	25	CC	carb. shale + coal
9507B[3]		8776	2675.6	27	0.79	0.66-0.94	16	C	carb. silty shale.
4200[2]		8776	2675.6	27	0.69			C	carb. silty shale
10110[1]	B669	8790	2679.1	27	0.65	0.61-0.69	25	C	carb. pyritic sst.
10111[1]	B670	9351	2850.9	28	0.89	0.77-1.00	25	C	shaly siltstone, fine silty sandstone
9508[3]		9351	2850.9	28	0.82	0.64-1.03	27	C	shaly siltstone, fine silty sandstone

Table No. 1 (p.4)

W.U. Sample No	Esso Sample No.	Depth Ft.	Depth m	Core No.	$\overline{R_o max}$ %	Range $R_o$max %	N	Sample Type	Description
4201[2]		9351	2850.9	28	0.83			C	coal.
9509[3]		9850	3003.0		0.96	0.78-1.08	18	B	slst, s'st, shale + minor coal
9510[3]		10110	3082.3		0.90	0.77-0.97	20	B	carb. shale, slst. + minor coal
9511[3]		10160	3097.6		0.95	0.77-1.11	18	B	shale, slst, s'st + minor coal
9512[3]		10290	3137.2		0.87	0.75-1.00	13	B	s'st, silty shale, carbonate (?cavings)
9513[3]		10540	3213.4		1.16*	1.04-1.30	13	B	coal, carb. shale, silty s'st, carbonate
10112[1]	B671	10909	3324.9	31	0.95	0.89-1.02	25	C	carb. shale
4202[2]		10909	3324.9	31	1.07			C	carb. fine silty sandstone
9514[3]		10910'6"	3326.4	31	1.14	1.06-1.20	10	C	shale
9514A[3]		11533	3516.2	32	<1.40			C	fine s'st + carbonate
4203[2]		11533	3516.2	32	1.0			C	siltstone, fine sandstone
10113[1]	B672	11608-11	3538.4	33	1.03	1.00-1.07	25	CC	coal + sst
903	S71[4]	11611	3539.9	33	1.02			C	thin vitrite layers in coarse qtz sst
10114[1]	B673	11614-17	3540.2	33	1.09	1.00-1.19	25	CC	coal + sst

[1] Analysis by L.L. Ingram 1979, 1980

[2] Analysis by G.C. Smith 1975, 1976

[3] Analysis by A.J. Kantsler 1980

[4] Analysis by A.C. Cook 1971

C - core sample

CC - core sample containing prominent coal bands

B - cuttings

* - samples heat affected during drying at well-site.

TABLE 2

TUNA NO. 2

Vitrinite Reflectance Analyses

W.U.

Sample No.	Esso Sample No.	Depth Ft.	Depth m	Core No.	$\bar{R}_o max$ %	Range $R_o max$ %	N	Sample Type	Description
9294	B696	4433-6	1351.5	2	0.39	0.34-0.44	24	C	laminated carb. silty shale + coarse qtz sst.
9295	B697	4533-9	1382.5	4	0.39	0.34-0.47	25	C	sandy slst.
9296	B698	4536-9	1383.0	4	0.33	0.26-0.41	15	C	sandy slst.
9297	B699	4539-42	1383.9	4	0.33	0.27-0.40	25	C	carb. slst.
9298	B700	4565-68	1391.8	5	0.53	0.47-0.57	25	C	carb. sandy slst.
9299	B701	6595-8	2010.5	6	0.54	0.45-0.62	26	C	carb. silty sst.
9300	B702	6600-1	2011.7	6	0.56	0.53-0.59	25	C	coal + carb. shale
9301	B703	6604-7	2013.3	6	0.48	0.45-0.52	25	C	coal + minor sandy slst.
9302	B704	6619-22	2017.8	7	0.52	0.47-0.57	28	C	coal + carb. silty shale + chalcopyrite
9303	B705	6621-25	2018.6	7	0.52	0.49-0.55	25	C	coal + carb. silty shale
9304	B706	6625-28	2019.7	7	0.52	0.46-0.61	25	C	silty carb. shale + coal
9305	B707	6634-37	2022.4	7	0.50	0.46-0.54	25	C	carb. shale + coal + fine sst.
9306	B708	6637-40	2023.3	7	0.56	0.51-0.62	24	C	coal + carb. shale
9307	B709	6640-43	2024.2	7	0.51	0.47-0.54	25	C	coal + carb. sandy slst.
9308	B710	6643-46	2025.1	7	0.54	0.51-0.59	25	C	coal + carb. shale
9309	B711	6646-49	2026.1	7	0.50	0.45-0.56	25	C	carb. shale + minor coal
9310	B712	6654-55	2028.2	7	0.57	0.51-0.63	25	C	coal + carb. shale
9311	B713	6658	2029.3	7	0.52	0.46-0.59	25	C	coal + fine sandy slst.
9312	B714	6662-64	2030.8	7	0.55	0.50-0.60	25	C	coal
9313	B715	6670-72	2033.2	7	0.54	0.49-0.58	25	C	coal + carb. shale
9314	B716	7221-24	2201.5	8	0.55	0.48-0.64	25	C	coal + carb. shale
9315	B717	7230-33	2204.3	8	0.54	0.51-0.59	26	C	coal + carb. shale
9316	B718	8020-21	2445.1	9	0.51	0.46-0.55	28	C	coal

TABLE 3

TUNA NO. 3

Vitrinite Reflectance Analyses

W.U. Sample No	Esso Sample No.	Depth Ft.	Depth m	Core No.	$\bar{R}_o max$ %	Range $R_o max$ %	N	Sample Type
9317	B719	4584-7	1397.6	3	0.42	0.36-0.46	21	Carb. silty fine sst.
9318	B720	4587-90	1398.5	3	0.41	0.37-0.45	18	silty fine s'st
9319	B721	6406-9	1952.9	4	0.50	0.46-0.54	25	laminated silty sst
9320	B722	6418-9	1956.3	4	0.49	0.45-0.54	25	coal + slst
9321	B723	6421-4	1957.4	4	0.52	0.47-0.57	25	coal + massive pyrite
9322	B724	6424-7	1958.4	4	0.52	0.47-0.57	24	
9323	B725	6446-9	1965.1	5	0.55	0.52-0.59	25	coal
9324	B726	6452-5	1966.9	5	0.58	0.54-0.64	25	coal
9325	B727	6458-61	1968.8	5	0.54	0.51-0.58	25	sst + minor coal fragments
9326	B728	6482-6	1976.2	6	0.56	0.50-0.62	25	coal
9327	B729	6498-6501	1980.9	6	0.56	0.51-0.62	25	coal fragments
9328	B730	6504-7	1982.8	6	0.58	0.54-0.64	25	coal + carb. shale
9329	B731	6507-10	1983.7	6	0.59	0.54-0.65	25	coal + carb. shale
9330	B732	6519-22	1987.3	6	0.55	0.50-0.61	24	coal
9331	B733	6522-8	1988.7	6	0.57	0.52-0.64	25	coal + fine qtz. sst.
9332	B734	6621-4	2018.4	7	0.54	0.48-0.61	25	coal + mudstone
9333	B735	6639-42	2023.9	7	0.54	0.51-0.59	25	coal
9334	B736	6642-4	2024.7	7	0.54	0.51-0.58	25	coal + silty carb. shale
9335	B737	6645-8	2025.8	7	0.51	0.47-0.55	30	coal + carb. shale
9336	B738	6689-92	2039.2	8	0.51	0.43-0.57	27	coal + qtz. sst.

Table 4

TUNA A-5

Vitrinite Reflectance Analyses

Sample No.	Esso Sample No.	Depth m	Core No.	$\overline{R_o}$max %	Range $R_o$max %	N	Sample Description
9291	B693	1340.6	1	0.41	0.37-0.45	25	Coal + carb. shale
9292	B694	1392.0	7	0.40	0.36-0.44	12	laminated carb. slst + chalcopyrite
9293	B695	1396.4	8	0.41	0.34-0.50	25	slst + carb. silty sh.
10065	B624	1975.2	11	0.55	0.50-0.59	25	vitrite scares in slst
10066	B625	1982.0	11	0.53	0.50-0.56	25	coal + carb. sh.
10067	B626	1992.5	12	0.54	0.49-0.61	25	vitrite scares in carb. sh.
10068	B627	2003.5	13	0.55	0.51-0.58	25	brown coal
10069	B628	2003.8	13	0.55	0.50-0.61	25	carb. silty sh.
10070	B629	2004.4	13	0.55	0.52-0.59	25	vitrite in carb. sh.
10071	B630	2020.5	15	0.55	0.51-0.60	26	vitrite scares in sst.
10072	B631	2039.5	17	0.56	0.51-0.61	25	vitrite scares in sst.
10073	B632	2051.6	18	0.57	0.52-0.61	25	coal

Table 5

TUNA A-15

Vitrinite Reflectance Analyses

Sample No.	Esso Sample No.	Depth m	Core No.	$\overline{R_o}max$ %	Range $R_o max$ %	N	Sample Description
10074	B633	2372.8	1	0.57	0.53-0.61	25	Laminated siltstone, shale, s'st, coal
10075	B634	2378.2	1	0.58	0.55-0.63	25	Coal + carb. sh.
10076	B635	2388.3	2	0.55	0.52-0.59	25	coal scares in sst.
10077	B636	2408.4	5	0.57	0.53-0.61	25	coal + carb. sh.
10078	B637	2431.5	7	0.57	0.53-0.61	25	sst. interlam. with carb. sh. + coal

LIST OF ABBREVIATIONS USED IN TABLES

V	vitrinite
I	inertinite
E	exinite
N	total no. of analyses
sst	sandstone
c	coal
sh	shale
slst	siltstone
mdst	mudstone
calc	calcareous

TABLE 6 Isothermal and gradthermal estimates of palaeotemperature in the Tuna-1 well

Depth m	Age MyBP	$\overline{R}_o$max %	Tpres °C	Tiso	Tgrad	Tpres-Tgrad	Teff	Tpres-Teff
2000	75	0.50	86	<40	<60	+26	90	-4
2700	85	0.70	107	60	90	+17	122	-15
3500	94	1.00	130	92	141	-11	155	-25

TABLE 7 Maceral Composition above M-1.2 reservoir in Tuna-1

Sample No.	Description	Depth (m)	DOM V	DOM I	DOM E	Total DOM
9283	calc. mdst.	1157.8	1	-	1	2

TABLE 8.1 Maceral Composition in M-1.2 reservoir in Tuna-1

Sample No.		Depth (m)	V	DOM I	DOM E	Total DOM	COAL V	COAL I	COAL E
9284	c + slst	1320.2	9	-	2	11	98	-	-
9285	silty sst	1367.4	13	-	3	16			
9286	"	1370.2	18	-	4	22			
9287	"	1374.4	13	-	4	17			
9288	"	1379.0	7	1	tr	8			
9289	"	1379.9	14	tr	2	16			
9290	"	1381.7	23	-	3	26	94	2	-
10080	"	1384.5	9	-	-	9			
10081	"	1386.3	6	-	2	8			
10082	sst	1387.2	3	-	-	3			
10083	c	1390.0					100	-	tr
10084	sst	1392.7	tr	-	-	tr			
10085	"	1393.6	3	-	-	3			
10086	sandy slst	1404.4	7	-	-	7			
10087	"	1408.4	4	-	1	5			
		Total	129	1	21	151	292	3	tr
		Ave	10	0	2	12	97	1	
		N	13	13	13	12	3	3	
		Range	3-23	0-1	0-4	3-26	94-100	0-2	

TABLE 8.2 Maceral Composition of M-1.2 Reservoir in Tuna-2

Sample No.		Depth (m)	V	DOM I	DOM E	Total DOM
9294	silty sh + sst	1351.2	23	2	3	28
9295	sandy slst	1382.5	4	tr	3	7
9296	"	1383.0	7	1	6	14
9297	slst	1383.9	1	tr	3	4
9298	"	1391.8	9	2	2	13
		TOTAL	44	5	17	66
		N	5	5	5	5
		Ave	9	1	3	13
		Range	1-23	0-2	2-6	4-28

TABLE 8.3 Maceral Composition of M-1.2 Reservoir in Tuna-3

Sample No.	Descr.	Depth (m)	DOM V	DOM I	DOM E	Total dom	COAL V	COAL I	COAL E
9317	silty sst	1397.6	4	-	2	6	96	-	2
9318	" "	1398.5	7	-	2	9			
		Total	11	0	4	15			
		N	2	2	2	2			
		Ave	5.5	0	2	7.5			
		Range	4-7	0	2	6-9			

TABLE 8.4 Maceral Composition of M-1.2 Reservoir in Tuna A-5

Sample No.	Descr.	Depth (m)	DOM V	DOM I	DOM E	Total dom	COAL V	COAL I	COAL E
9291	c	1340.6					92	-	-
9292	slst	1392.0	5	-	1	6			
9293	"	1396.4	7	-	2	7			
		Total	12	-	3	13	92		
		N	2	2	2	2			
		Ave	6	-	1.5	6.5			
		Range	5-7	-	1-2	6-7			

TABLE 9 Maceral Composition between M-1 and T-1 reservoirs in Tuna-1

Sample No.	Descr.	Depth (m)	DOM V	DOM I	DOM E	Total dom	COAL V	COAL I	COAL E
10088	sh	1636.2	14	1	12	27			
10089	c + sh	1638.2	28	2	11	41	100	-	-
10090	c	1638.5					100	-	-
10091	c + sh	1886.6	24	1	10	35	100	tr	tr
10092	mdst	1887.8	8	1	3	12	100	-	-
10093	c + sh	1892.1	27	-	11	38	82	3	16
10094	c	1893.6					84	8	8
		Total	101	5	47	193	566	11	24
		Ave	20	1	9	39	94	2	4
		N	5	5	5	5	6	6	6
		Range	8-28	0-2	3-12	12-41	82-100	0-8	0-16

TABLE 10.1 Maceral Composition in T-1 reservoir

Sample No.	Descr.	Depth (m)	DOM V	DOM I	DOM E	Total dom	COAL V	COAL I	COAL E
10095	sh + sst	1972.3	20	3	5	28			
10096		1973.6	25	1	4	30	99		1
10097	c	1980.9					100	tr	tr
10098		1986.3	11	1	3	15	98		2
10099	sh + sst	1996.3	29	-	5	34			
10100	sh	2010.7	14	5	4	23			
10101	sst + c	2011.6	1	-	-	1	87	6	7
10102	c + sh	2020.9	33	1	10	44	100	-	tr
10103	c + sst	2024.5	8	-	1	9	97	1	2
		Total	141	11	32	184	581	7	12
		Ave	18	1	4	23	97	1	2
		N	8	8	8	8	6	6	6
		Range	1-33	0-5	0-10	1-44	37-100	0-6	4-7

TABLE 10.2 Maceral Composition of T-1 Reservoir in Tuna-2

Sample No.	Descr.	Depth (m)	DOM V	DOM I	DOM E	Total dom	COAL V	COAL I	COAL E
9299	sst	2010.5	3	5	4	12			
9300	c + sh	2011.7	41	5	8	54	100	-	tr
9301	c + sh	2013.3	21	9	4	34	72	12	10
9302	c + sst	2017.8	36	1	10	47	96	-	2
9303	c + sh	2018.6	27	2	8	37	98	-	1
9304	c + sh	2019.7	14	2	3	19	99	-	-
9305	sh + sst	2022.4	28	3	7	38	97	-	3
9306	c + sh	2023.3	34	tr	9	43	99	-	-
9307	c + sst	2024.2	14	1	2	17	92	-	4
9308	c + sh	2025.1	15	1	1	17	83	8	7
9309	c + sh	2026.1	20	1	3	24	99	-	1
9310	c + sh	2028.2	42	2	4	48	90	5	5
9311	c + sst	2029.3	9	tr	7	16	91	tr	9
9312	c + sh	2030.8	28	13	12	53	74	11	15
9313	c + sh	2033.2	26	1	2	29	96	-	3
		Total	358	45	84	488	1286	36	60
		Ave	24	3	6	33	92	3	4
		N	15	15	15	15	14	14	14
		Range	3-42	0-13	1-12	12-54	72-100	0-12	0-15

TABLE 10.3 Maceral Composition of T-1 Reservoir in Tuna-3

Sample No.	Descr.	Depth (m)	DOM V	DOM I	DOM E	Total dom	COAL V	COAL I	COAL E
9319	sst + slst	1952.9	6	17	2	25			
9320	c + slst	1956.3	8	-	2	10	97	2	2
9321	c	1957.5					89	-	2
9322		1958.4	24	-	5	29	97	-	2
9323	c	1965.1					99	-	-
9324	c	1966.9					97	2	2
9325	c + sst	1968.8	6	3	-	9	78	8	2
9326	c	1976.2					99	-	1
9327	c + mdst	1980.9	6	2	2	10	100	-	-
9328	c + sh	1982.8	13	3	2	18	99	-	1
9329	c+sst+sh	1983.7	9	2	1	12	82	1	6
9330	c + sh	1987.3					83	6	5
9331	c + sst	1988.7	8	tr	tr	8	79	3	12
9332	c + mdst	2018.4	5	-	1	6	98	-	1
9333	c	2023.9					100	-	-
9334	c + slst	2024.7	13	2	6	21	99	-	tr
9335	c + sh	2025.8	29	2	5	36	99	-	1
9336	sst + c	2039.2	16	4	-	20	99	2	-
		Total	143	35	26	204	1594	24	37
		N	12	12	12	12	17	17	17
		Ave	12	3	2	17	94	1	2
		Range	5-29	0-17	0-6	6-36	78-100	0-8	0-6

TABLE 10.4 Maceral Composition of T-1 Reservoir in Tuna A-5

Sample No.	Descr.	Depth (m)	DOM V	DOM I	DOM E	Total dom	COAL V	COAL I	COAL E
10065		1975.2	15	tr	1	16			
10066	c + sh	1982.0	19	6	6	31	99		
10067	sh	1992.5	31	9	6	46			
10068	c	2003.5					100		
10069	sh	2003.8	9	1	3	13			
10070	c + sh	2004.4					71	7	10
10071	sst	2020.5	8	3	tr	11			
10072	sst	2039.5	11	2	1	14			
10073	c	2051.6					71	14	10
		Total	93	21	17	131	341	21	21
		Ave	16	4	3	22	85	5	5
		N	6	6	6	6	4	4	4
		Range	8-31	0-9	0-6	11-46	71-100	0-14	0-11

TABLE 10.5 Maceral Composition of T-1 Reservoir in Tuna A-15

Sample No.	Descr.	Depth (m)	DOM V	DOM I	DOM E	Total dom	COAL V	COAL I	COAL E
10074	sh + sst	2372.8	16	4	2	22			
10075	c + sh	2378.2	26	12	5	43	99	-	-
10076	sst	2388.2	6	1	3	10			
10077	c + sh	2408.4	47	1	9	57	100	-	-
10078	sst + sh	2431.5	13	3	3	19			
		Total	108	21	22	151	199	-	-
		N	5	5	5	5	2		
		Ave	22	4	4	30	99.5		
		Range	6-47	1-12	2-9	10-57	99-100		

TABLE 11.1 Maceral Composition below T-1 Reservoir

Sample No.	Descr.	Depth (m)	DOM V	DOM I	DOM E	Total dom	COAL V	COAL I	COAL E
10104	silty sst	2265.0	8	6	tr	14			
10105	c + sh	2459.2	20	4	8	32	99	-	1
10106	sh + sst	2663.4	9	1	5	15	93	-	6
10107	sst + sh	2667.0	7	1	2	10			
10108	c + sh	2667.9	23	2	5	30	100	-	-
10109	sh + c	2674.8	15	1	2	18	99	-	1
10110	sst	2679.1	9	1	-	10			
10111	sh + sst	2850.0	5	7	1	13			
10112	sh	3324.9	7	3	-	10			
10113	sst	3538.4	18	8	3	28			
10114	sst	3540.2	14	11	tr	25			
		Total	135	45	26	206	391	0	8
		Ave	12	4	2	19	98	0	2
		N	11	11	11	11	4	4	4
		Range	7 23	1 11	0 8	10 32	93-100	0	0-6

TABLE 11.2 Maceral Composition below T-1 reservoirs in Tuna-2

Sample No.	Descr.	Depth (m)	DOM V	DOM I	DOM E	Total dom	COAL V	COAL I	COAL E
9314	sh + c	2201.5	3	tr	8	11	81	6	13
9315	c + sh	2204.3	23	-	3	26	99	-	tr
9316	c + sh	2445.1	44	-	9	53	96	-	4
		Total	70	-	20	90	276	6	17
		Ave	23	-	7	30	92	2	6
		N	3	3	3	3	3	3	3
		Range	3 44	-	3 9	11 53	81 99	0 6	0 13

Table 12 Average Maceral Composition at various levels in Tuna Field

Level		Tuna 1 Dom	Tuna 1 Coal	Tuna 2 Dom	Tuna 2 Coal	Tuna 3 Dom	Tuna 3 Coal	Tuna A5 Dom	Tuna A5 Coal	Tuna A15 Dom	Tuna A15 Coal	Overall Dom	Overall Coal
Above M-1 Res.	Vit.	0.5										0.5	
	Inert.												
	Ex.	1										1.0	
	Av. Dom	1.5										1.5	
	N	2										2	
M-1 Reservoir ± 10m	Vit.	10.0	97.0	8.8		5.5	96	6.0	92			9	96.0
	Inert.	-	0.7	1.0		-	1	0				0	0.4
	Ex.	1.6	-	3.4		2.0	2	1.5	-			2	0.4
	Av. Dom	11.6		14.0		7.5		7.5				11	
	N	13	3	5		2	1	2		22		22	5
Between M-1 and T-1 Reservoirs	Vit.	20.2	94.3									20.2	94.3
	Inert.	1.0	1.8									1.0	1.8
	Ex.	9.4	4.0									9.4	4.0
	Av. Dom	30.6										30.6	
	N	5	6									5	6
T-1 Reservoir ± 10m	Vit.	17.6	96.8	23.4	92.0	11.9	93.5	15.5	85.2	21.6	100.0	18.3	93.0
	Inert.	1.4	1.2	3.1	2.7	2.9	1.4	3.5	5.3	4.2	-	2.9	2.1
	Ex.	4.0	2.0	5.6	4.1	2.2	2.2	2.8	5.3	4.4	-	3.9	3.0
	Av. Dom	23.0		32.4		16.9		21.2		30.0		25.0	
	N	8	6	15	14	12	16	6	4	5	2	46	43
Below T-1 Reservoir	Vit.	12.3	97.8	23.3	92.0							14.6	95.2
	Inert.	4.1	-	2.0	2.0							3.2	0.9
	Ex.	2.4	2.0	6.7	5.7							3.3	3.6
	Av. Dom	18.6		30.0								21.1	
	N	11	4	3	3							14	7

All photomicrographs taken with Leitz Orthomat Camera System using EKTACHROME 400 ASA slide film. Field width 0.34mm across unless stated otherwise.

Fluorescence mode photomicrographs taken using violet excitation with a K490 barrier filter.

Plate 1 WU9493A 3800'(T-1) Lakes Entrance Fm.

Dinoflagellate/acritarch cyst showing bright yellow fluorescence; characteristic of thermal immaturity. Such phytoplankton are relatively rare. R_o=0.23%

Plate 2 WU9289 4526'(T-1) M-1.2 Reservoir

Oblique section through phytoclast of poorly preserved vitrinite (V), surrounded by a thick mantle of red-brown cutinite, and associated with minor pyrite (P) in a matrix of quartz sandstone (Q). R_o=0.42%.

Plate 3 As above.

The cutinite is highly structured, the texture being derived from the palisade cells which immediately underlie it.

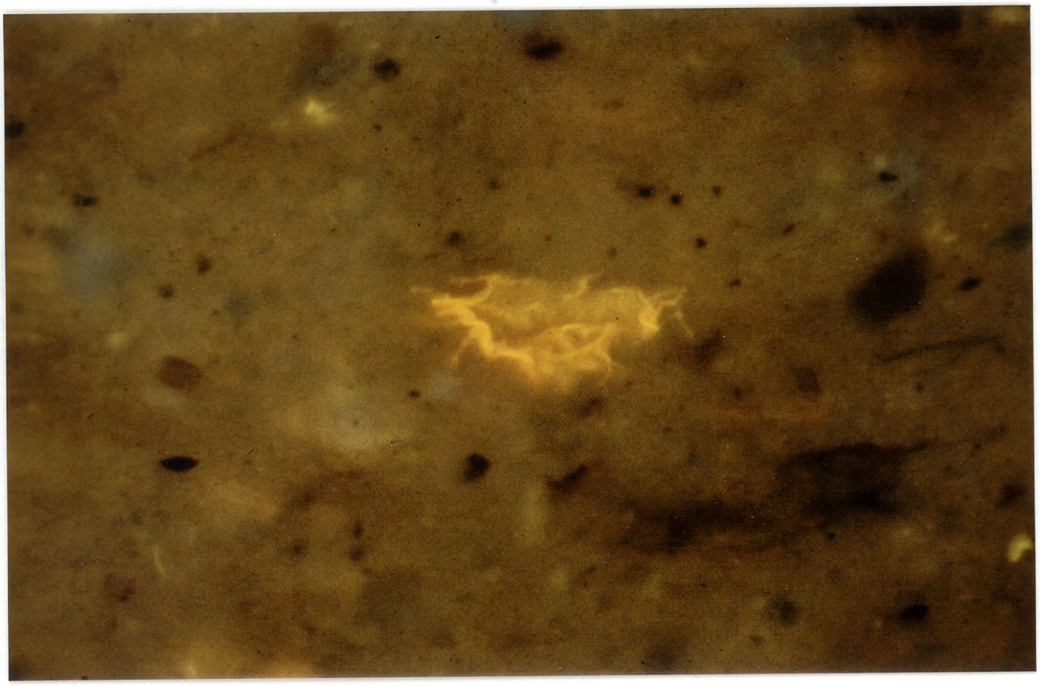

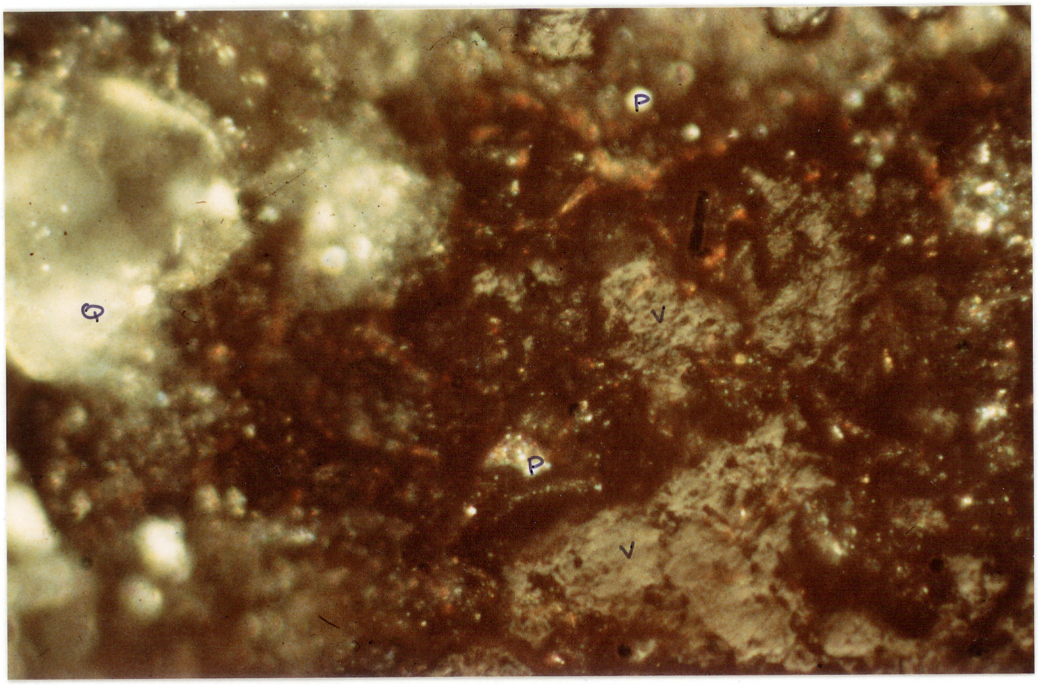
P
Q
V
P
V

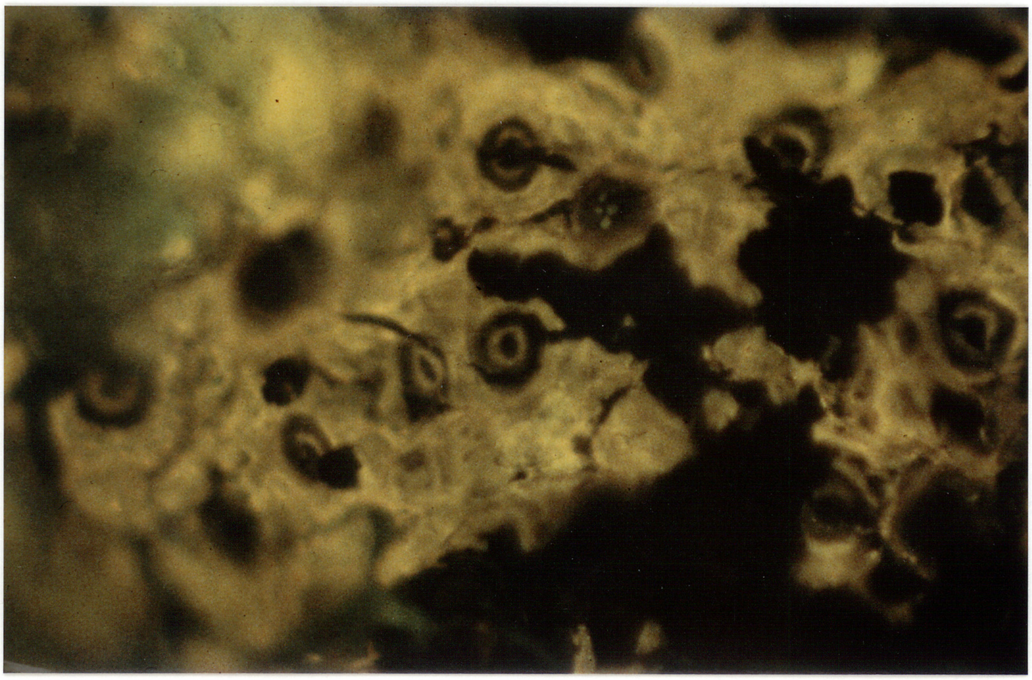

Plate 4 WU9289 4526'(T-1) M-1.2 Reservoir

Layer of coal comprised almost entirely of vitrinite, which itself is comprised largely of cellular infillings known as phlobaphinite or corpohuminite. Corpohuminite generally tends to have a slightly higher reflectance than the more massive varieties of vitrinite such as ex-ulminite or collinite. R_o=0.42%

Plate 5 WU9497 5375'(T-1) Between M-1.2 and T-1

Exsudation of pale-green fluorescing oil from fracture in a vitrinite layer. R_o=0.45%

Plate 6 As above.

Note how the oil has etched the surface of the vitrinite.

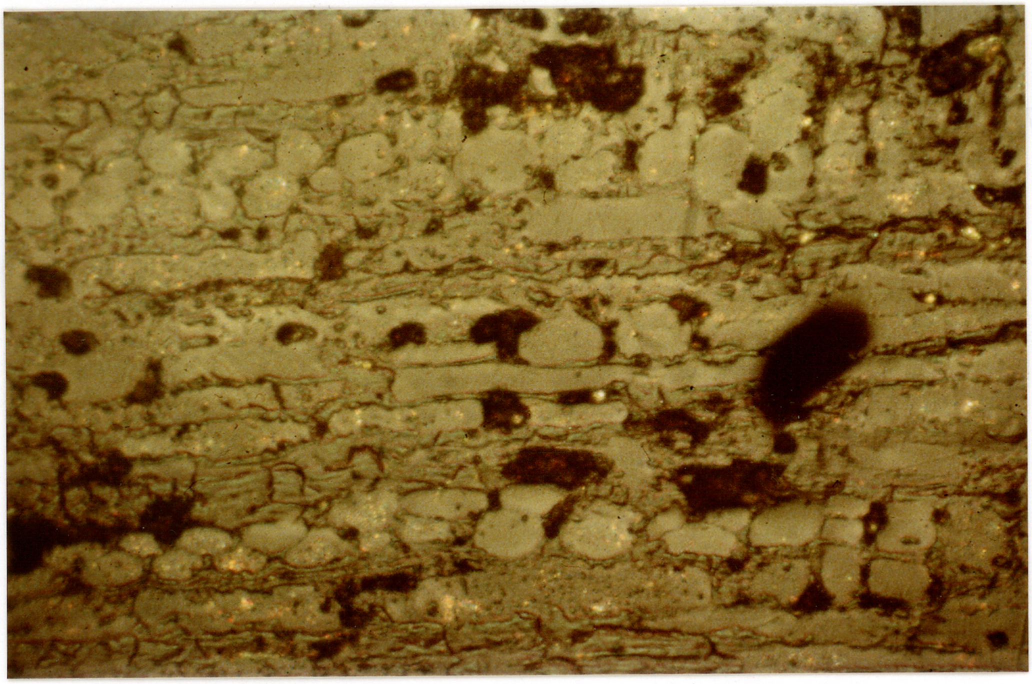

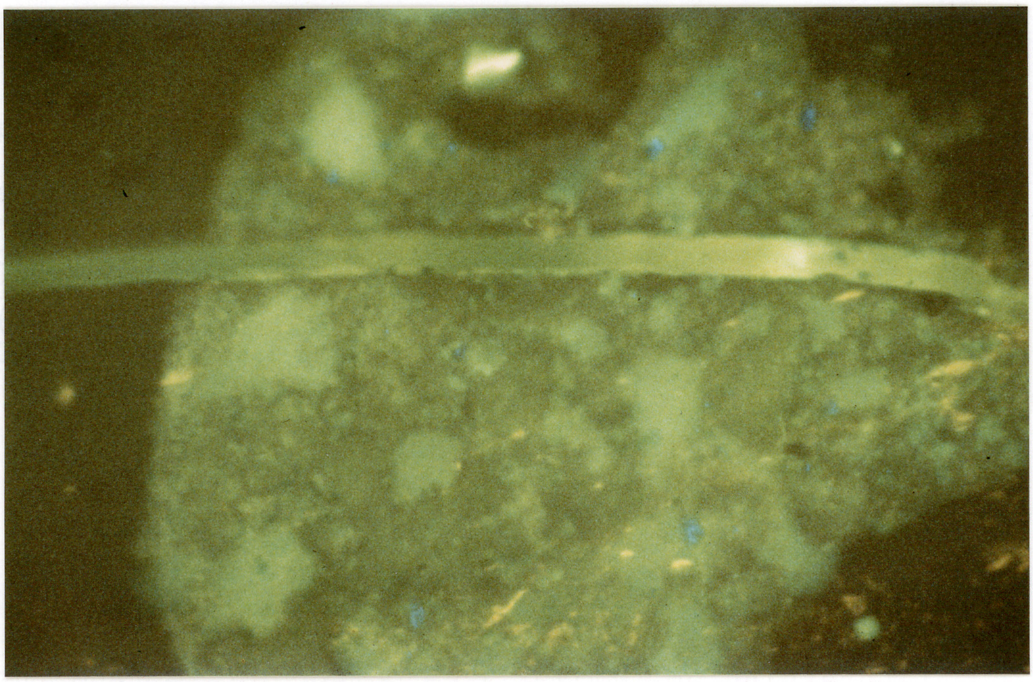

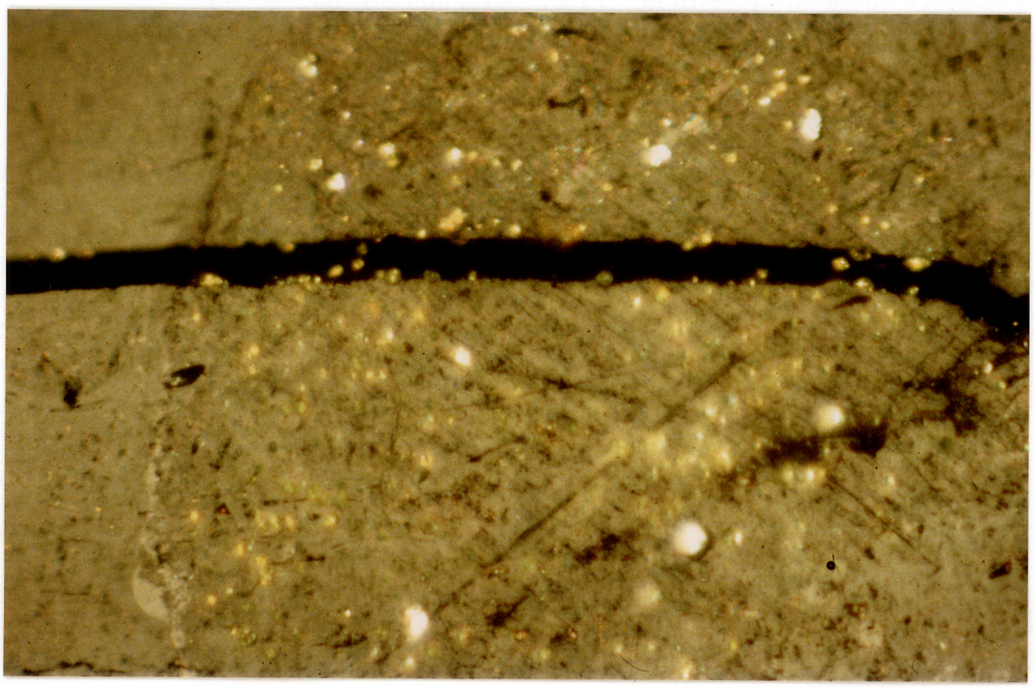

Plate 7 WU9501 5920'(T-1) Between M-12 and T-1

Vitrinite layer comprised of corpocollinite-filled cell lumens surrounded by thin walls of suberinite (an exinite maceral). In the lower part of the field of view this association shows numerous internal reflections. R_o=0.48%

Plate 8 WU9493 5210'(T-1) Between M-1.2 and T-1

Coal layer comprised of the microlithotype clarite. This clarite is made up of large amounts of sporinite (S) and liptodetrinite (L-an exinite not capable of identification because of its small size) in a matrix of a vitrinite variety known as desmocollinite (D). Minor corpocollinite (C). Minor pyrite (P). R_o=0.52%

Plate 9 As above.

Sporinite and liptodetrinite show strong fluorescence, characteristic of low-rank coals.

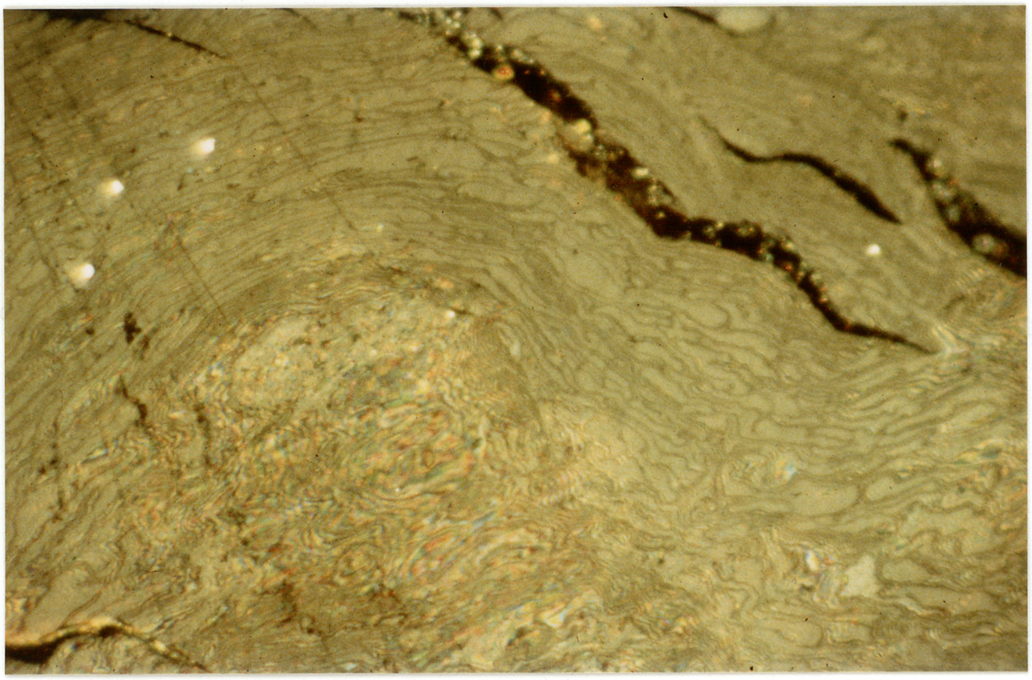

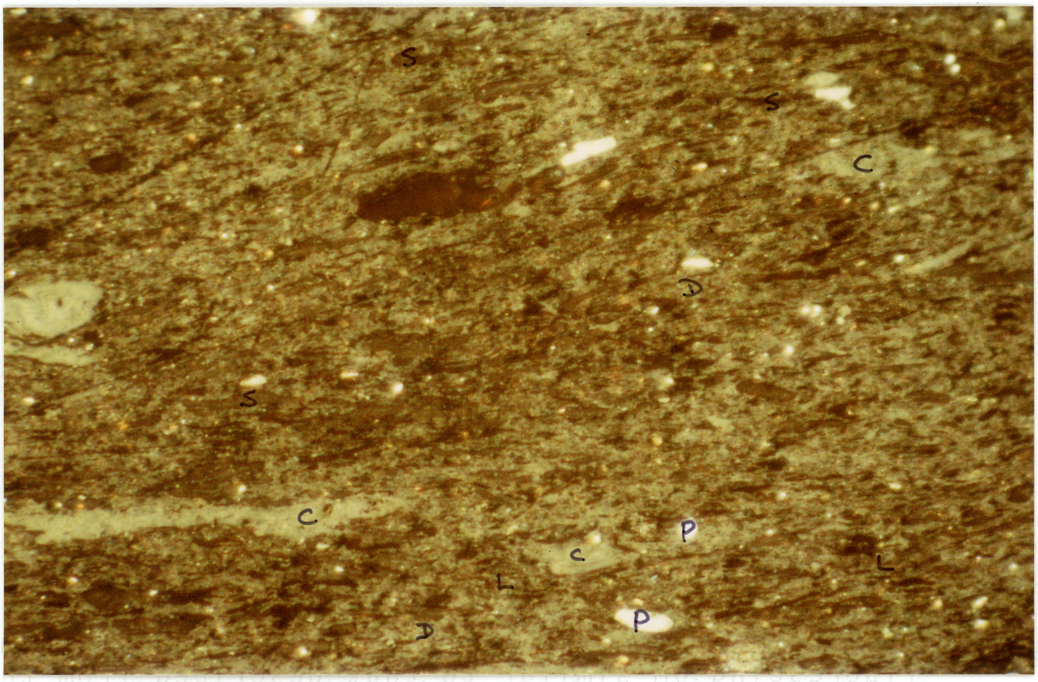
S
S
C
D
S
C
P
C
L
L
D
P

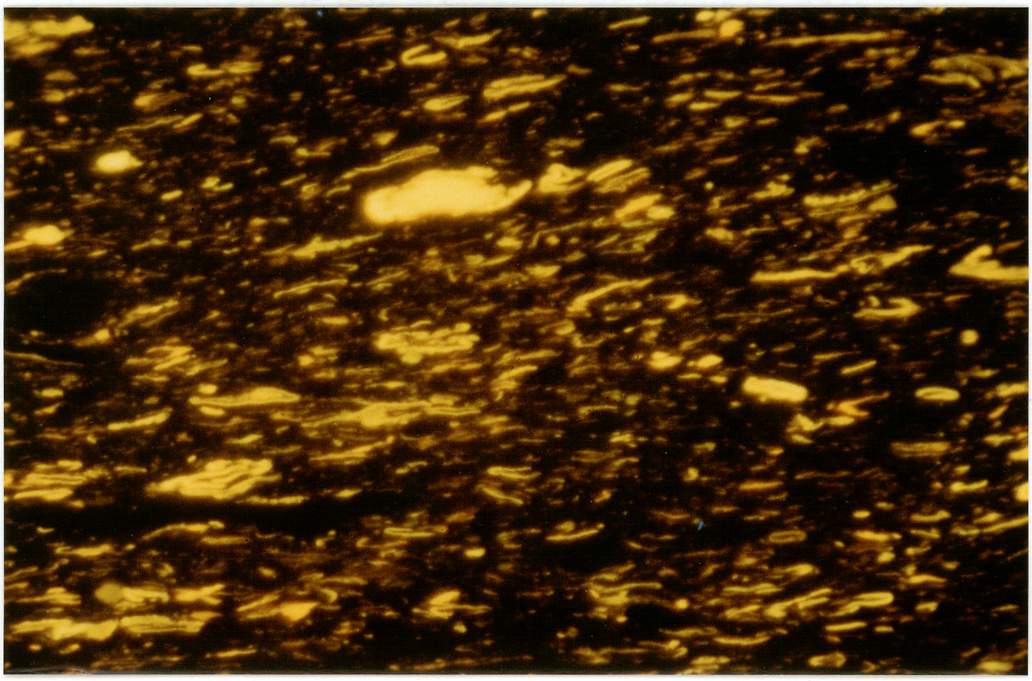

Plate 10 WU9501 5920'(T-1) Between M-1.2 and T-1

Coal-rich layer in carbonaceous shale made up of large amounts of sporinite (S), lesser vitrinite (V) and minor pyrite (P). R_o=0.48%

Plate 11 As above

Sporinite shows bright yellow fluorescence. Unlike the clarite figured in Plates 8 and 9, the groundmass layers show a weak fluorescence.

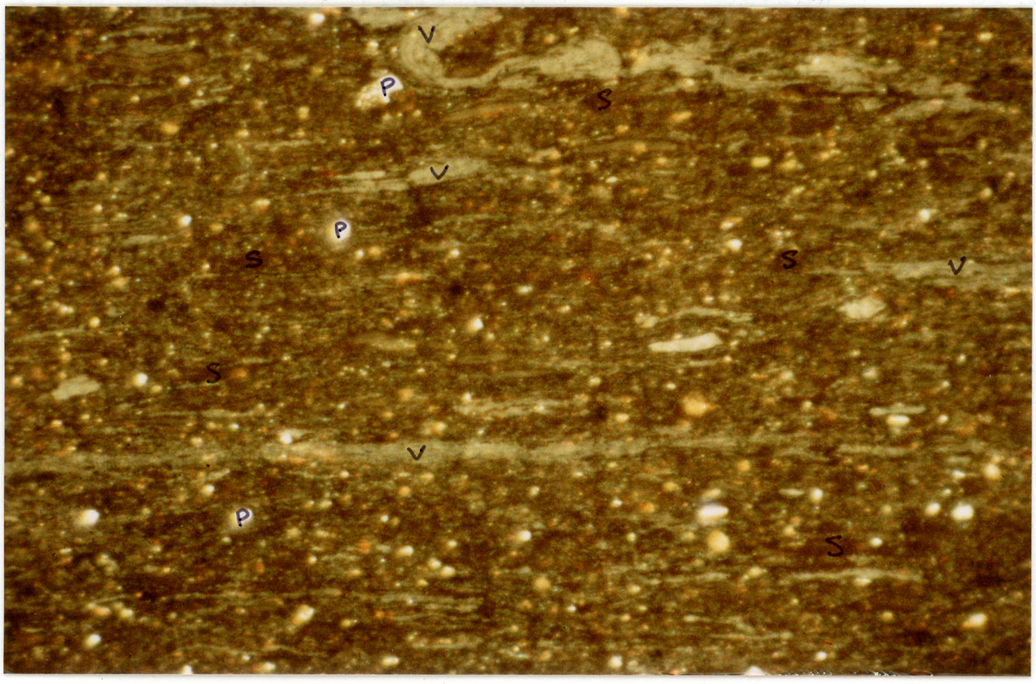
V
P
S
V
P
S
S
V
S
V
P
S

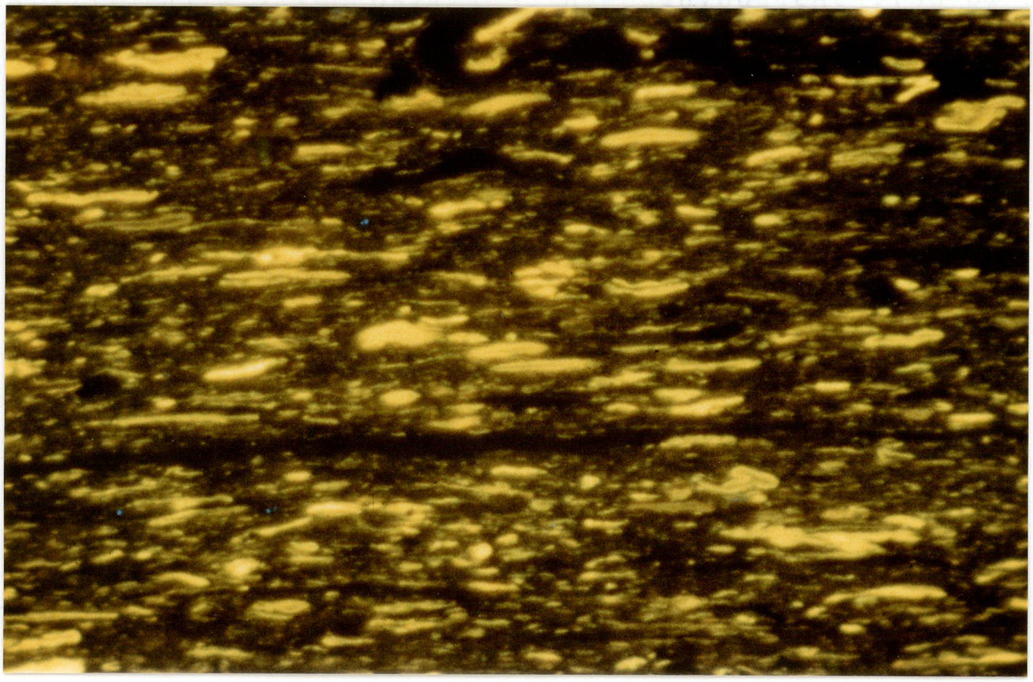

Plate 12 WU9495 5230'(T-1) Between M-1.2 and T-1

Cuttings grains showing minor vitrinite (V) and inertinitic (I) dom with common pyrite (P) against a background of quartz grains. R_o=0.43%

f.o.v. 0.28mm across.

Plate 13 As above.

In fluorescence mode these grains show very common fluorescing OM similar to that described from the Rundle oil shale i.e. Alginite B.

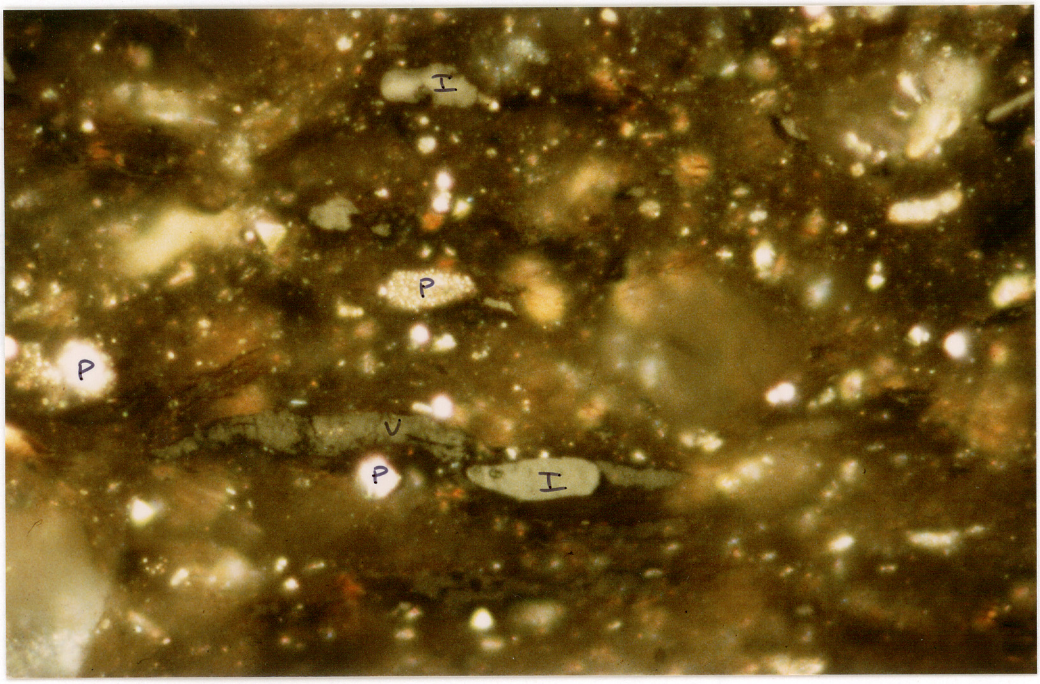
I
P
P
V
P
I

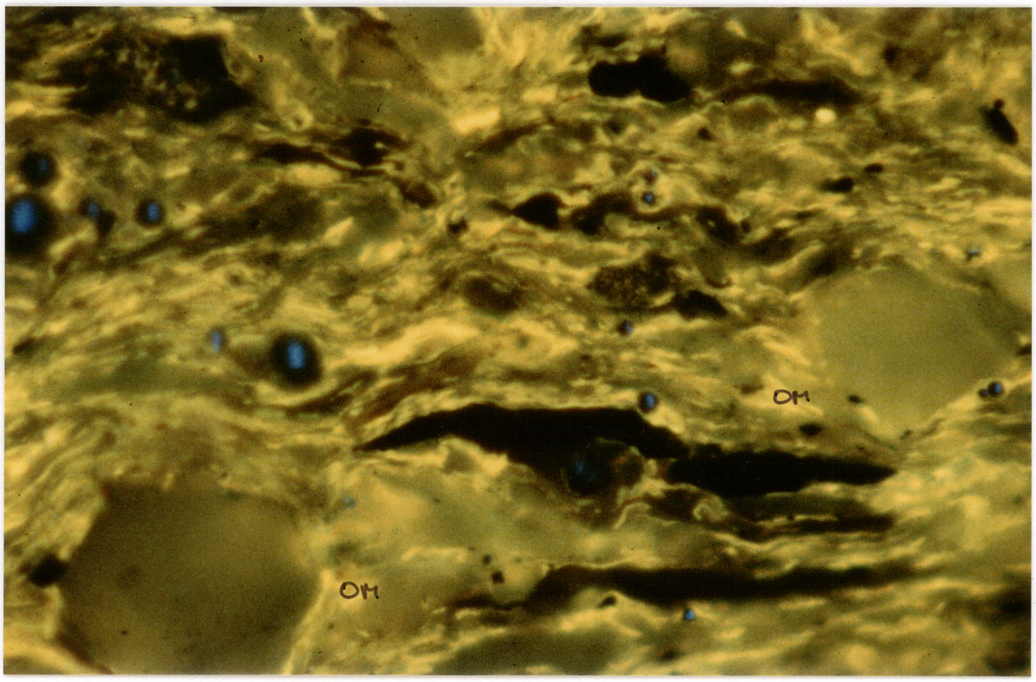
OM
OM

Plate 14 WU9306 6637'(T-2) T-1 Reservoir

Layer of vitrinite showing only partially compressed cell structure. Layers of corpocollinite (phlobaphinite) alternate with layers of texto- and eu-ulminite (TU, EU). Both are transected by layers of corpocollinite-filled cells which represent former canals for the transport of fluids. R_o=0.56%

Plate 15 WU9304 6625'(T-2) T-1 Reservoir

Layers of phlobaphinite filled cells with cross-cutting phlobaphinite filled canals. R_o=0.52%
f.o.v. 0.56mm across.

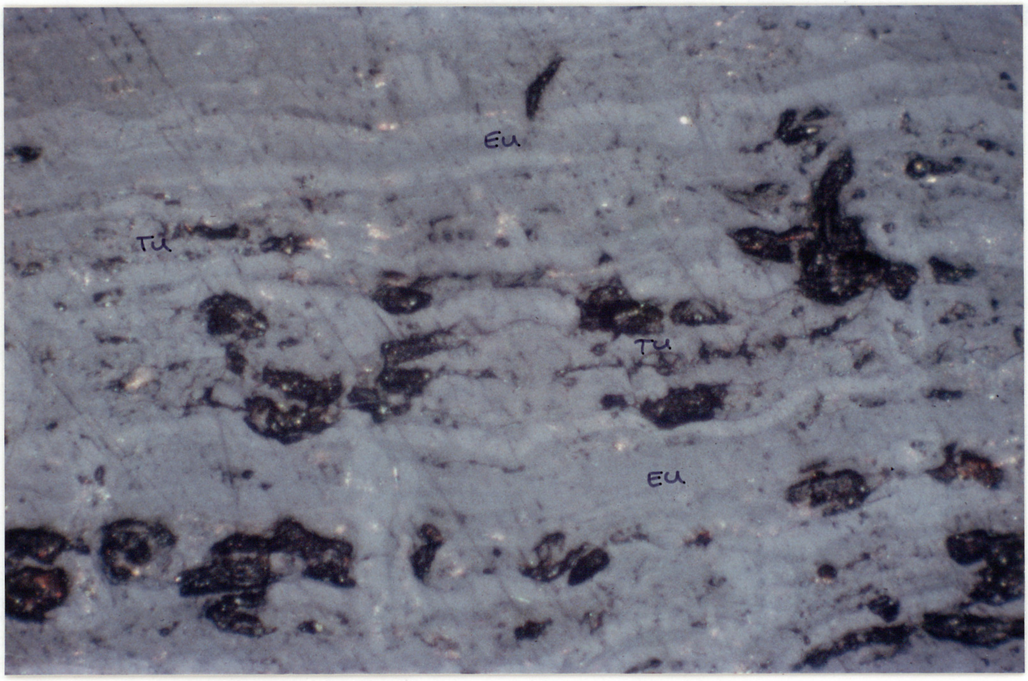
Eu
Tu
Tu
Eu

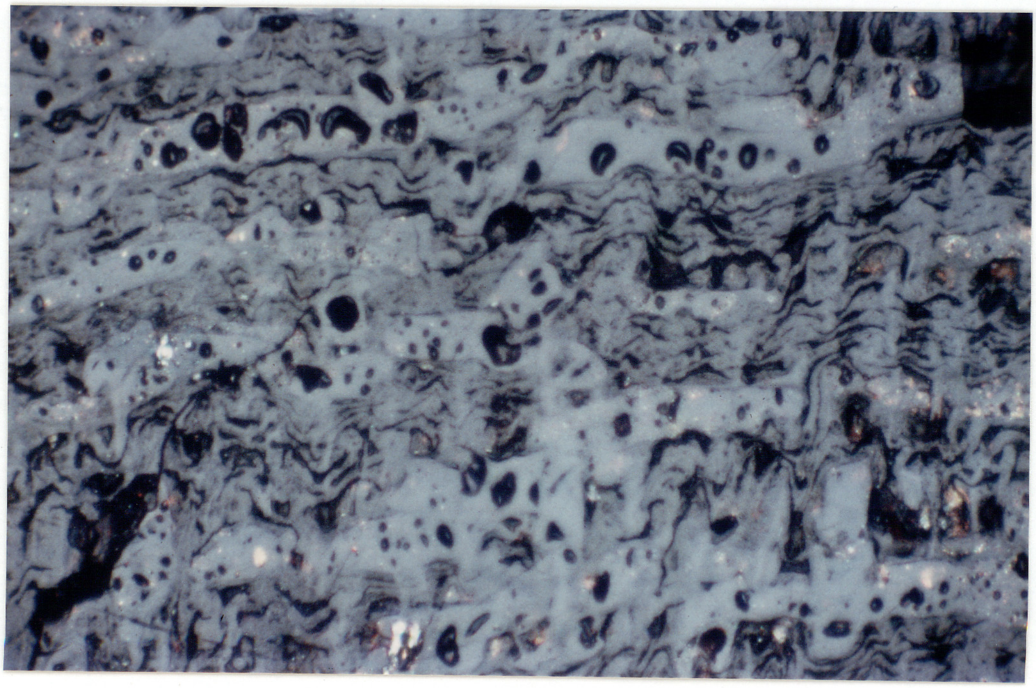

Plate 16 WU9303 6621' (T-2) T-1 Reservoir

Cells filled with phlobaphinite and surrounded by suberinite. R_o=0.52%

Plate 17 WU9311 6658'(T-2) T-1 Reservoir

Cell lumens infilled with either phlobaphinite (PH) or porigelinite (PO). R_o=0.52%

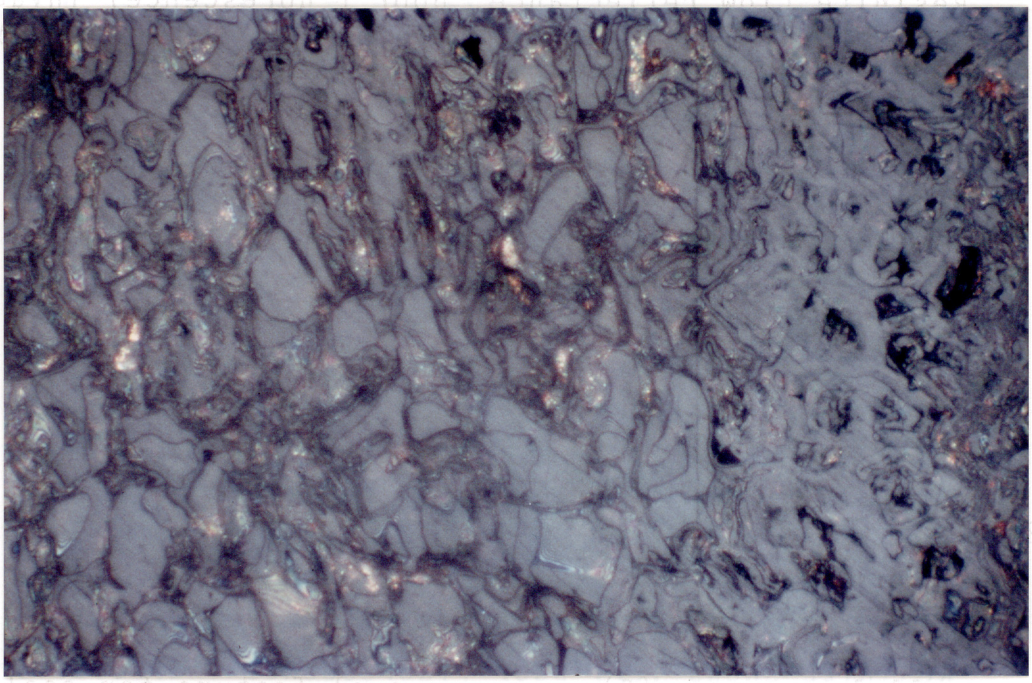

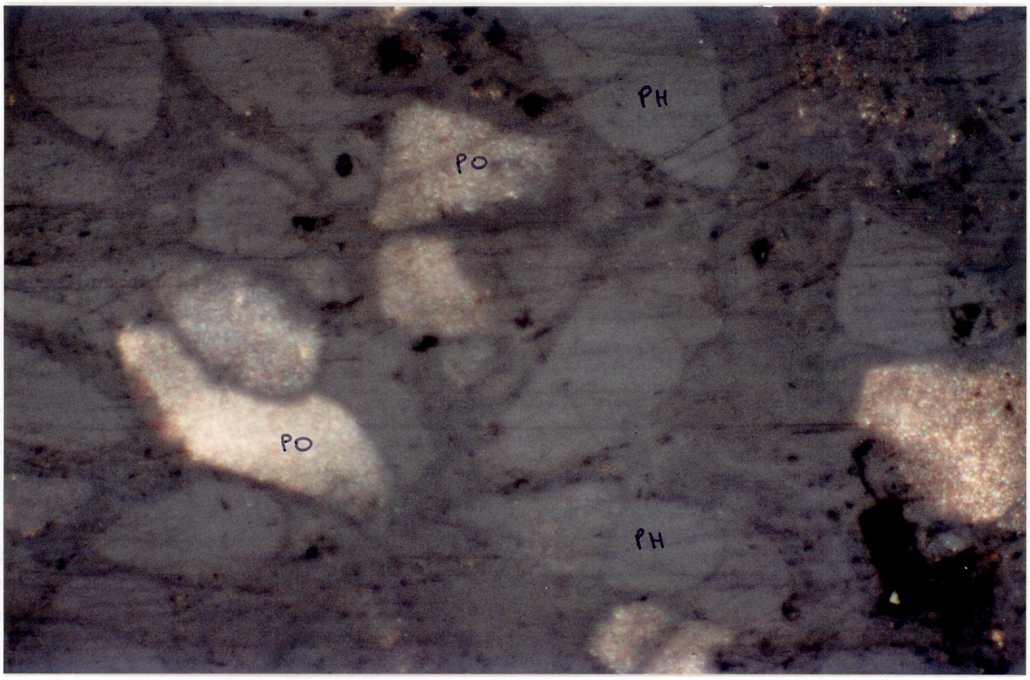
PH
PO
PO
PH

Plate 18 WU9313 6662'(T-2) T-1 Reservoir

Cell lumens in vitrinite layer infilled with relatively high reflectance resinite. R_o=0.54%
f.o.v. 0.56mm across.

Plate 19 As above.

Resinite shows very poor fluorescence characteristics indicating that its chemical composition is controlled more by the composition of its precursor materials and factors such as oxidative polymerization rather than thermal maturation.

Plate 20 WU9326 6482' (T-3) T-1 Reservoir

Highly fluorescing resinite in vitrinite of the same rank as the vitrinite illustrated above. Such physical differences typify the wide range of resinite commonly found in coals.

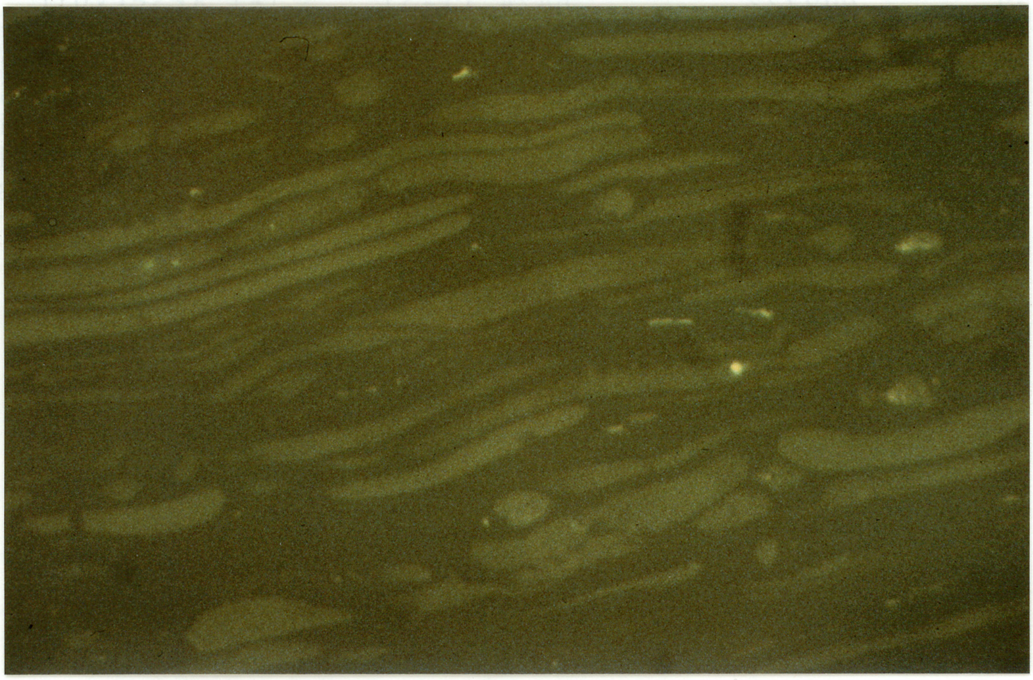

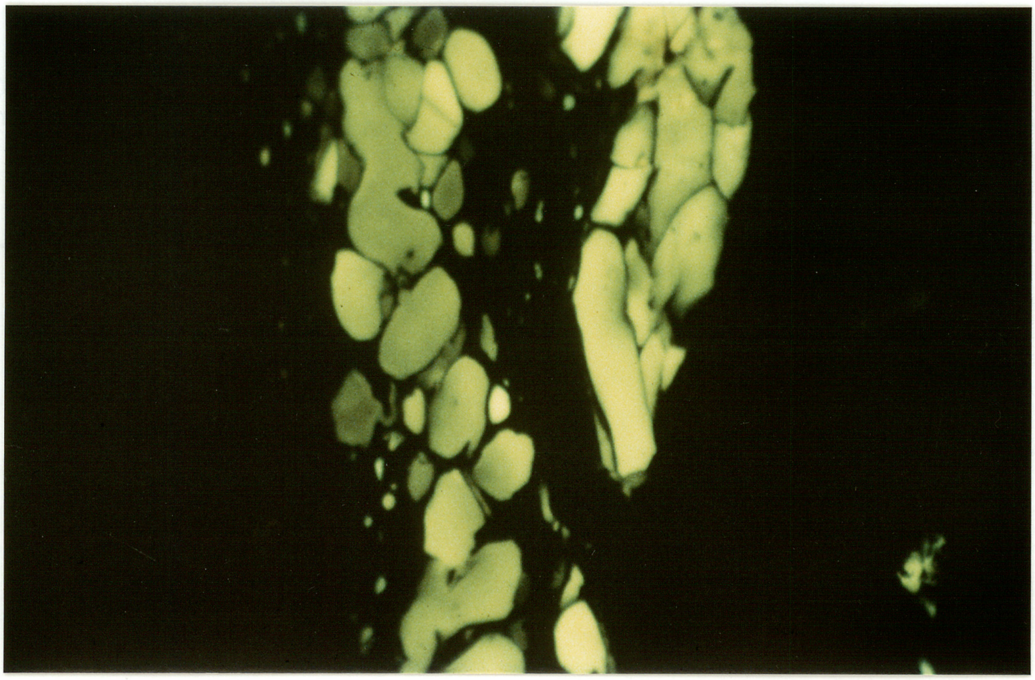

Plate 21 WU9503 6551'(T-1) T-1 Reservoir

Resinite (low reflectance, poor fluorescence) invading cell walls and some cell lumens in what is probably wound (scar) tissue. R_o=0.56%
f.o.v. 0.26mm across.

Plate 22 WU9322 6424'(T-3) T-1 Reservoir

Layer of vitrinite comprised of corpohuminite (CO) and texto-ulminite (TU). The corpohuminite shows variable reflectance and the texto-ulminite displays open intercellular spaces (C) — an unusual feature for coals buried to depths of nearly 2km, since it is inconsistent with the load pressures which obtain at such depths.
R_o=0.52%

Plate 23 As above.

Intercellular spaces and ?partly vacant cell lumens (the vitrinite associated with internal reflections in the plate above) are associated with a pale-green fluorescence presumed to represent an oil stain. It may be that the fluid pressure regime of the T-1 reservoir has prevented the collapse of the texto-ulminite described above.
f.o.v. 0.26mm across.

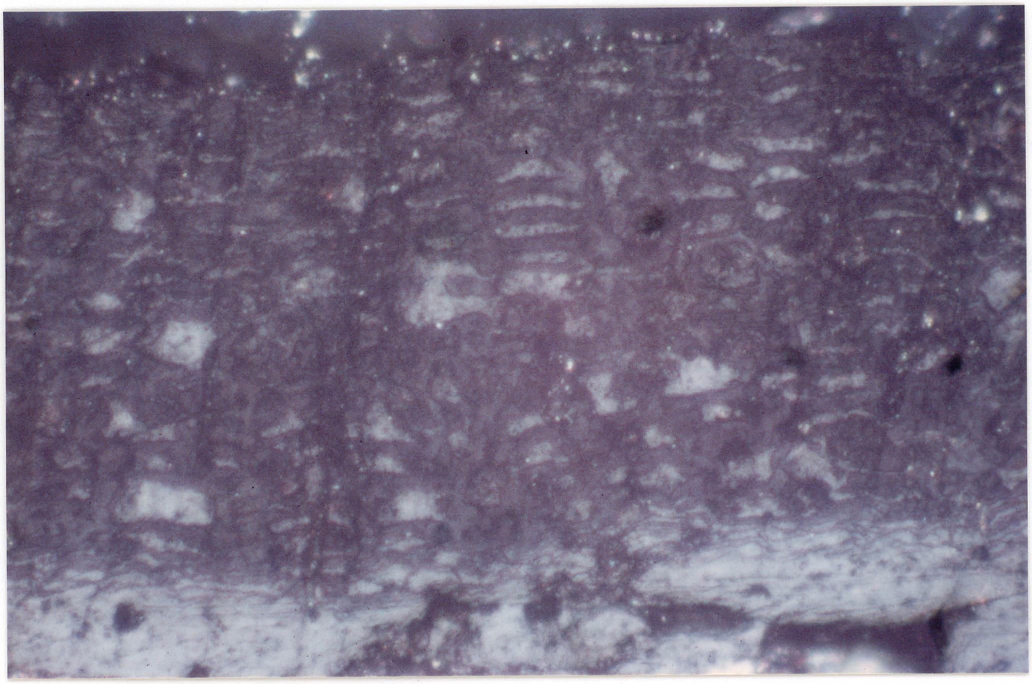

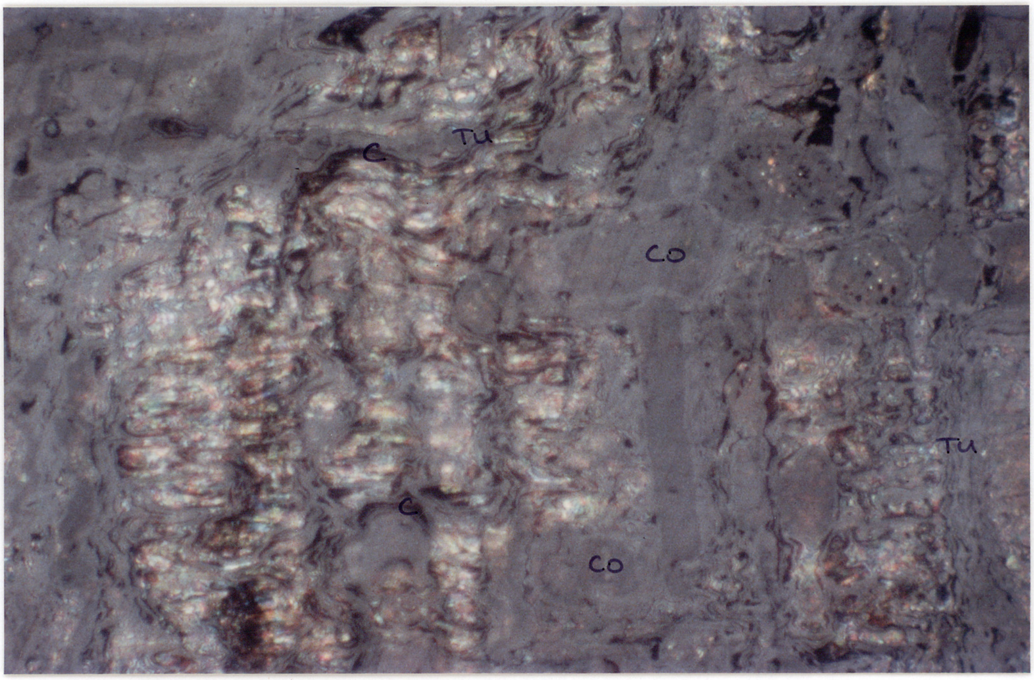

C
TU
CO
TU
C
CO

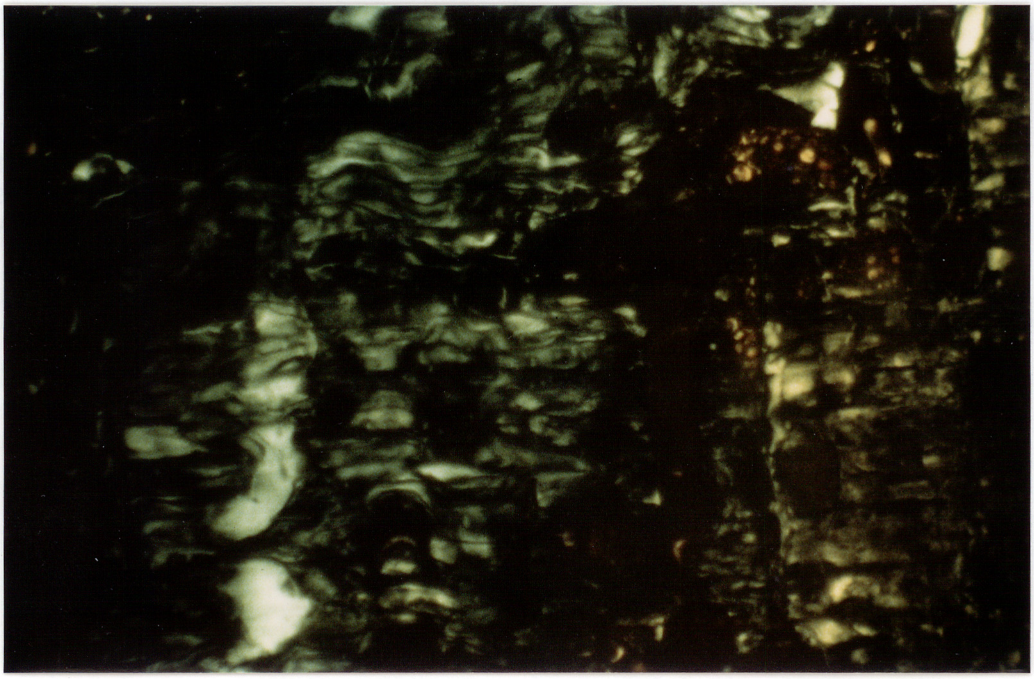

Plates 24 and 25   WU9322   6424' (T-3)   T-1 Reservoir

Description is as for plates 22 and 23. R_o=0.52%
f.o.v.   0.26mm across.

Plate 26   WU9320   6418'(T-3)   T-1 Reservoir

Phlobaphinite filled cell lumens associated with dark oil stain. As there is no smearing associated with the oil stain it is presumed to have occurred after final polishing of the sample took place — i.e. oil is emanating from the fine porous structure of the vitrinite. R_o=0.49%
f.o.v.   0.26mm across.

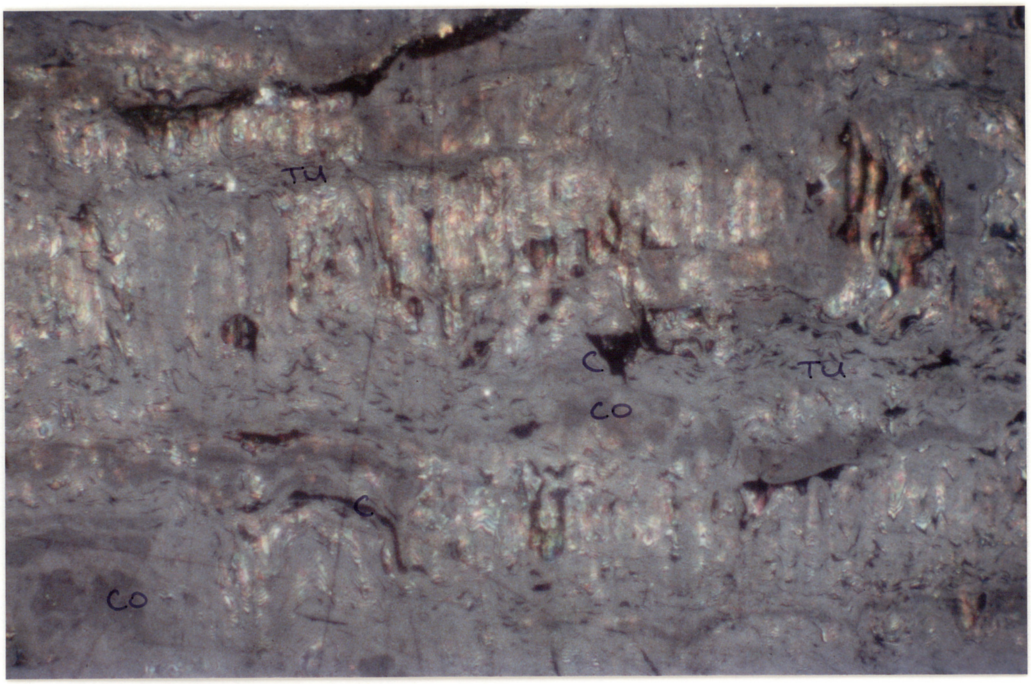
TU
C
TU
CO
C
CO

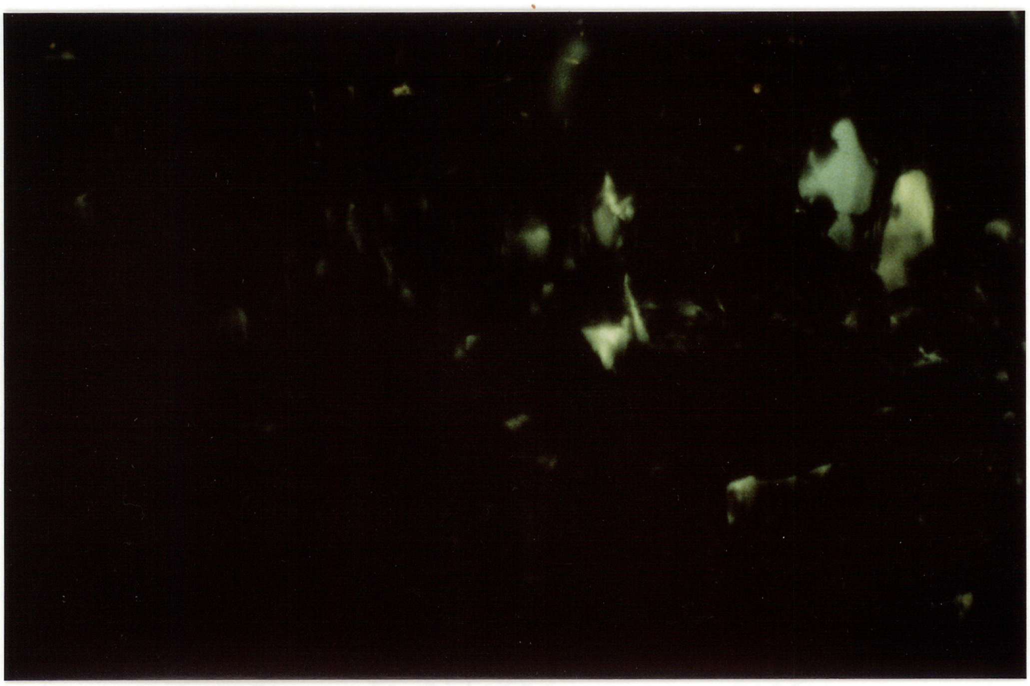

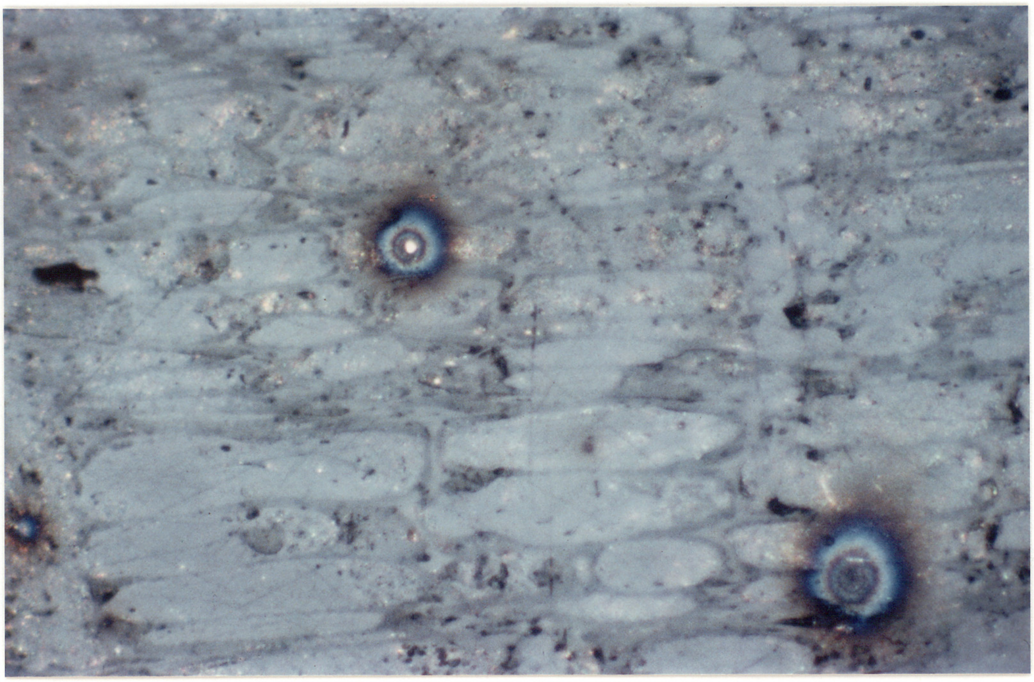

Plate 27 WU9321 6421'(T-3) T-1 Reservoir

Oil released from vitrinite during the grinding/polishing procedure staining polished vitrinite surface. R_o=0.52%

Plate 28 WU9312 6662'(T-2) T-1 Reservoir

As for Plate 27. R_o=0.55%

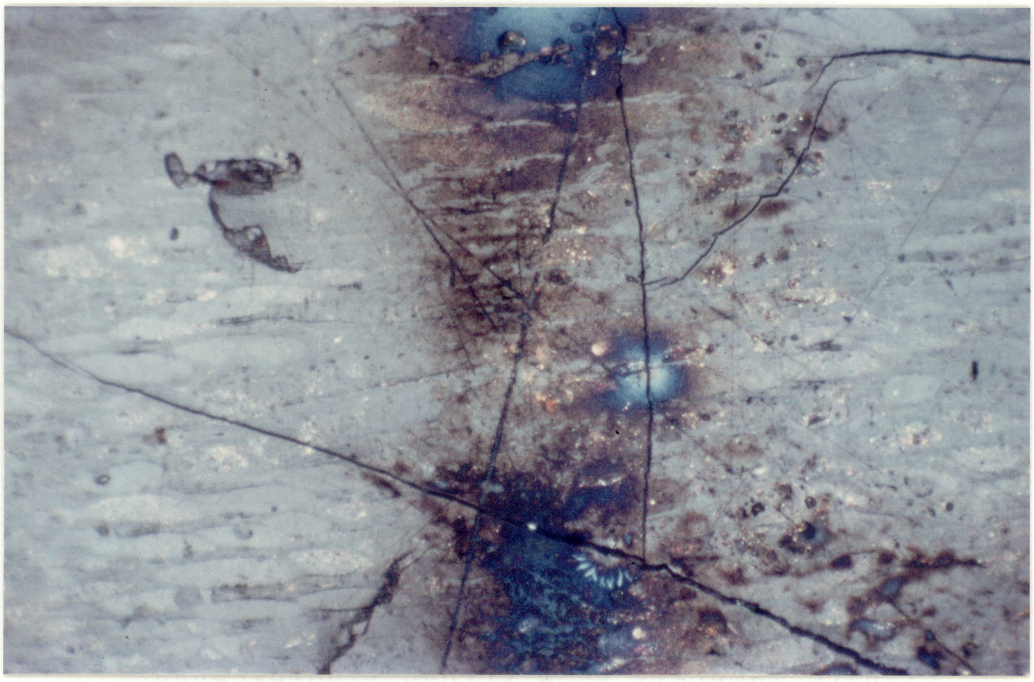

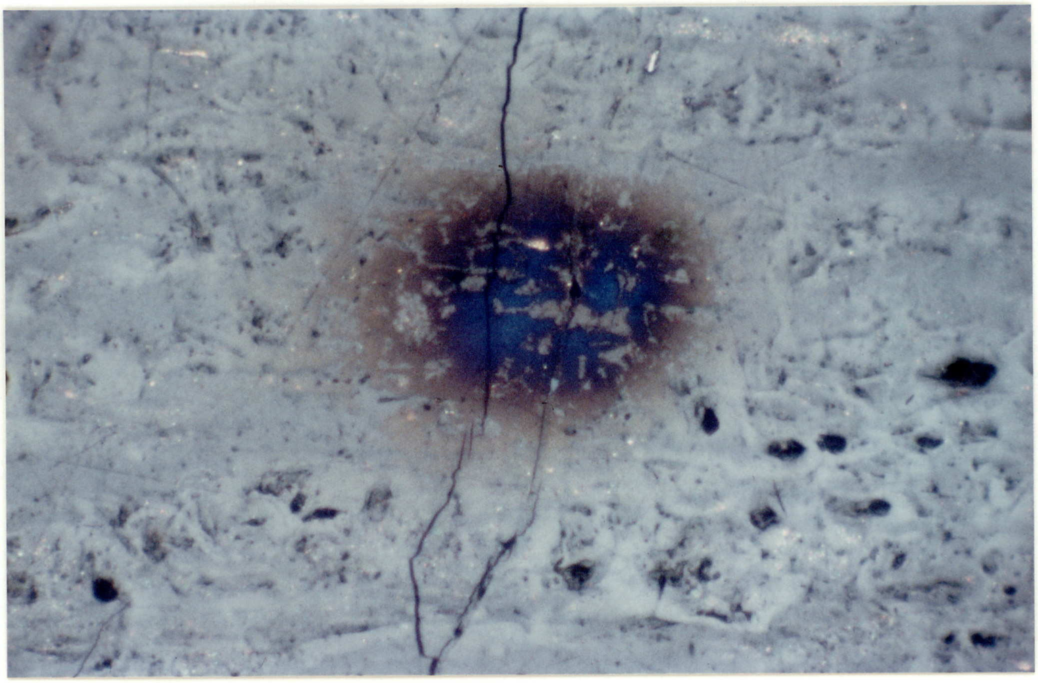

Plate 29 WU9313 6670'(T-2) T-1 Reservoir

Layer of duroclarite type coal. Coal is comprised of semifusinite (SF) and inertodetrinite (I), the exinite macerals sporinite (S) and cutinite (C), all in a matrix of desmocollinite-type vitrinite. R_o=0.54%

Plate 30 As above.

Exinite macerals show strong fluorescence.

Plate 31 WU9325 6458'(T-3) T-1 Reservoir

Dirty coal associated with quartz (Q) and clay (CL). R_o=0.54%

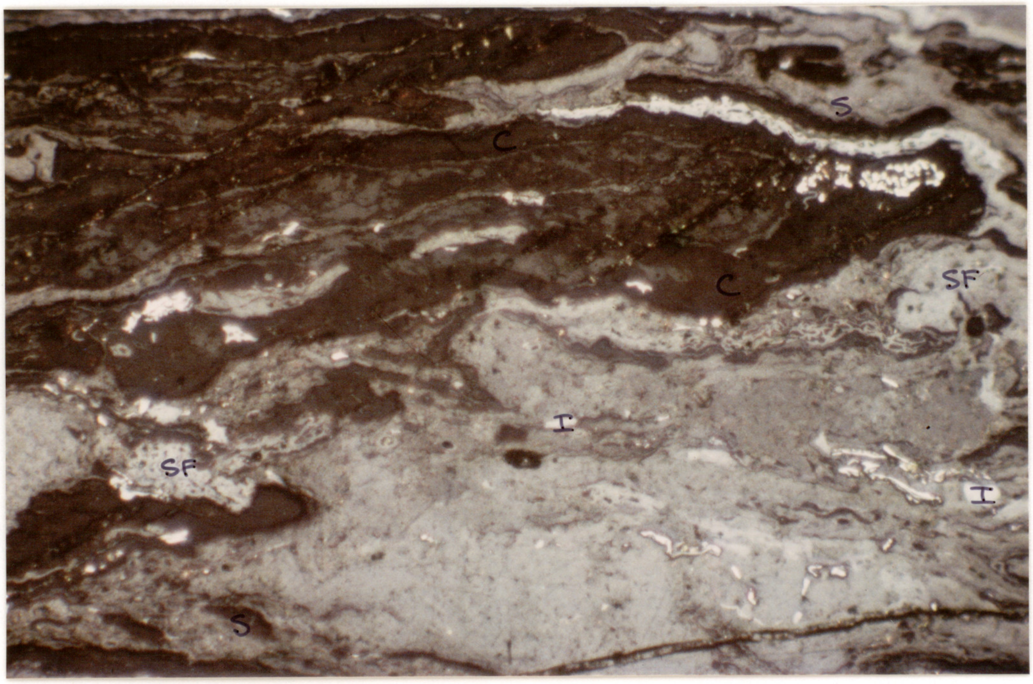
S
C
C
SF
I
SF
I
S

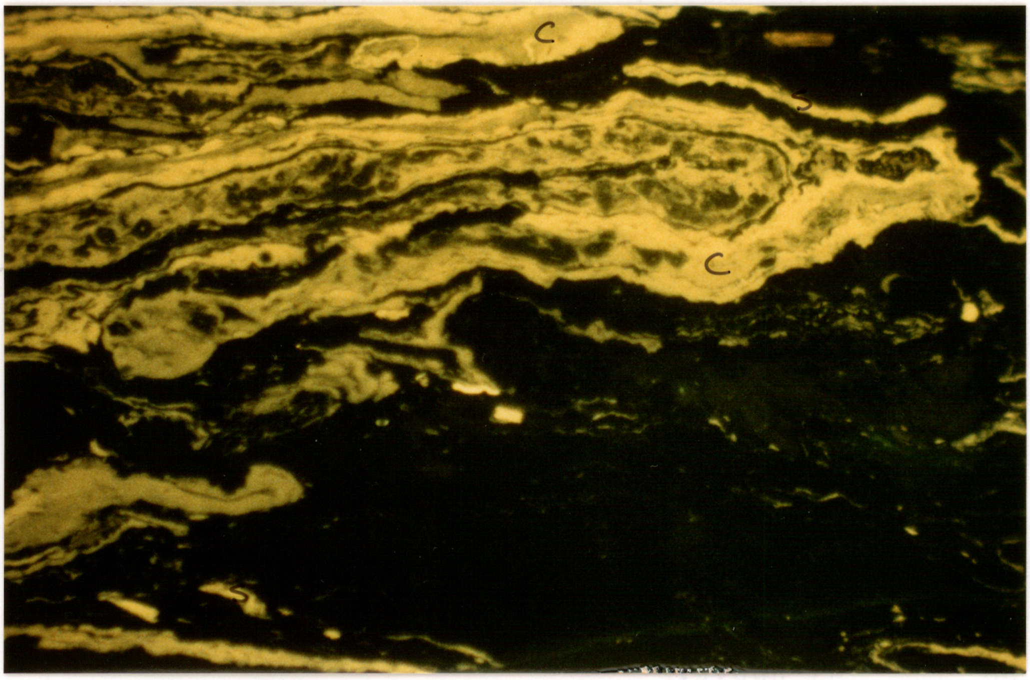
C
S
C
S

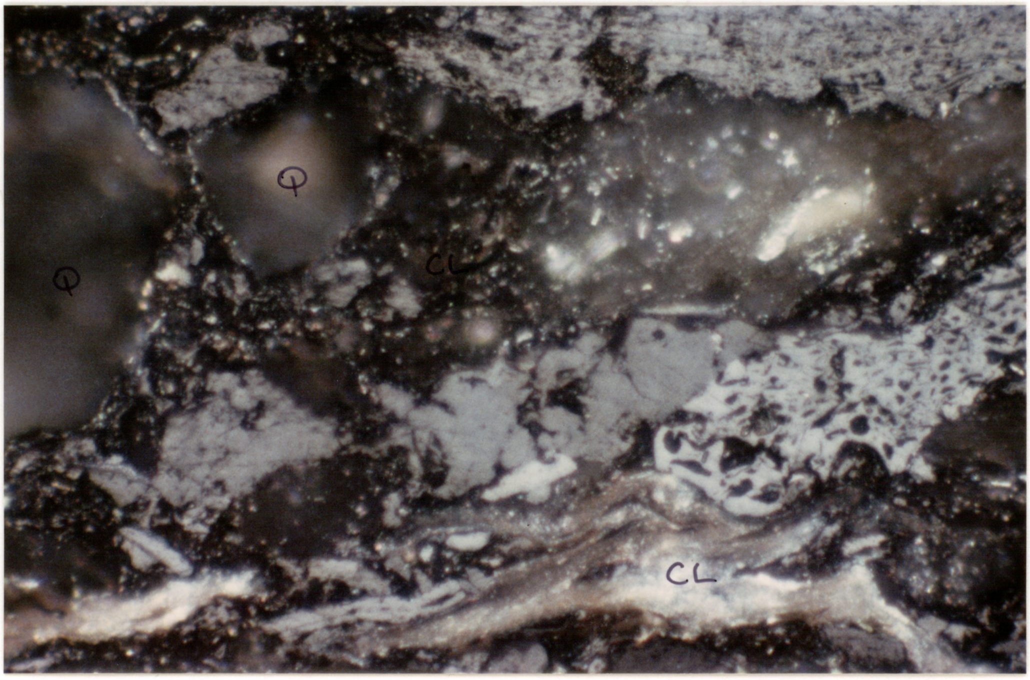
Q
Q
CL
CL

Plate 32 WU9312 6662'(T-2) T-1 Reservoir

Clarodurite layer. Thick layer of cutinite (C) shows high reflectance (possibly due to oxidative polymerization) and surrounds the resin-rich (R) interior of a leaf. The leaf fragment is surrounded by coaly detritus rich in semifusinite and exinite, the latter including resinite and sporinite. Vitrinite absent. R_o=0.55%

Plate 33 As above.

The cutinite has very poor to almost no fluorescence whereas the resinite is characterized by a strong yellow fluorescence.

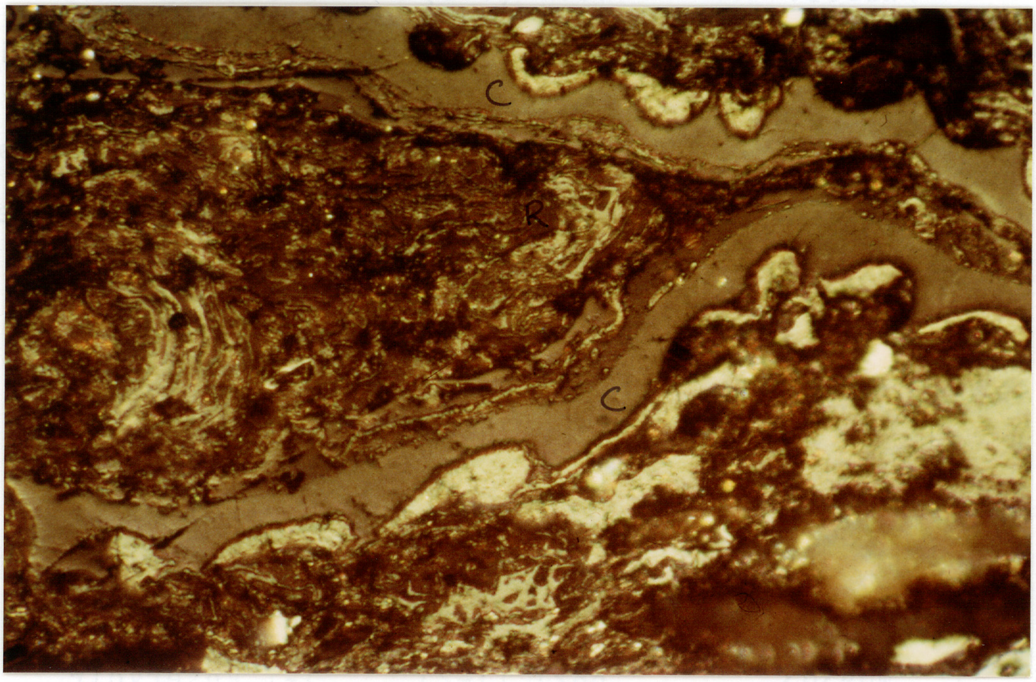
C
R
C

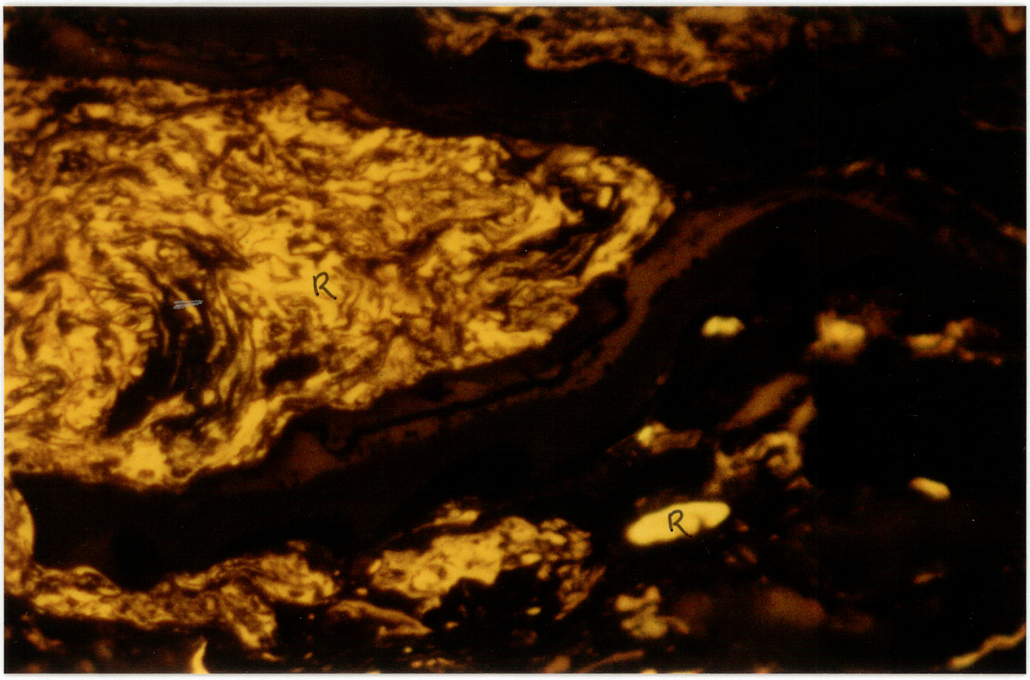
R
R

Plate 34 WU9310 6654'(T-2) T-1 Reservoir

Uncompressed fusinite. Usually at such depths inertinite is crushed into fragments similar to those in the centre of the field of view. It is possible that hydrocarbon fluids infilling such vacant cell lumens have preserved the inertinite structure but it is a curious anomaly that polished surfaces of inertinite are rarely oil stained. $R_o=0.57\%$

f.o.v. 0.56mm across.

Plate 35 WU9303 6621'(T-2) T-1 Reservoir

Well preserved cell structure in semifusinite. Pits in cell walls and inter-mural pores for plant respiration still visible. Some development of micrinite (M) in infilled cell lumens. Other comments as above. $R_o=0.52\%$

Plate 36 WU9302(T-2) T-1 Reservoir

'Dirty' coal showing gradation into carbonaceous shale/carbonaceous fine sandstone. Common vitrinite (V) interstitial to quartz grains (Q) and clay (CL). Minor inertodetrinite (I). $R_o=0.52\%$

f.o.v. 0.56mm across.

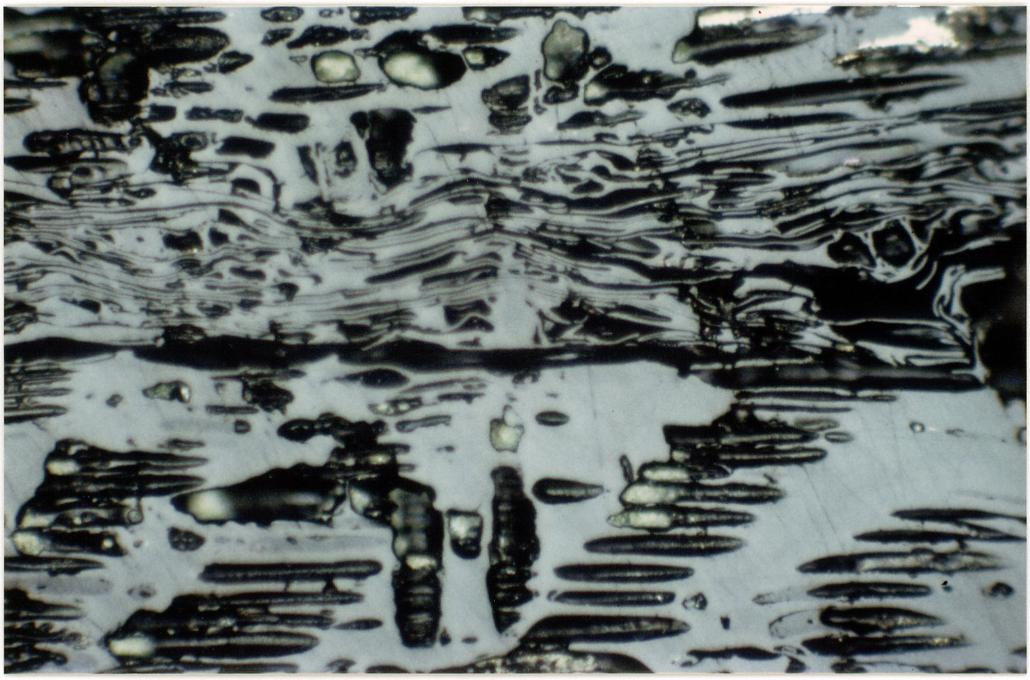


M
M

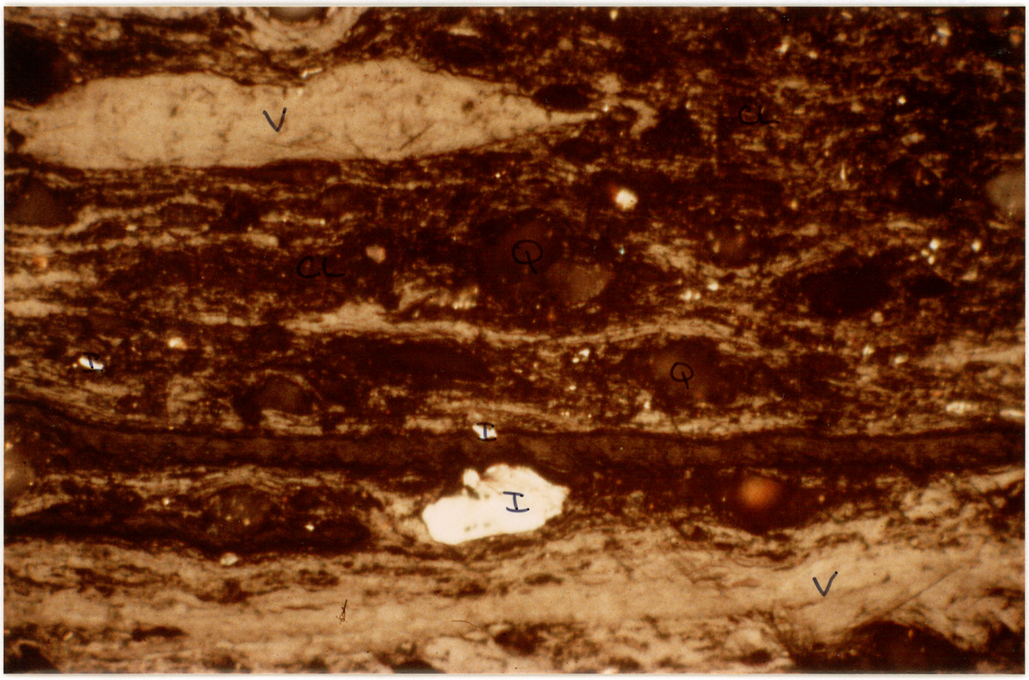
V
CL
Q
CL
Q
I
I
V

Plate 37 WU9503 6551'(T-1) T-1 Reservoir

Carbonaceous siltstone/sandy siltstone comprising scattered vitrinitic and inertinitic dom in a matrix of fine sand and clay. R_o=0.55%

Plate 38 As above

Common sporinite and liptodetrinite are also present and show strong yellow fluorescence. Most siltstones throughout the Tuna Field contain similar amounts of exinitic dom.

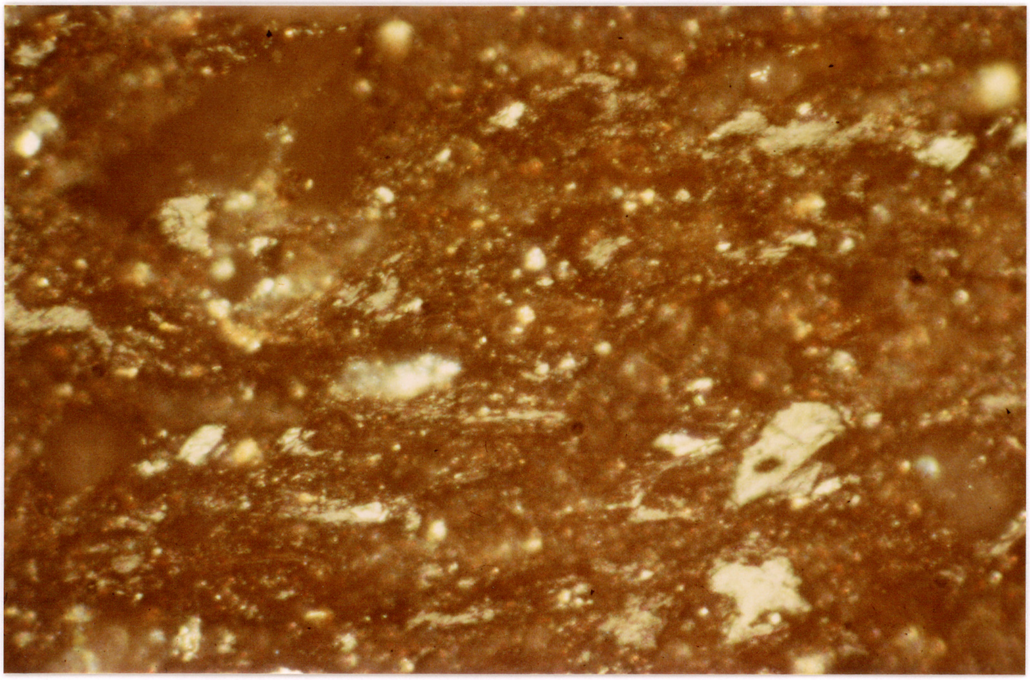

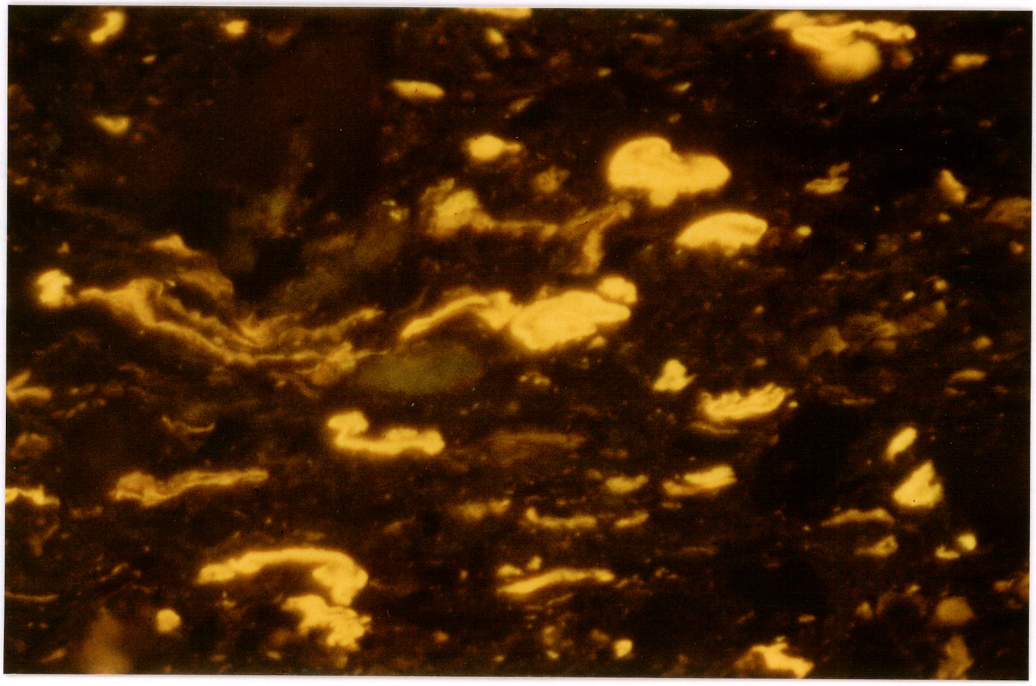

Plate 39 WU9505 7670'(T-1) Below T-1 Reservoir

Large grains of asphaltic pyrobitumen interstitial to carbonate (? dolomite). R_o=0.55%

Plate 40 WU9505 7670'(T-1) Below T-1 Reservoir

?Mineral/?Matrix (?oil) fluorescence in fine grained sediment.